

Introduction to some geo-topics on Early Earth & present-day earth

*What do we know?
What do we dont know?
How do we know?*

Bettina Scheu, Earth & Environmental Sciences LMU

How did the Early Earth look alike? Hot <-> cold? Only a water world? What atmosphere did it had?

How likely was an exposed land surface on early Earth?



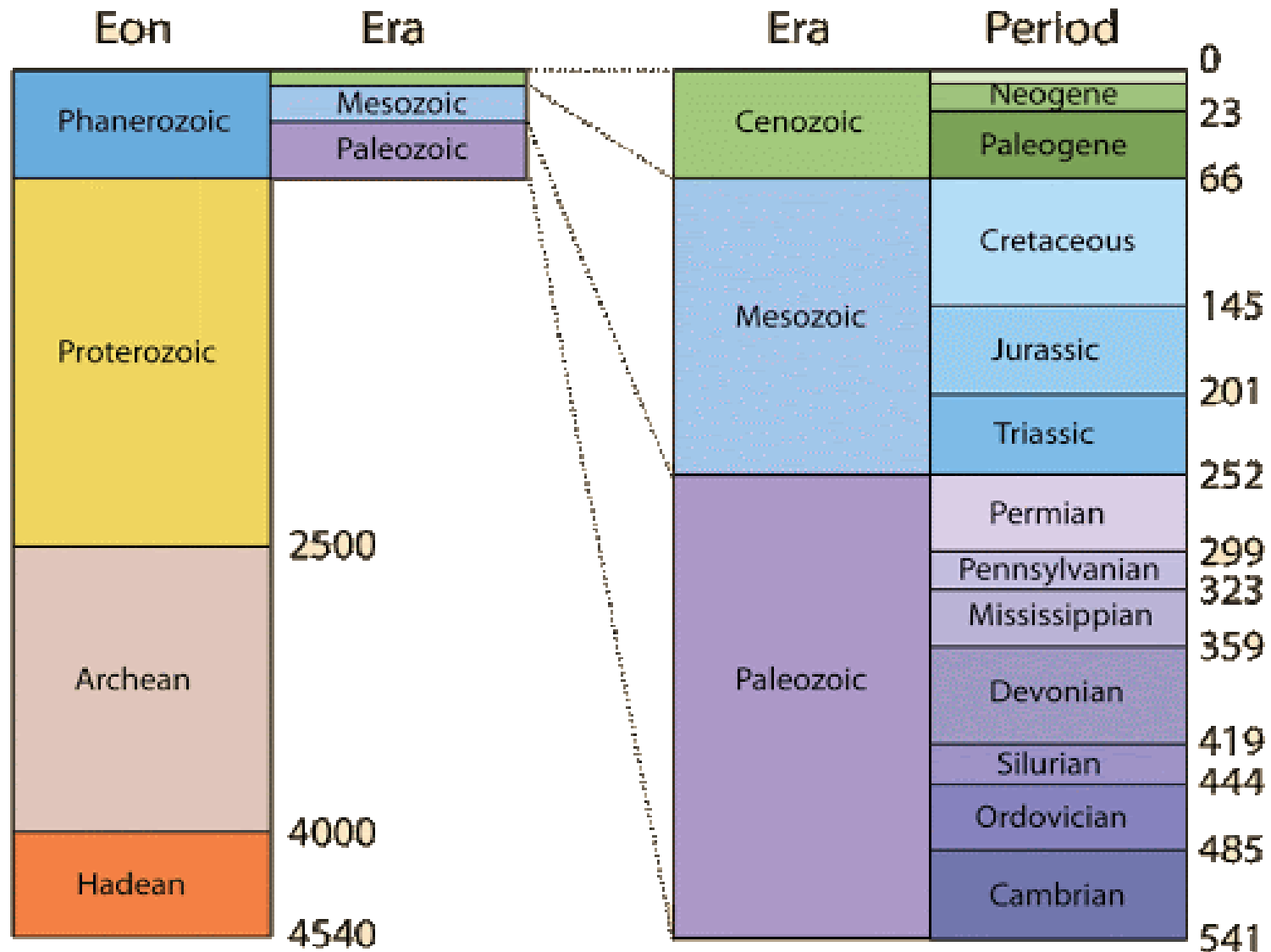
Modern Origins of Geology & Geochemistry

- James Hutton (1726-1797), is known as the “Father of Geology”
- Alfred Wegener 1915 Theorie zur Drift der Kontinente -> Plattentektonik
- Physical Chemistry and Geology were effectively combined by establishment in 1907 of the Geophysical Laboratory of the Carnegie Institute of Washington.
→ N.L. Bowen, a MIT-trained scientist, published “The Evolution of the Igneous Rocks (1928)
- V.M. Goldschmidt (1888-1947) is known as the father of Modern Geochemistry. His collected efforts are summarized in the book “Geochemistry”, Clarendon Press, Oxford, 1954.

Begriffe - Definitionen

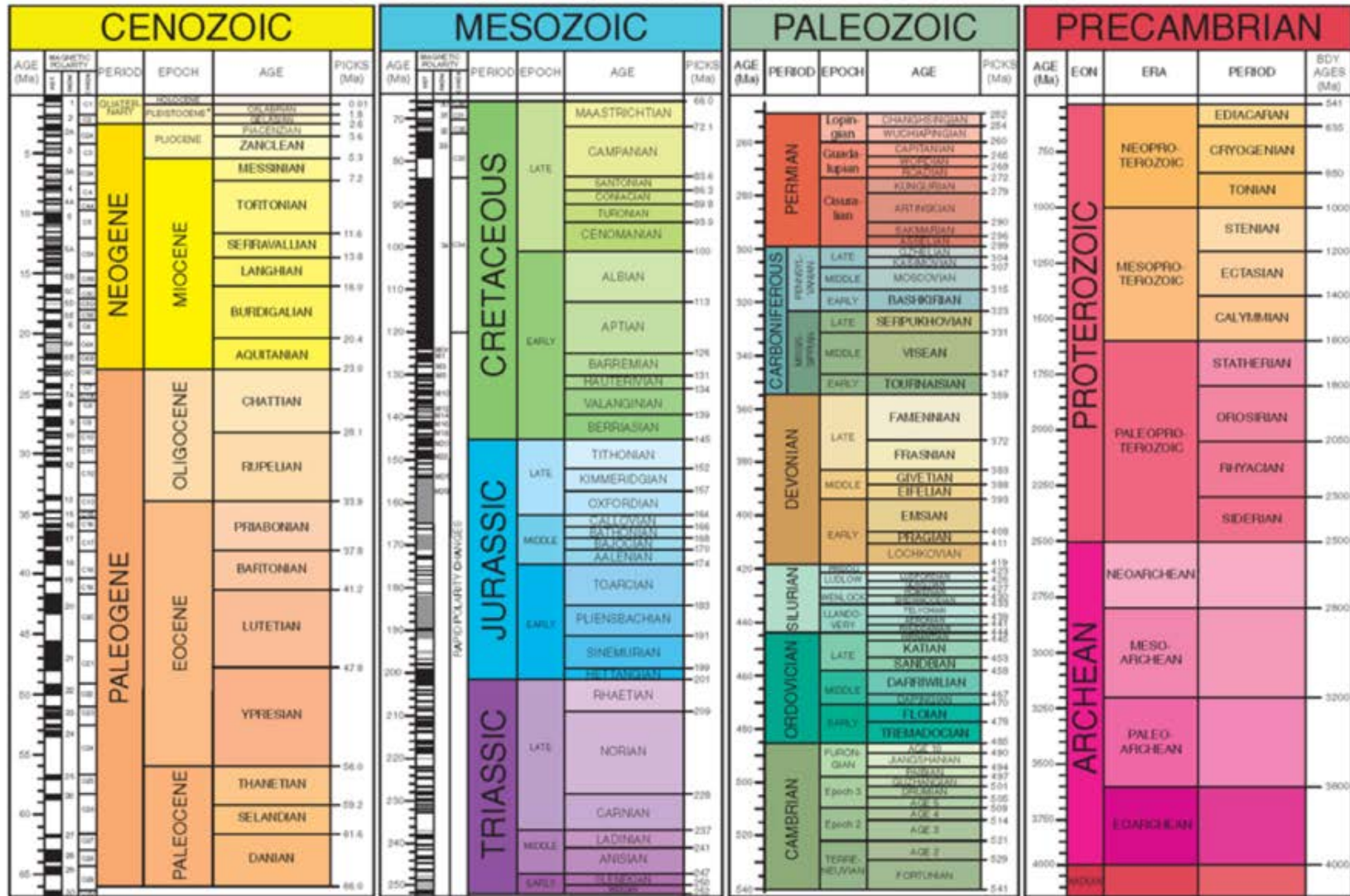
- **Mineral** = Natürlicher, homogener Festkörper, der meist in kristallisierter Form vorliegt.
- **Kristall** = Festkörper mit periodischer und streng regelmäßiger Anordnung von Atomen und Molekülen. Die streng geordnete Struktur wird Kristallgitter genannt.
- **Gestein** = Jedes natürliche Material, das im Wesentlichen aus mineralischen Komponenten besteht. Dazu zählen auch natürliche Gläser. Es gibt Festgesteine und Lockergesteine.
- **Natürliches Glas** = Durch geologische Prozesse entstandener anorganischer Festkörper ohne kristalline Ordnung (= amorpher Zustand).

Geologic time



Geologic time and the geologic column

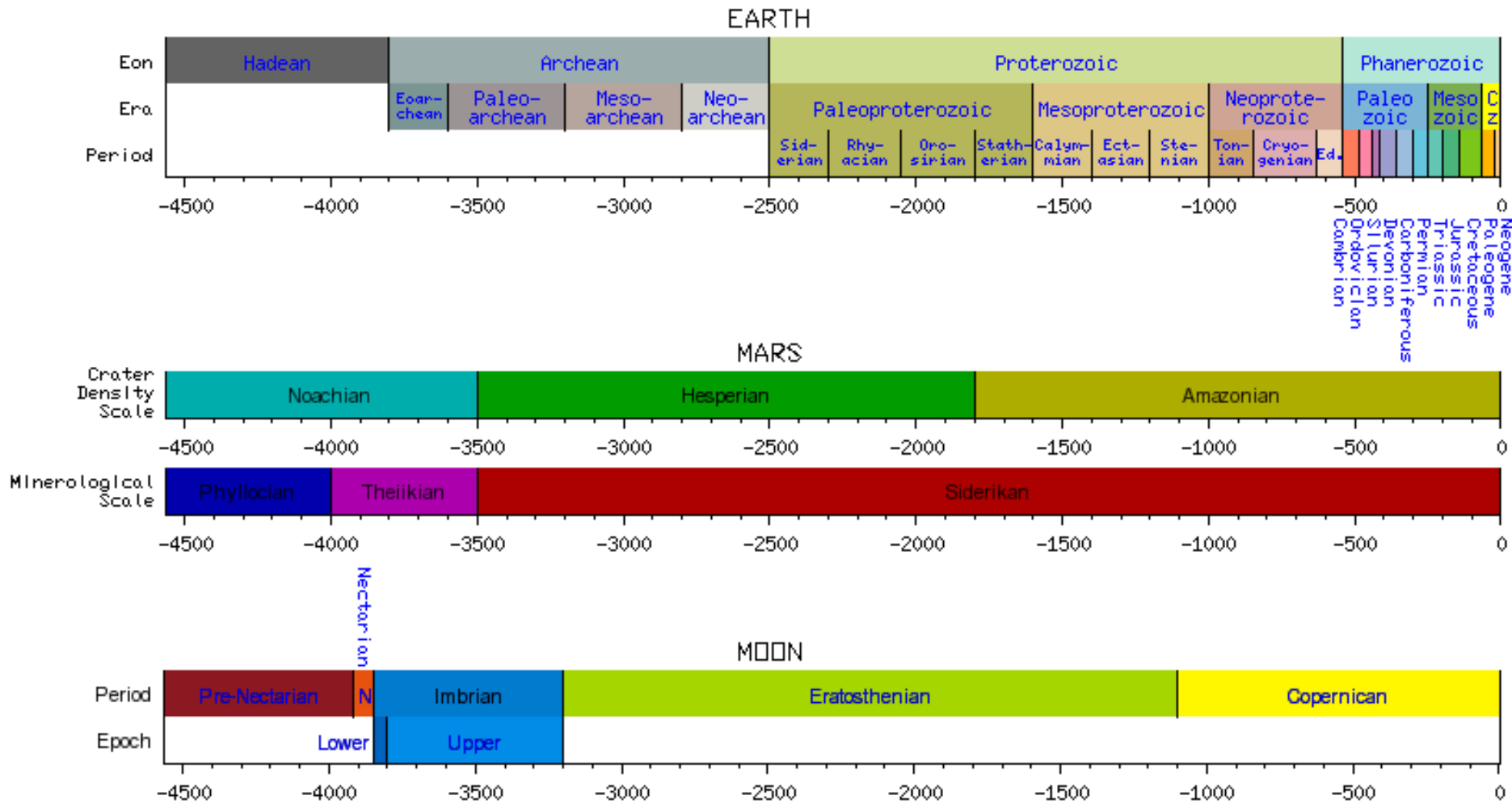
GSA GEOLOGIC TIME SCALE v. 4.0



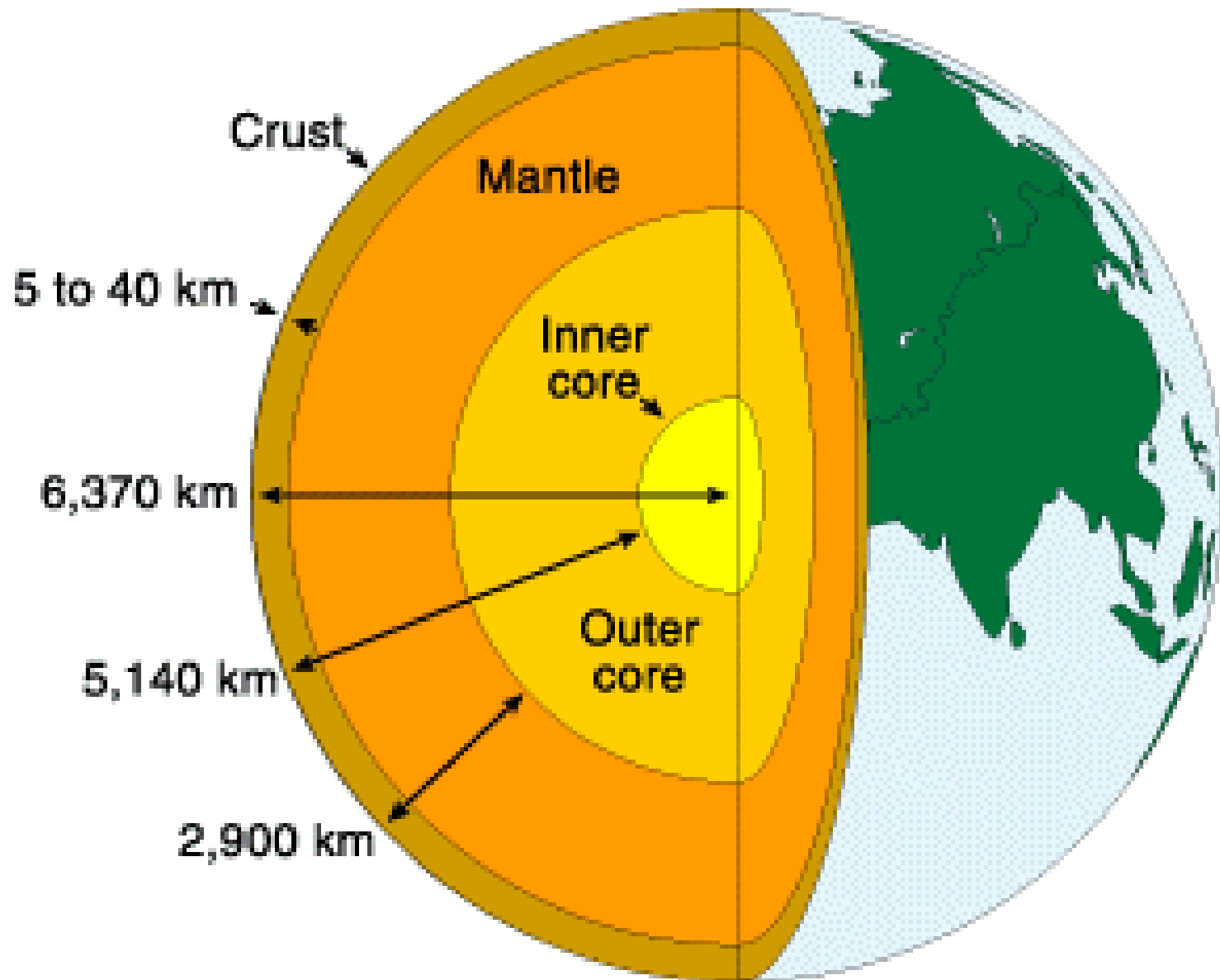
*The Pleistocene is divided into four ages, but only two are shown here. What is shown as Calabrian is actually three ages—Calabrian from 1.8 to 0.29 Ma, Middle from 0.78 to 0.13 Ma, and Late from 0.13 to 0.01 Ma. Walker, J.D., Gassman, J.W., Bowring, S.A., and Babcock, L.E., compilers, 2012, Geologic Time Scale v. 4.0. Geological Society of America, doi: 10.1130/2012.CT5004R0C. ©2012 The Geological Society of America. The Cenozoic, Mesozoic, and Paleozoic are the Eras of the Phanerozoic Eon. Names of units and age boundaries follow the Gradstein et al. (2012) and Cohen et al. (2012) compilations. Age estimates and picks of boundaries are rounded to the nearest whole number (1 Ma) for the pre-Cenomanian, and rounded to one decimal place (100 ka) for the Cenomanian to Pleistocene interval. The numbered epochs and ages of the Cambrian are provisional. REFERENCES CITED: Cohen, K.M., Finlay, S., and Gibbard, P.L., 2012, International Chronostratigraphic Chart: International Commission on Stratigraphy, www.stratigraphy.org (last accessed May 2012). (Chart reproduced for the 34th International Geological Congress, Brisbane, Australia, 5–10 August 2012.) Gradstein, F.M., Ogg, J.G., Schmitz, M.D., et al., 2012, The Geologic Time Scale 2012. Boston, USA: Elsevier, DOI: 10.1016/B978-0-444-59425-9.00004-4.



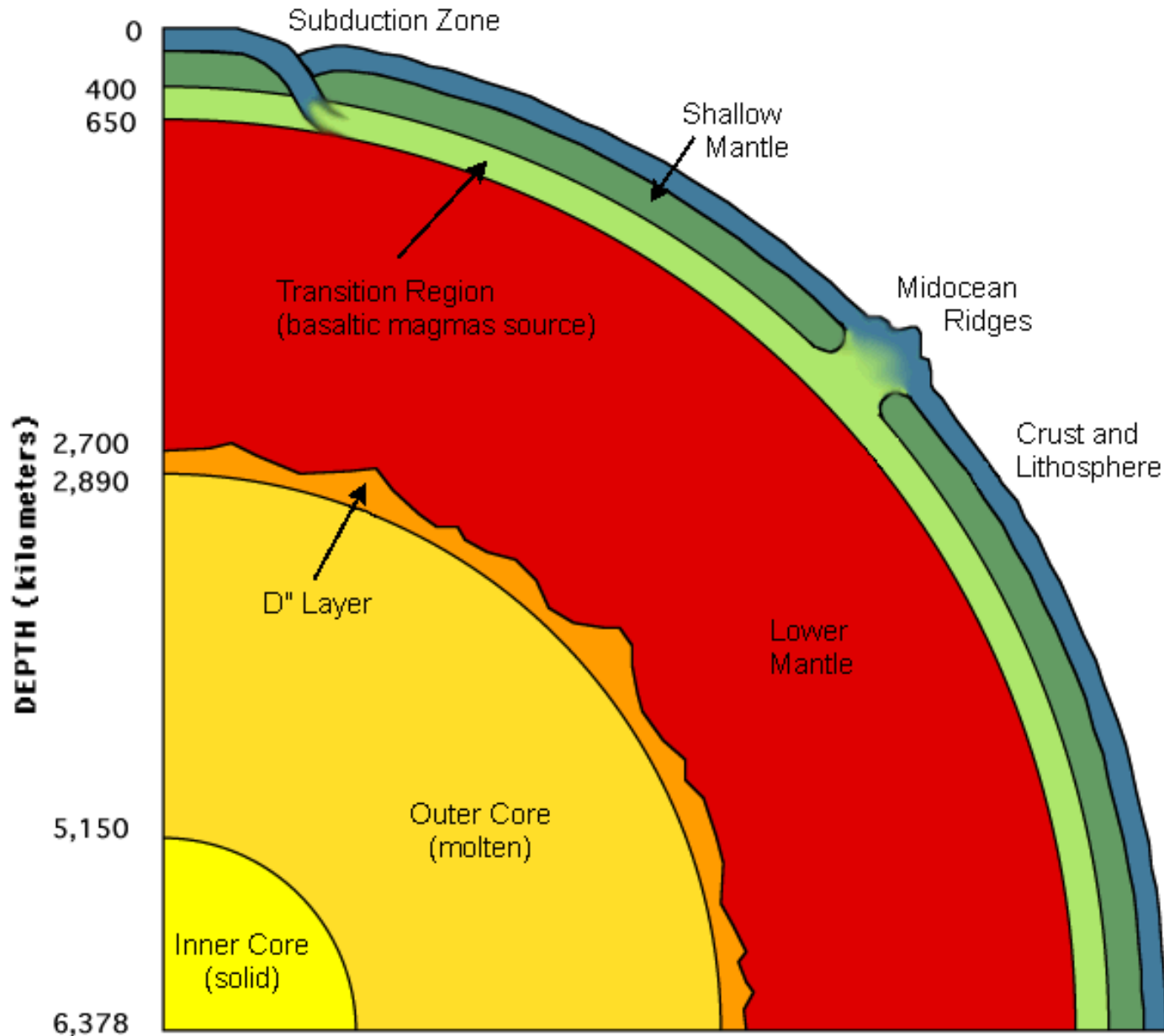
Geologic time – Earth – Mars - Moon



Present-day Earth Interior



Present-day Earth Interior



Present-day Earth Interior – How do we know?

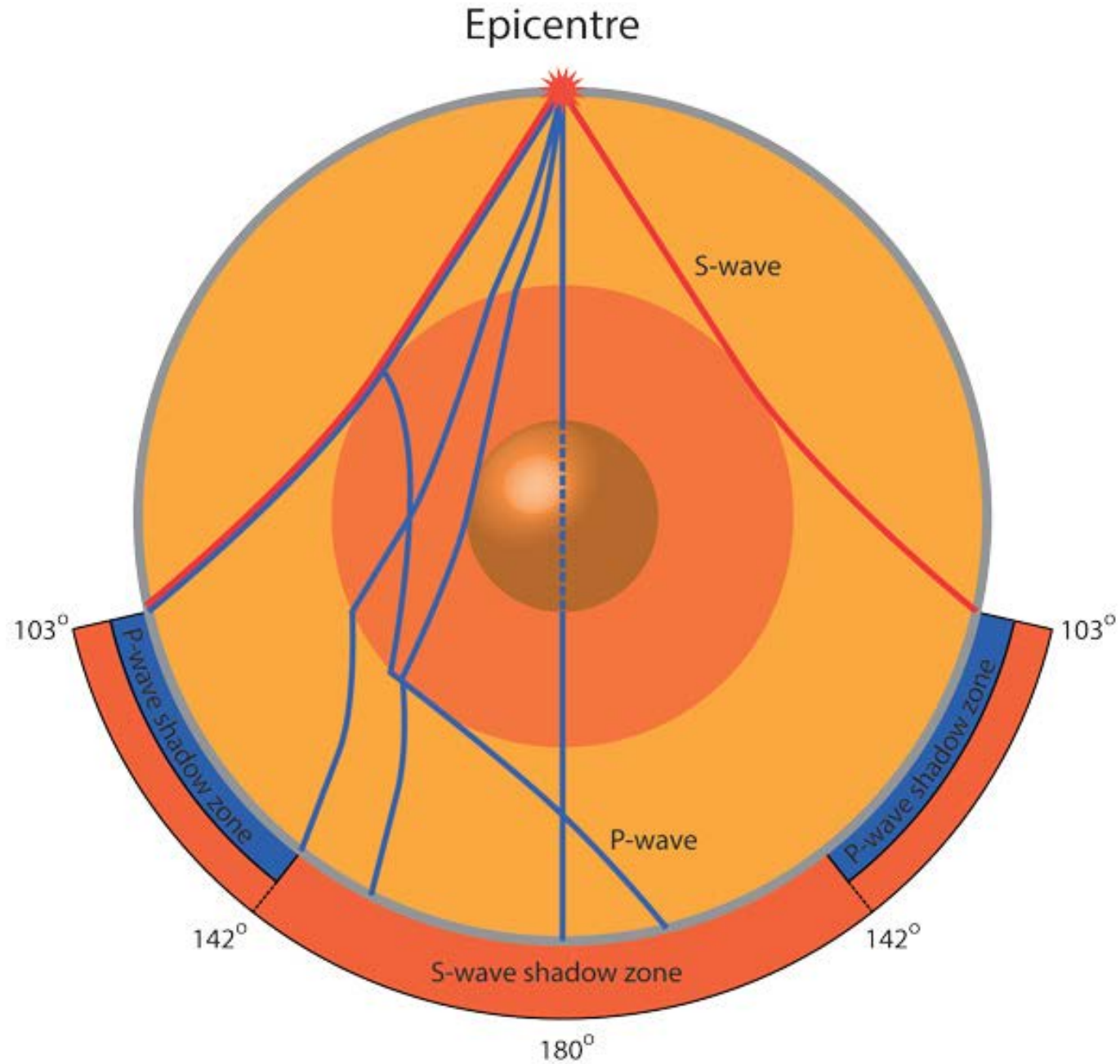
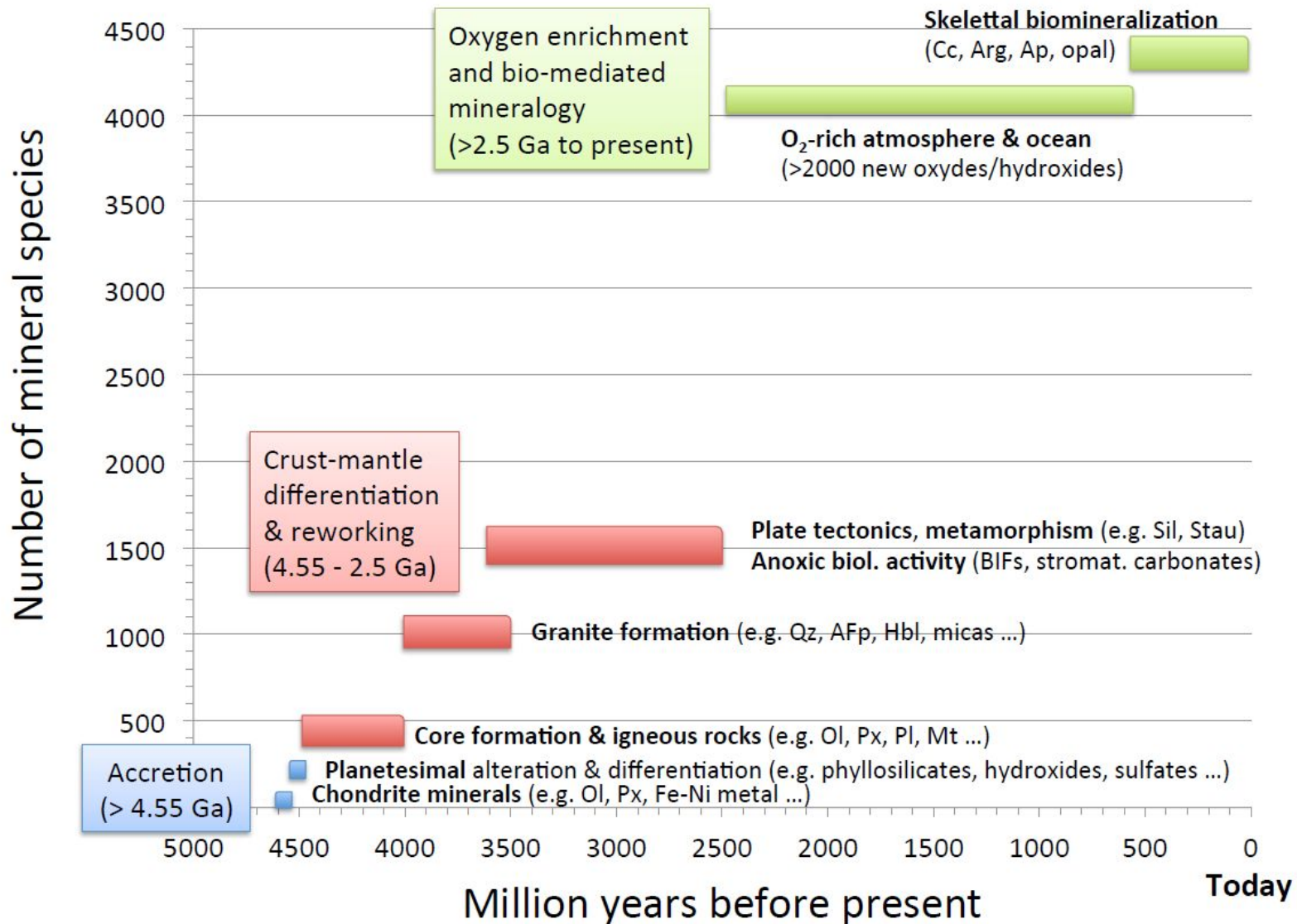


Tabelle 1.5. Häufigkeit wichtiger Minerale und Mineralgruppen in der **Erdkruste** (in Masse-%)

Feldspäte	58.0 %	Silikate 91.5 %
Pyroxene	16.5 %	
Amphibole		
Olivin		
Quarz	12.5 %	
Glimmer (3.5 %) und silikatische Tonminerale	4.5 %	
Eisenoxide	3.5 %	
Calcit	1.5 %	
alle anderen Minerale	3.5 %	
Summe	100 %	

(nach Rösler, 1991, S. 182)

Minerale – How many different?



Source: Hazen et al. (2008)

Minerale - Einteilung

Kristallchemische Gliederung

→ 9 Klassen

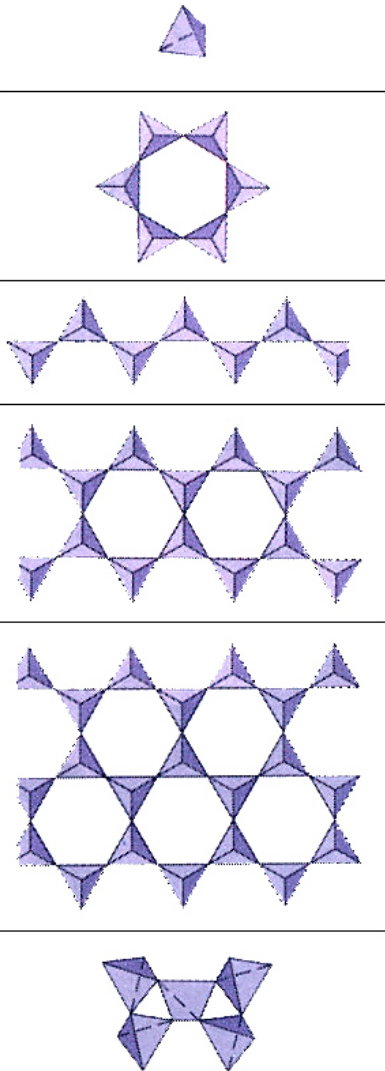
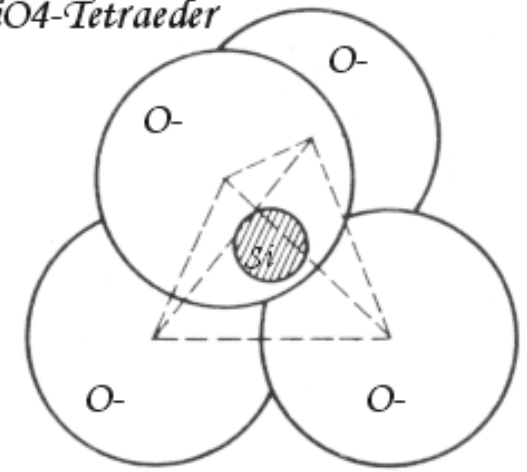
→ Beruht auf der dominierenden Stellung der Anionen

1. **Elemente**
2. **Sulfide**
3. **Halogenide**
4. **Oxide**, Hydroxide
5. Nitrate, **Karbonate**, Borate
6. **Sulfate**, Chromate, Molybdate, Wolframate
7. **Phosphate**, Arsenate, Vanadate
8. **Silikate**
9. Organische Minerale

Silikatstrukturen

Tetraeder-Polymerisation

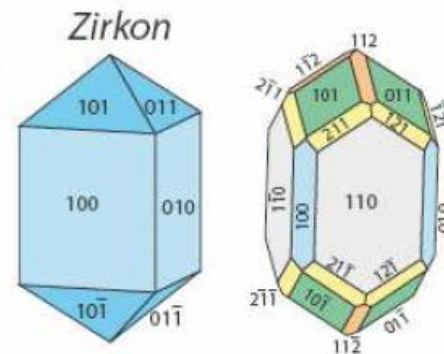
SiO₄-Tetraeder



- Inselsilikate z.B. Olivin
- Gruppensilikate z.B. Epidot
(ohne Grafik)
- Ringsilikate z.B. Beryll
- Kettensilikate z.B. Pyroxene (Augit)
- Bandsilikate z.B. Amphibole (Hornblende)
- Schichtsilikate z.B. Glimmer, Tonminerale
- Gerüstsilikate z.B. **Feldspäte**, Quarz*

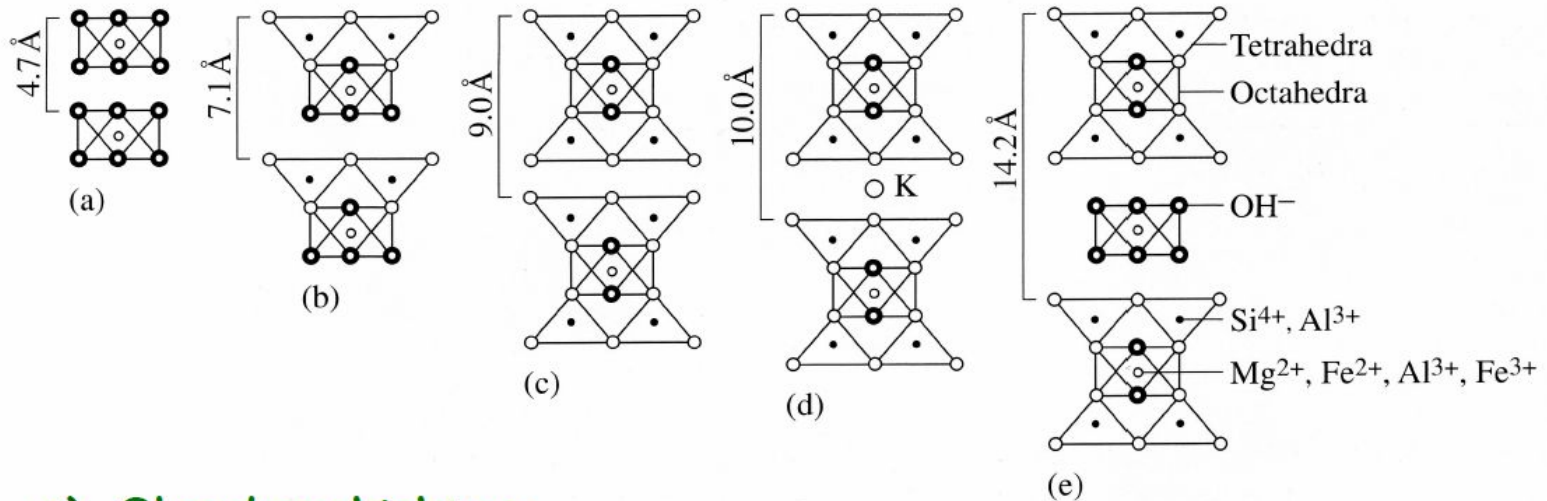
Insel silikate: Zirkon

Zirkon	ZrSiO_4
Kristallsystem:	tetragonal (Klasse 4/mmm)
Ausbildung:	Kristalle von prismatischem bis pyramidalem Habitus
Bruch:	eine unvollkommene Spaltbarkeit
Härte:	$7\frac{1}{2}$
Kristalle:	gut ausgebildete Kristallflächen selten; fast immer eingewachsen; sekundär in abgerollten Körnern
Glanz:	nichtmetallischer hoher Glanz
Farbe:	grau, braun, braunrot, seltener gelb, grün oder farblos
Vorkommen:	magmatisch und metamorph; sekundär in Sedimenten (wichti-



Schichtsilikate

Einteilung: Oktaeder-/Tetraederschichten



a) Oktaederschichten:

Brucitschicht $\text{Mg}(\text{OH})_2$ bzw. Gibbsschicht $\text{Al}(\text{OH})_3$

b) Zweischichtsilikat, z.B. Serpentin $\text{Mg}_3[\text{Si}_2\text{O}_5(\text{OH})_4]$









c) Dreischichtsilikat, z.B. Talk $\text{Mg}_3[\text{Si}_4\text{O}_{10}(\text{OH})_2]$

d) Glimmer (große Kationen zwischen den Schichten)

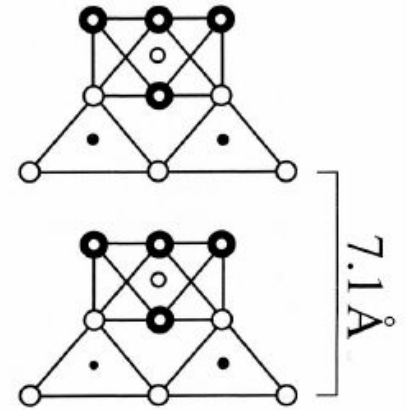
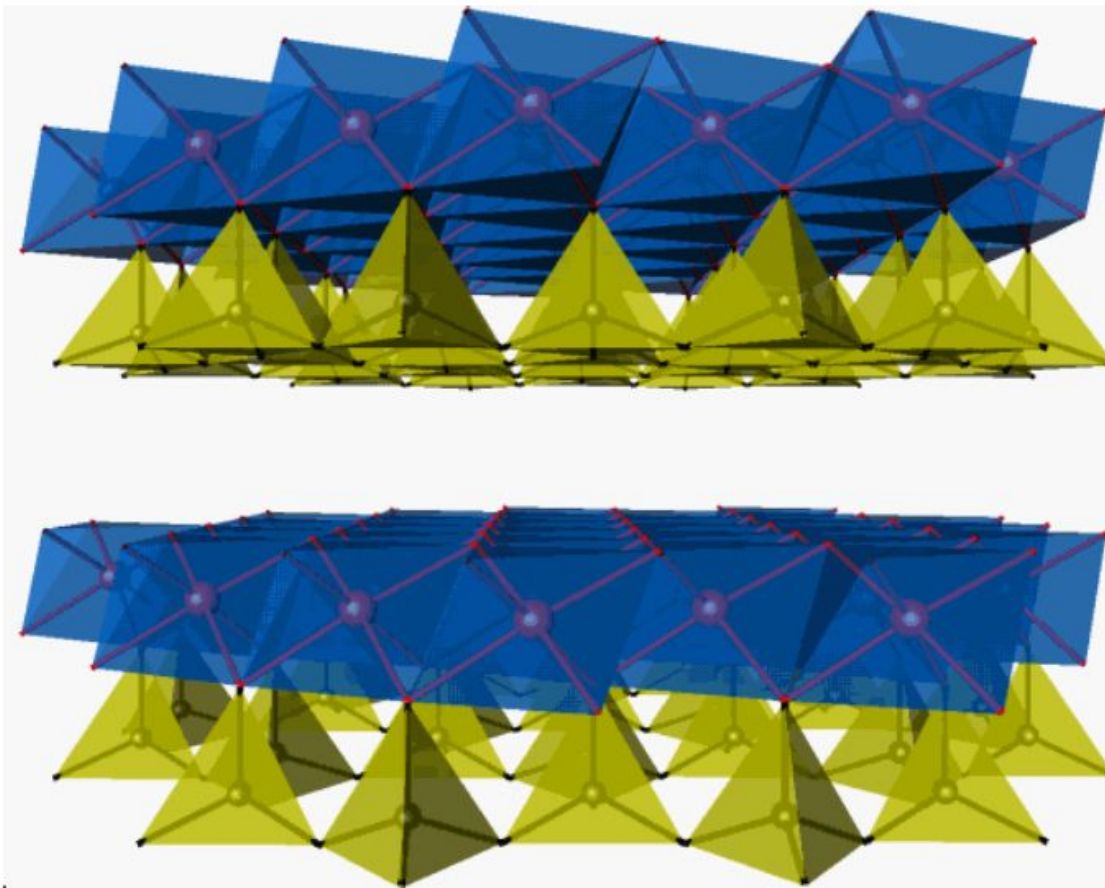
e) Chlorit (Vierschichtsilikat aus Talk-ähnlicher Schicht (TOT) und Brucit-ähnlicher Zwischenschicht)

Schichtsilikate

Systematik der Schichtsilikate

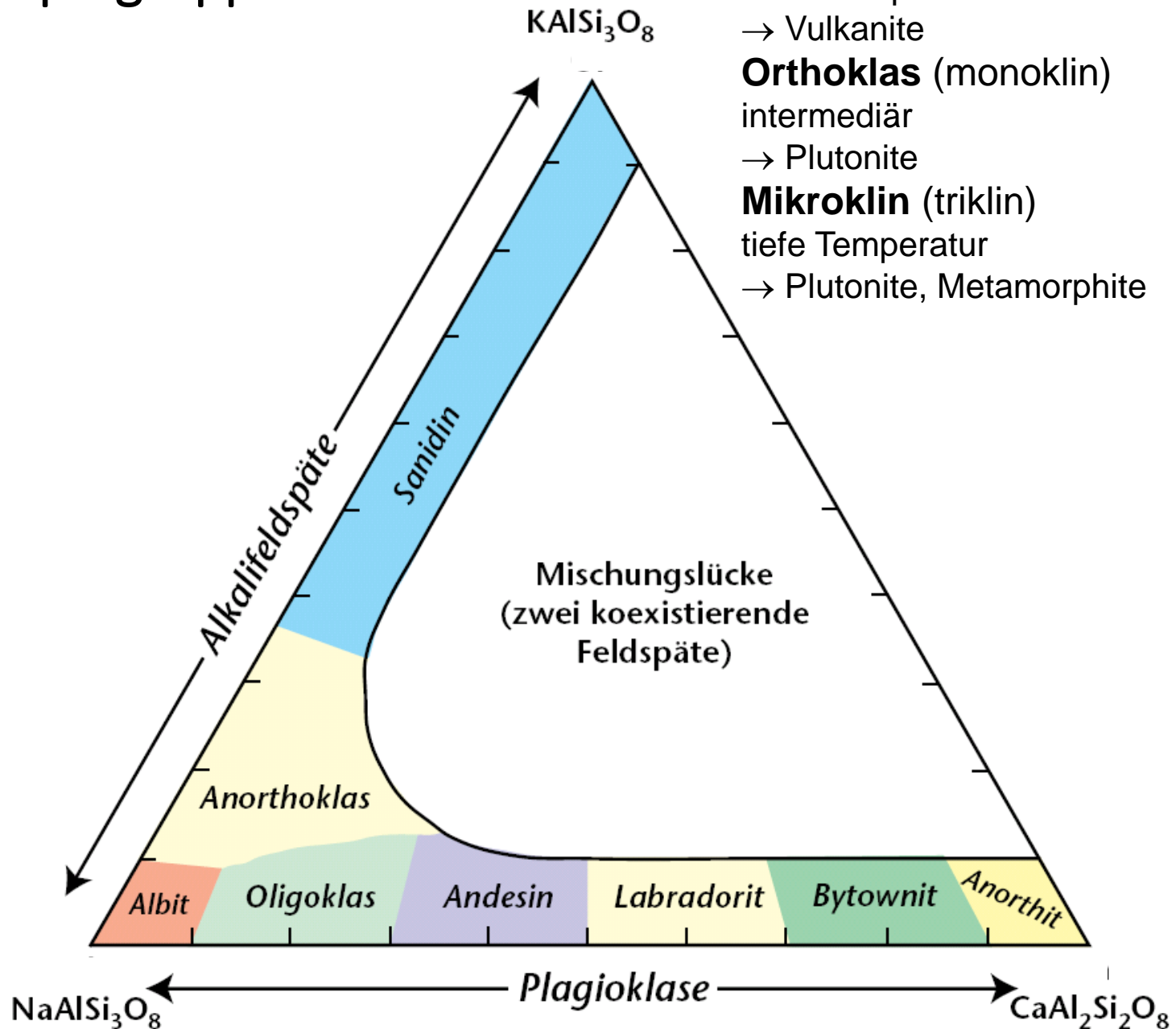
				trioktaedrisch	dioktaedrisch	
Serpentin, Kaolin	2-schichtsilikat		T	7 Å	Si_2O_5	Si_2O_5
			O		$\text{Mg}_3(\text{OH})_4$	$\text{Al}_2(\text{OH})_4$
Talk	3-schichtsilikat		T	9 Å	Si_2O_5	
			O		$\text{Mg}_3(\text{OH})_2$	
„Tonminerale“ z.B. Montmorillonit, Nontronit, Vermiculit			T	C ₀	Si_2O_5	
			T			
Biotit, Muskovit	3-schichtsilikat		T	10 Å	$\text{Al}_{0,5}\text{Si}_{1,5}\text{O}_5$	$\text{Al}_{0,5}\text{Si}_{1,5}\text{O}_5$
			O		$\text{Mg}_3(\text{OH})_2$	K
			T	C ₀	$\text{Al}_{0,5}\text{Si}_{1,5}\text{O}_5$	$\text{Al}_{0,5}\text{Si}_{1,5}\text{O}_5$
			T			
Chlorit	4-schichtsilikat		T	14 Å	Si_2O_5	
			O		$\text{Mg}_3(\text{OH})_2$	
			T	C ₀	Si_2O_5	
			O			$\text{Mg}_3(\text{OH})_6$
			O		Chlorit	

Serpentin $Mg_3[Si_2O_5(OH)_4]$



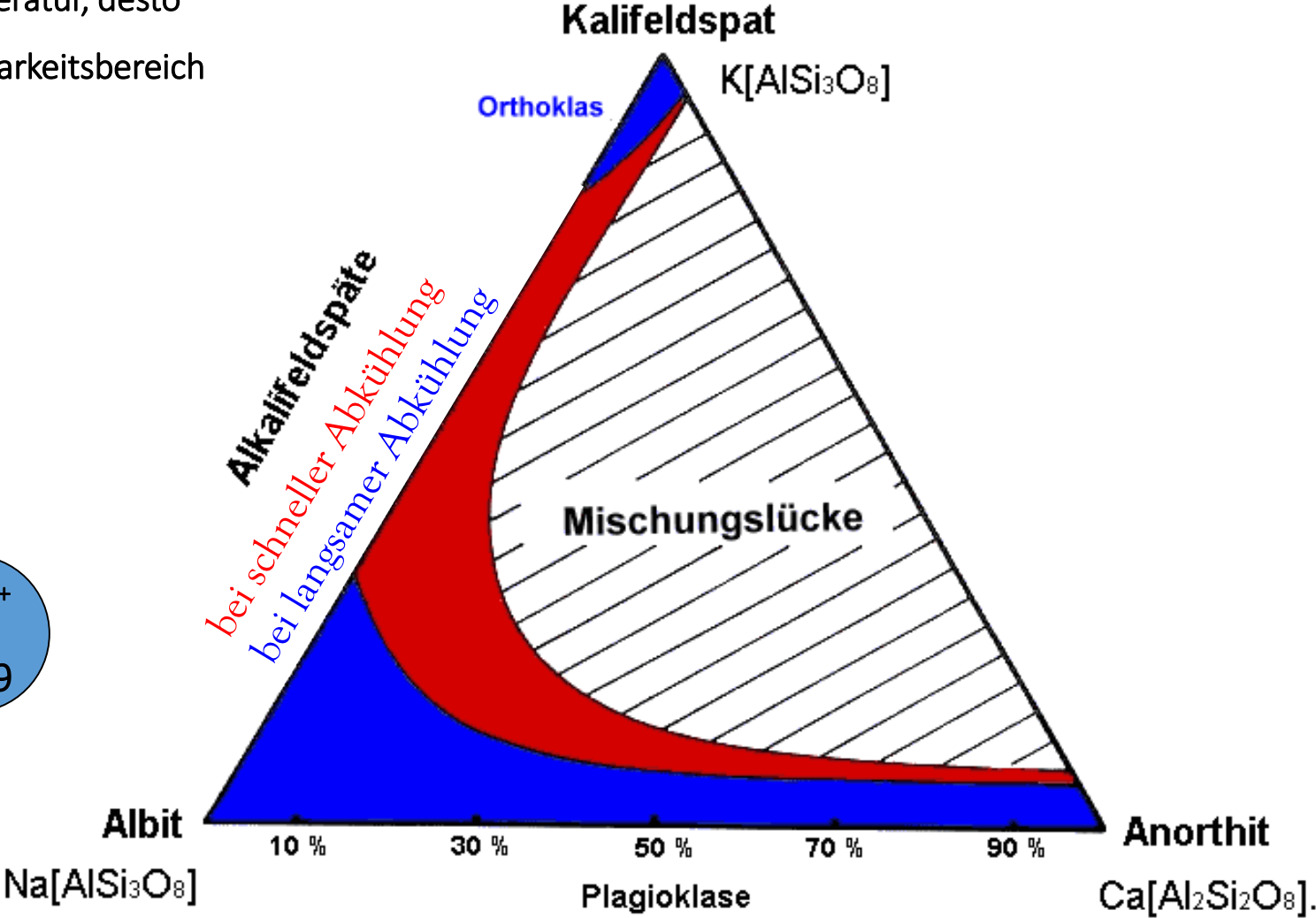
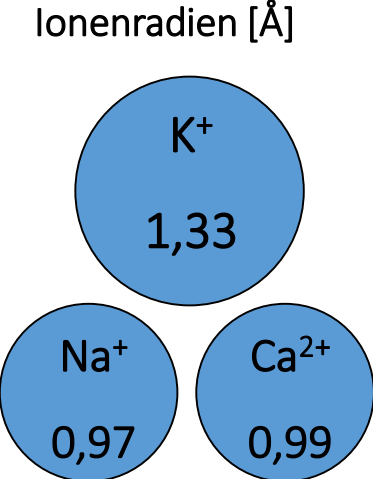
2-Schicht-Silikat

Feldspatgruppe



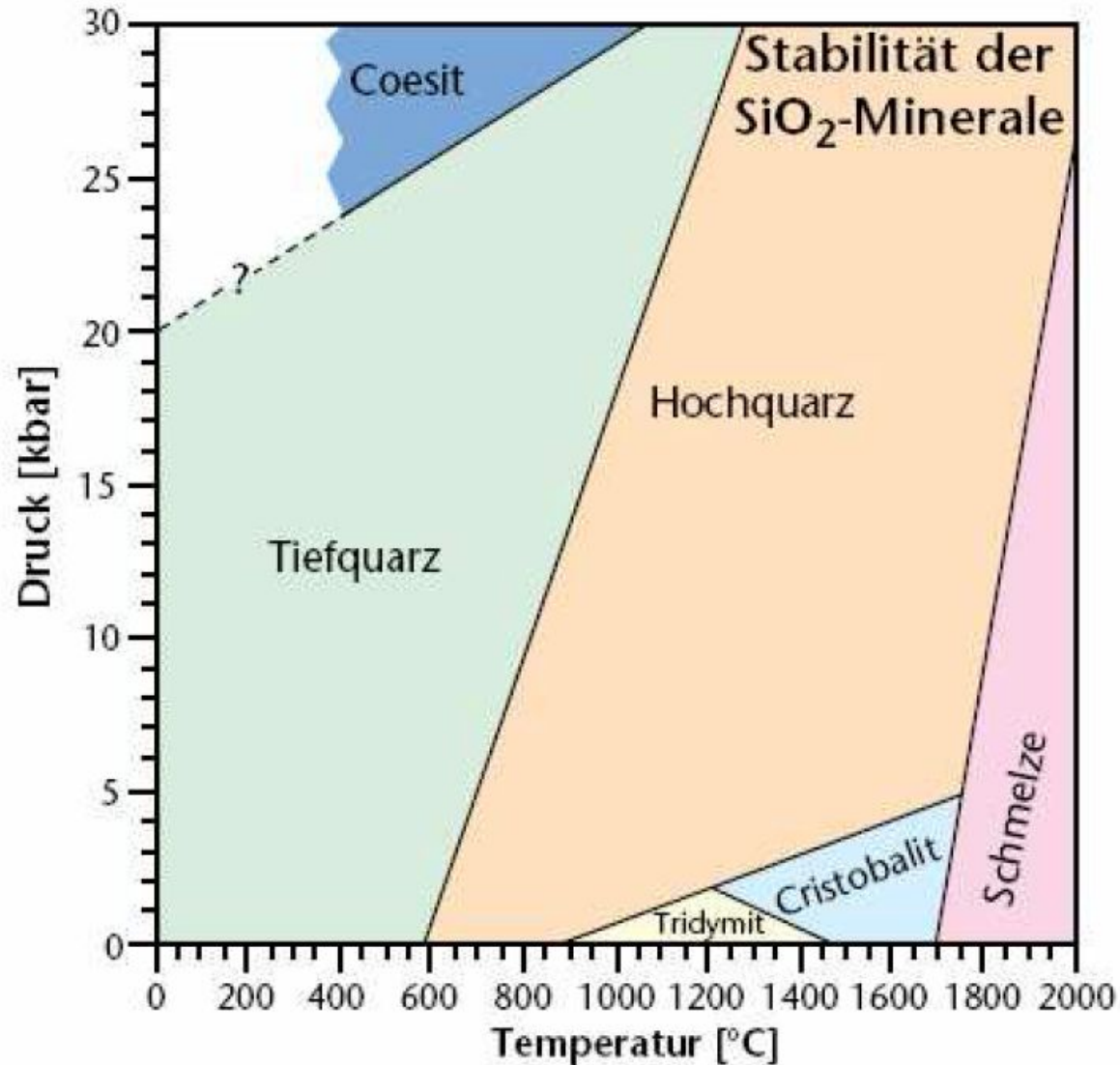
Einfluss der Temperatur auf die Mischbarkeit von Feldspäten

Je höher die Temperatur, desto größer der Mischbarkeitsbereich



Die Prozentangaben in der Plagioklasreihe beziehen sich auf den Anorthitgehalt.

Stabilitätsfelder der SiO_2 - Modifikationen



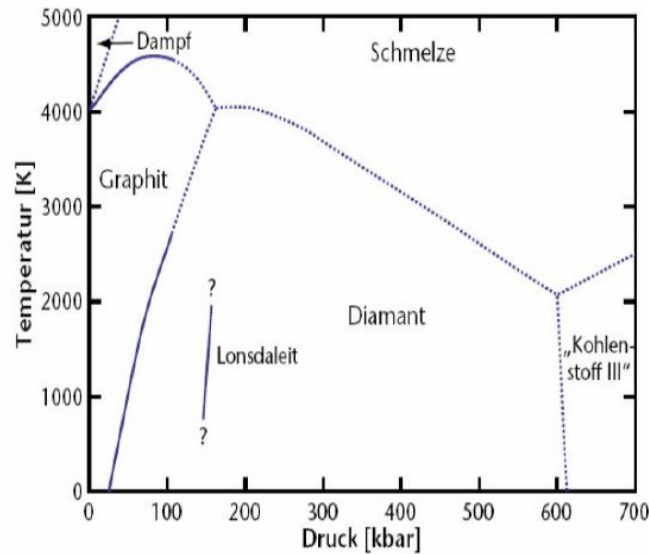
Kohlenstoff C

→ Polymorph: Als Polymorphie bezeichnet man das Vorkommen eines Elementes oder einer Verbindung in zwei oder auch mehreren kristallinen Phasen (Modifikationen)

Graphit ↔ Diamant



<http://de.wikipedia.org/wiki/Graphit>



<http://de.wikipedia.org/wiki/Diamant>

Gesteine - Rocks

- 3 major types:

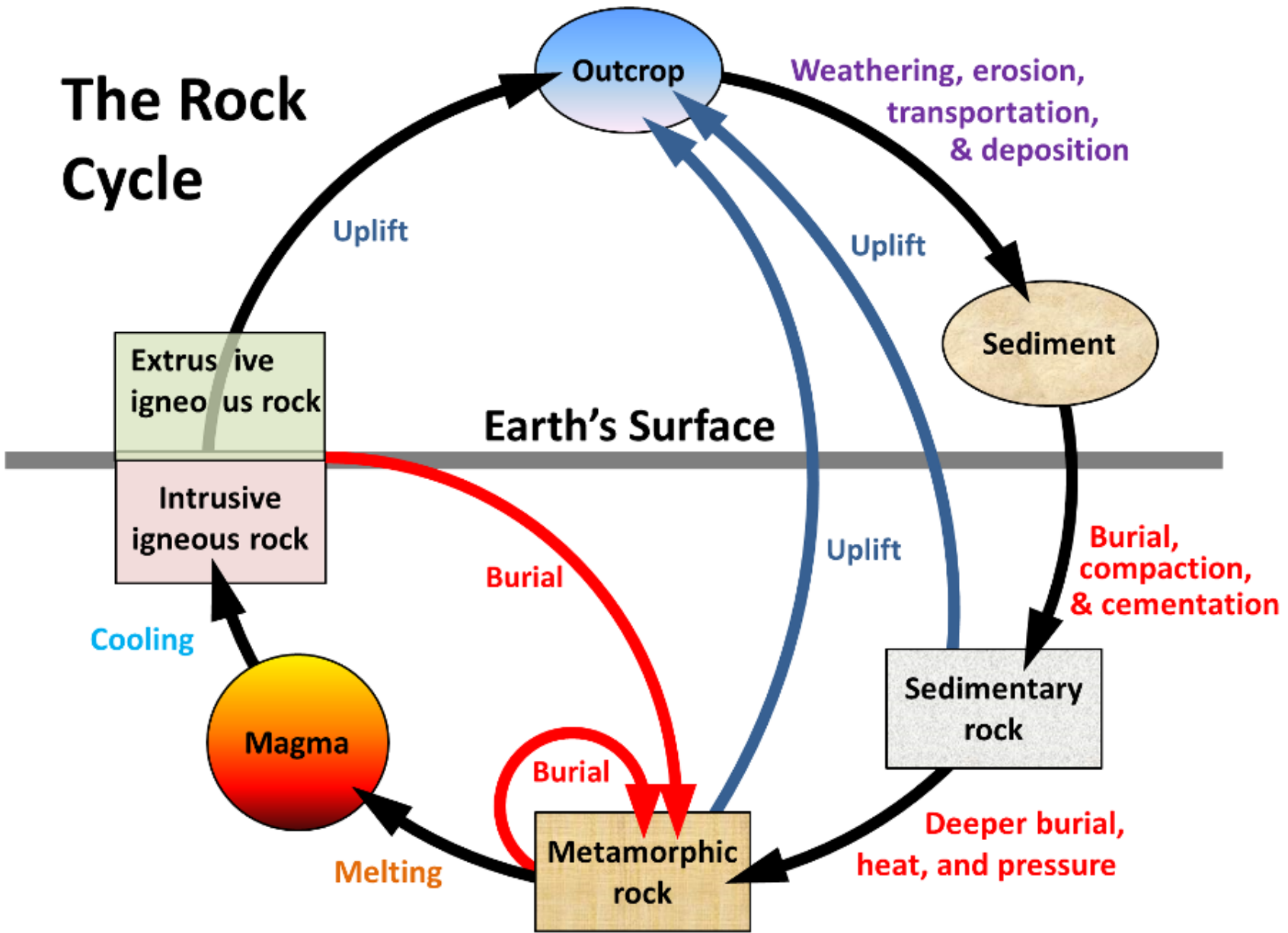
- 1) igneous rocks

- 2) sedimentary

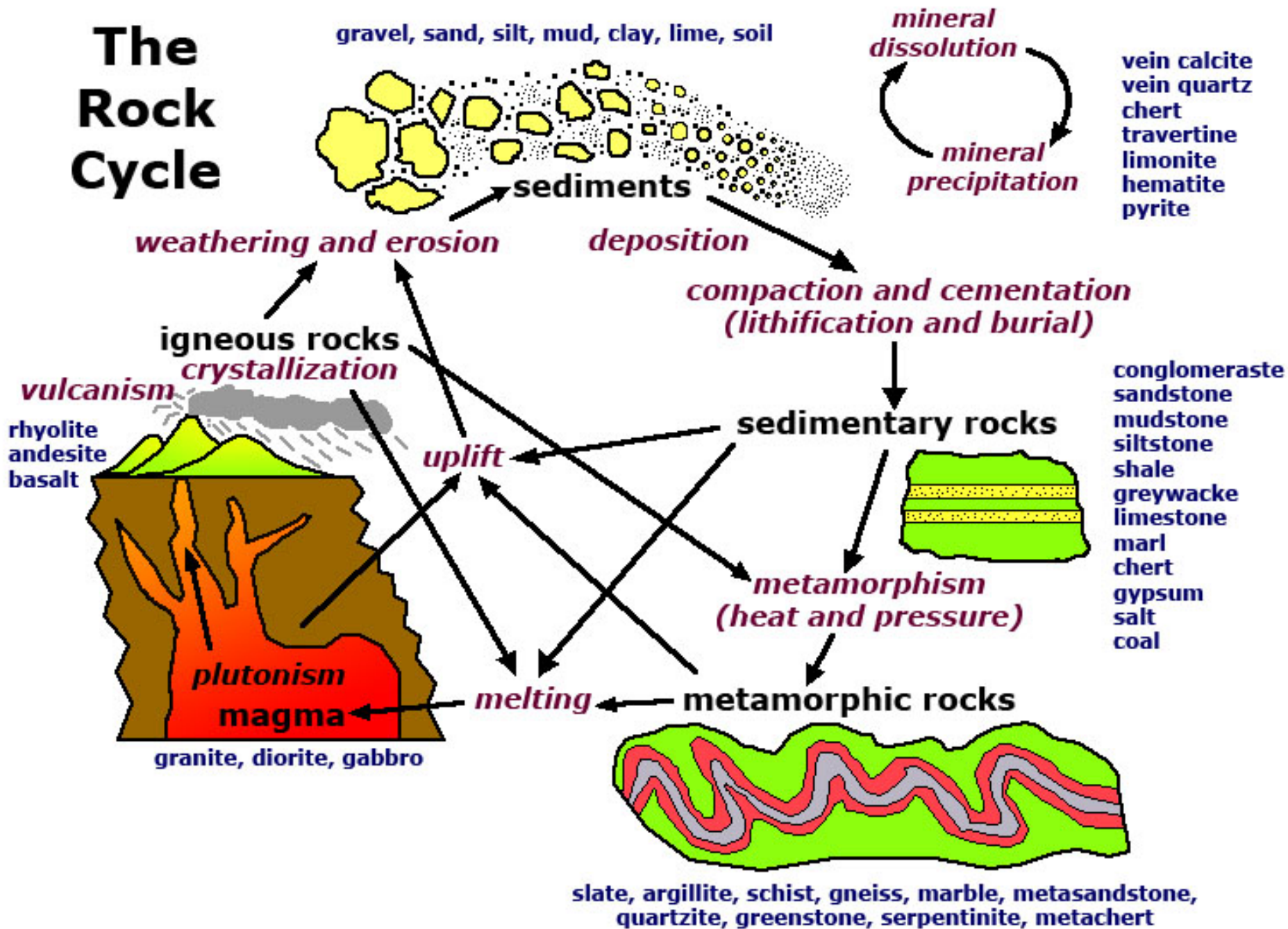
- 3) metamorphic rocks

→ Geological rock cycle

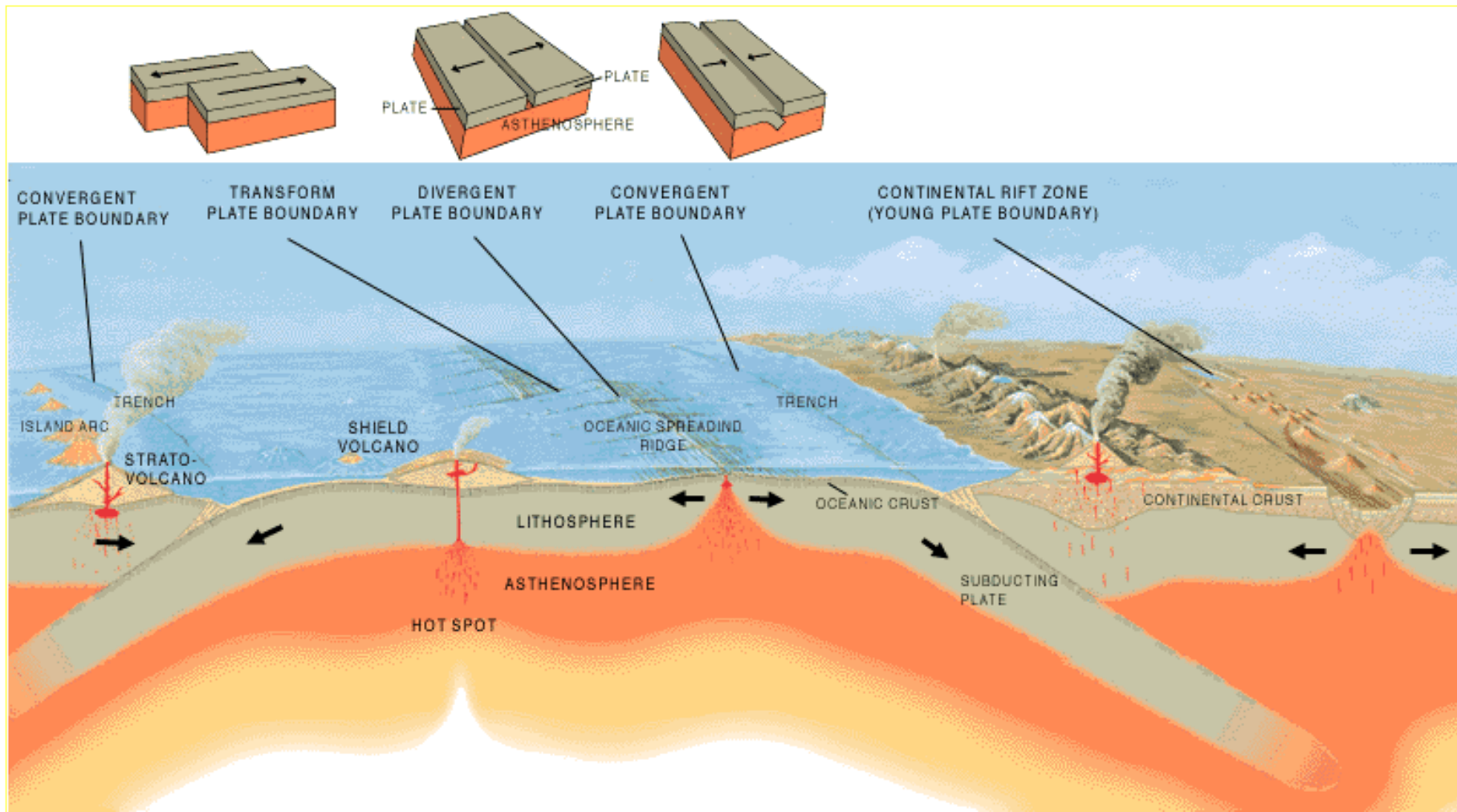
The Rock Cycle



The Rock Cycle



Volcanoes and tectonics



The lithosphere slides over the asthenosphere which is weakened due to it being near its solidus. The asthenosphere, though solid, flows by convection

Plate tectonics and magma composition

1. Divergent margins: Decompression melting

-> low volatile abundance, low SiO₂ (~50%), low viscosity basaltic magmas (e.g. Krafla, Iceland)

2. Convergent margins: Addition of volatiles

Melting of the mantle wedge below the continental crust, magmas commonly differentiate during their rise through the thicker and chemically distinct continental crust. High volatile abundance, intermediate SiO₂ (60-70%), high viscosity andesites and dacites (e.g. Montserrat, West Indies)

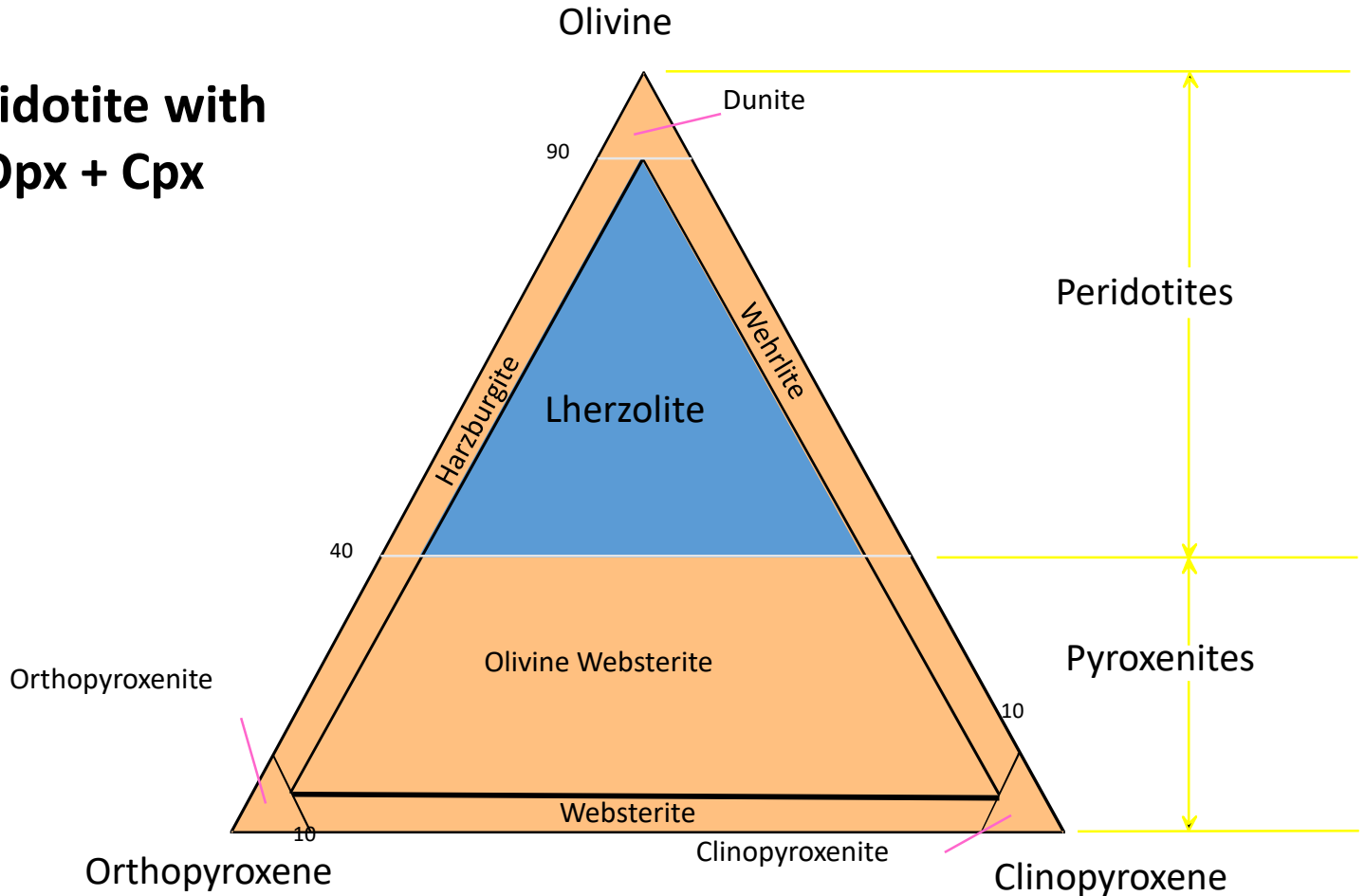
3. Intraplate `Hot-spot` settings: Temperature increase

A. Oceanic: Mantle plumes melt thin oceanic crust producing low viscosity basaltic magmas (e.g. Kilauea, Hawaii)

B. Continental: Mantle plumes melt thicker, silicic continental crust producing highly silicic (>70% SiO₂) rhyolites (e.g. Yellowstone, USA)

The Earth's mantle is a lherzolite

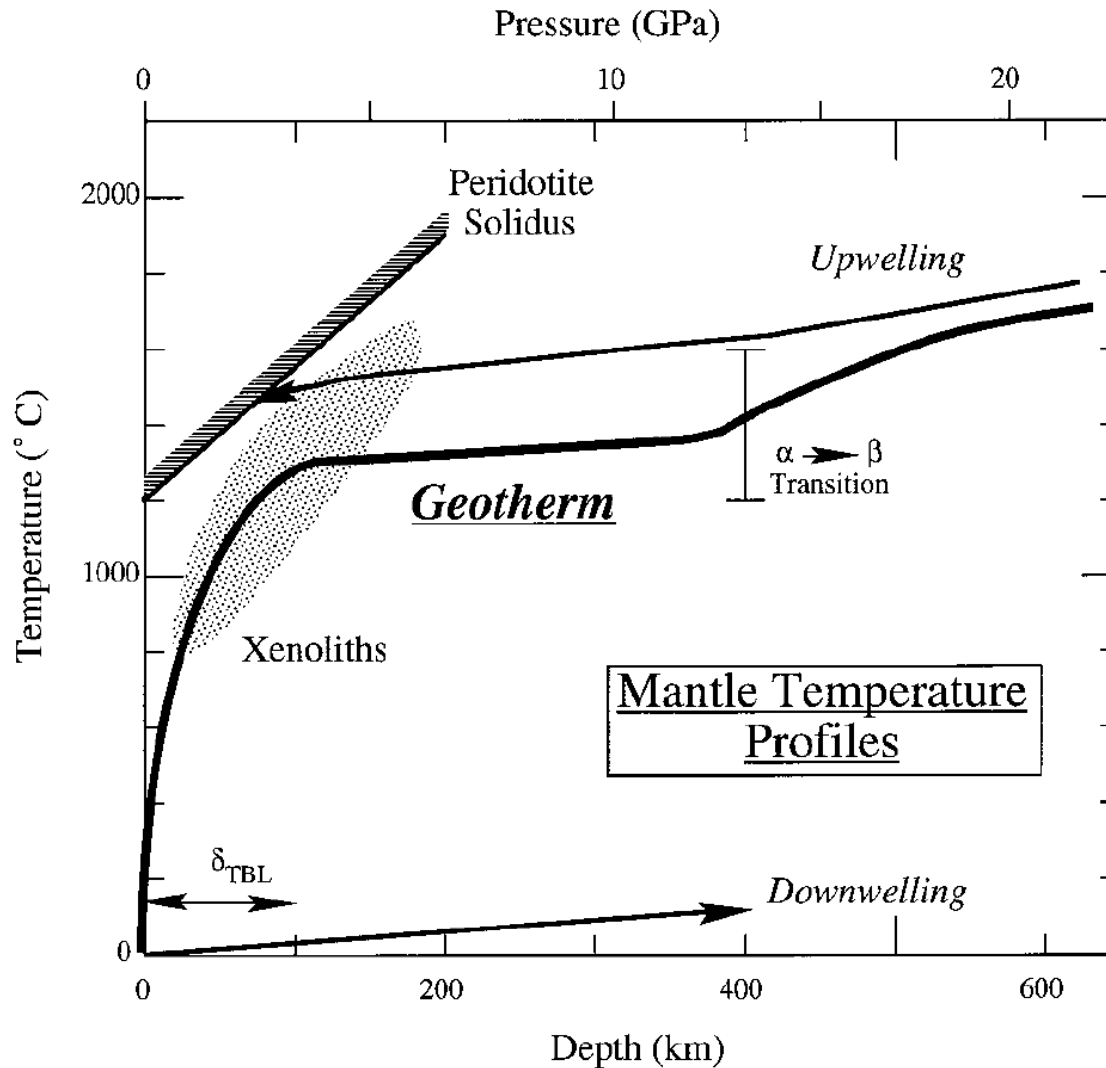
A type of peridotite with
Olivine > Opx + Cpx



Conductivity

The lithosphere cools conductively

The asthenosphere is very near to the solidus



1. Melting by temperature increase

Impact melting

- meteorite

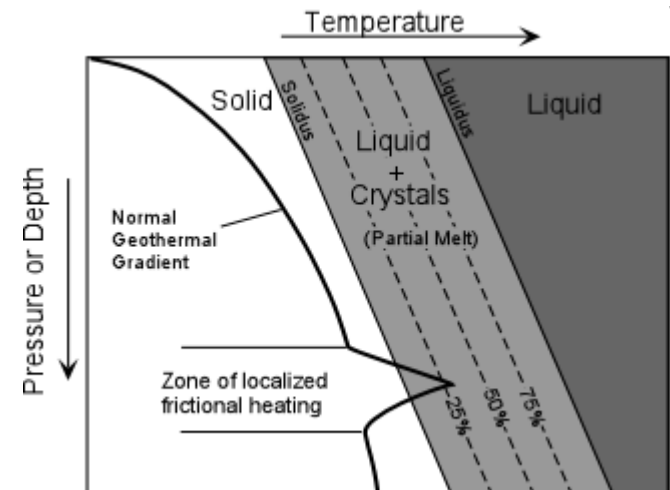
Radioactive heat generation

- planetary formation

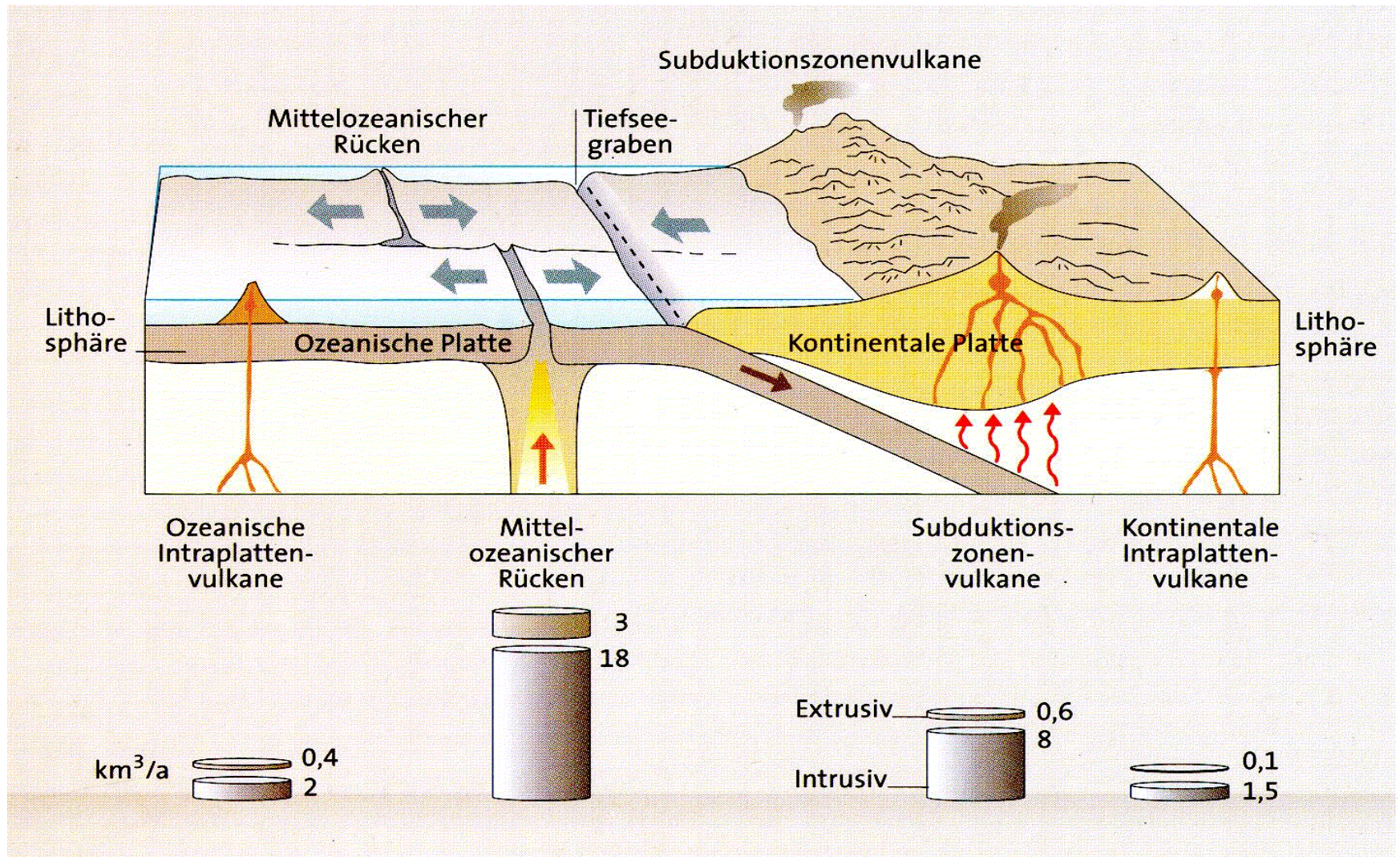
Conduction

- dyke/sill intrusion
- migmatism
- partial melting

Frictional heating and viscous dissipation

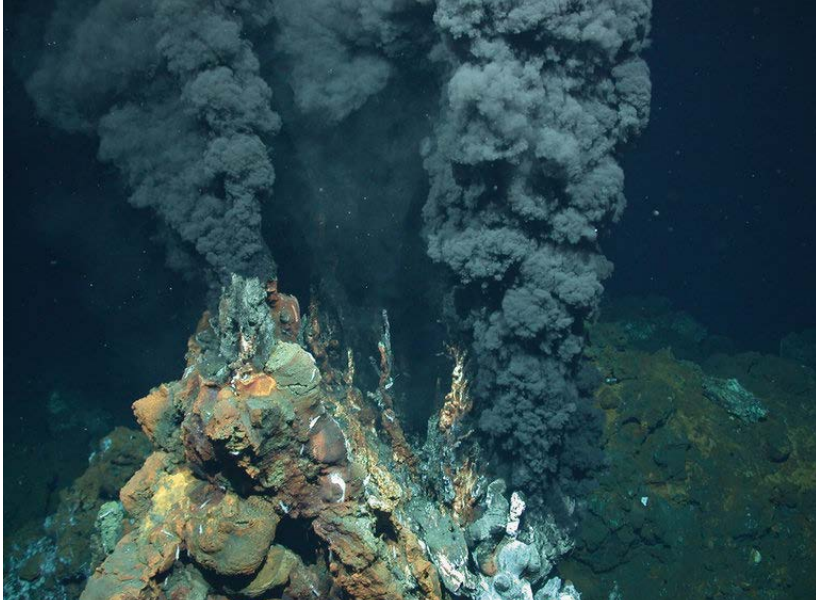


2. Melting by decompression

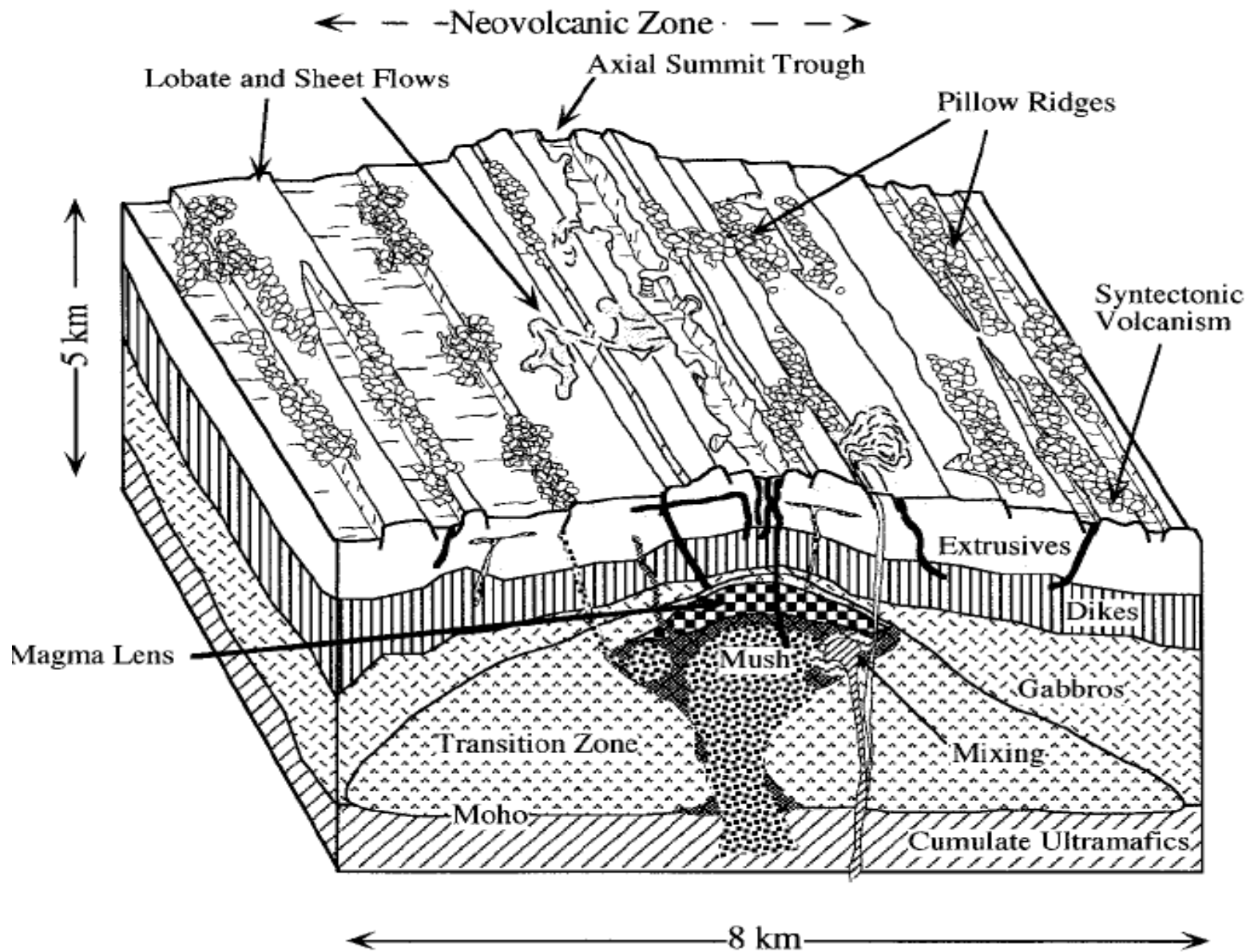


Melting by decompression prevails at Mid Ocean Ridges

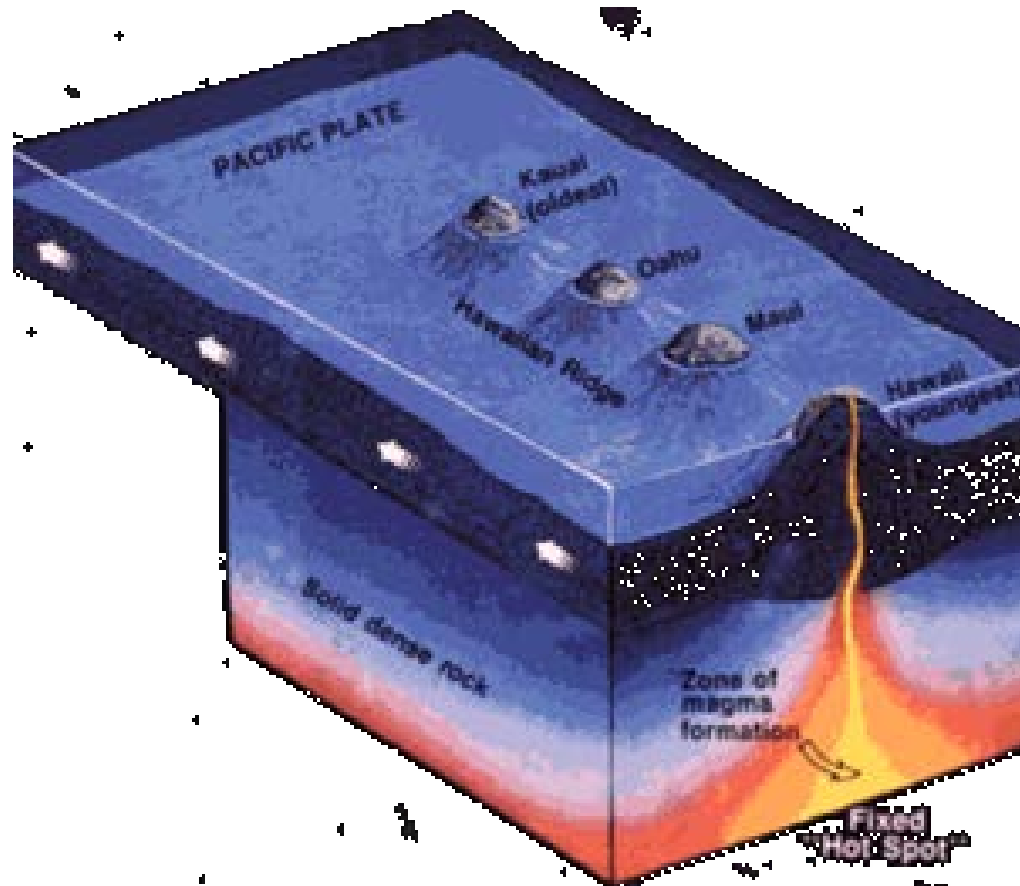
Mid Ocean Ridges



MOR



Melting at hotspots



Melting occurs as P-T profile across the plume intersects the solidus
(*c.f.*, as for the convecting mantle)

Intraplate magmatism

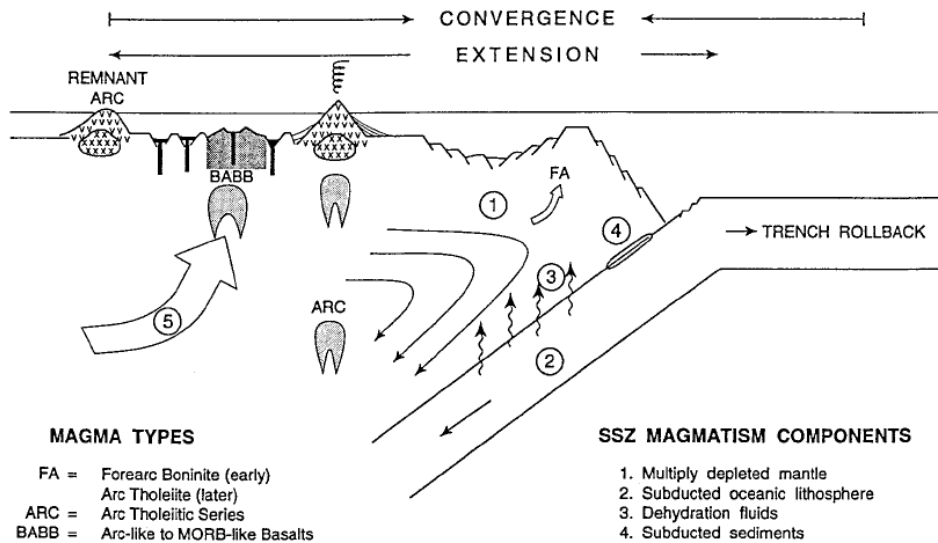


Plumes or Hotspots correlate with Geoid highs (*i.e.*, rise in the gravitational potential surface)

They may originate from the D'' layer at the CMB or U/LMB

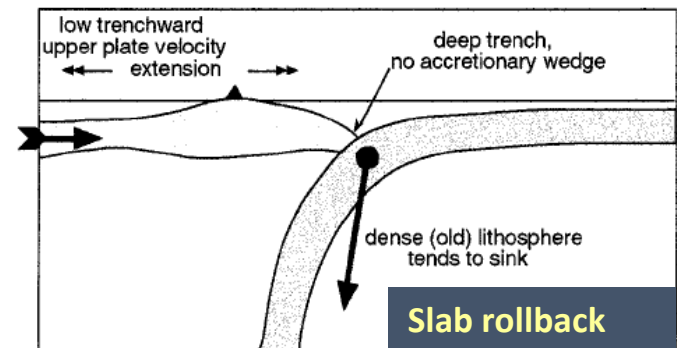
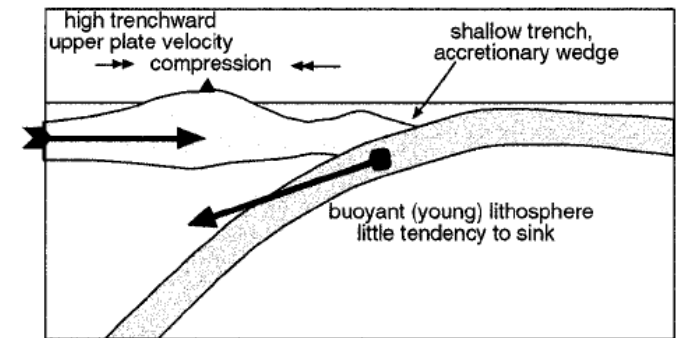
Hotspots are much 'hotter'?!? than the surrounding mantle: the generation of melt is accordingly high

3) Melting by chemical changes

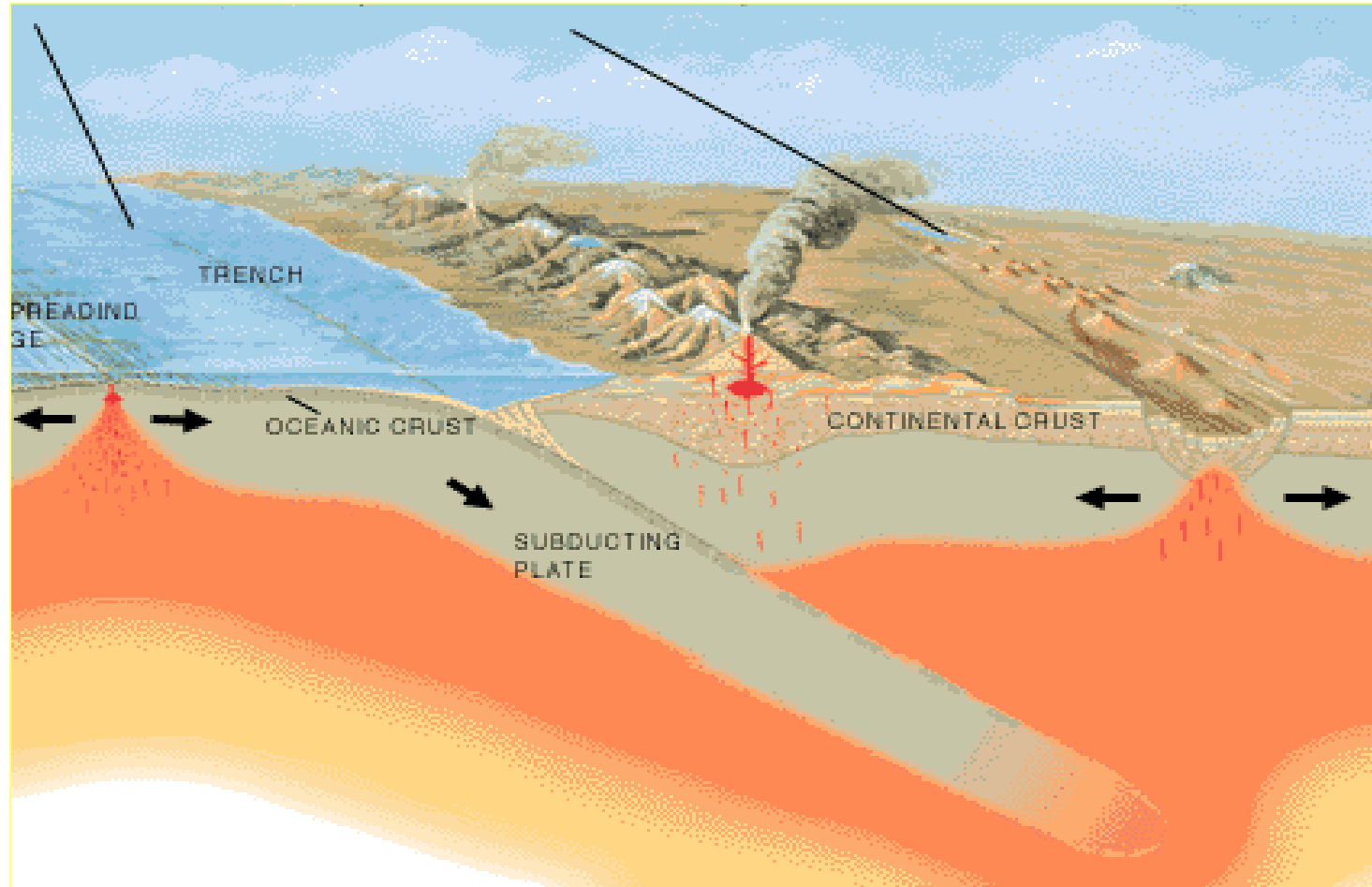


- Are volcanic arcs in compression or extension?

- Volcanic arcs parallel the trench
- Segmentation of the arc due to structure in the upper plate:
 - Ridge (NVZ)
 - Windows (CVZ)
 - Flat subduction (SVZ) – may produce adakite
 - Lateral motion (W Aleutian)



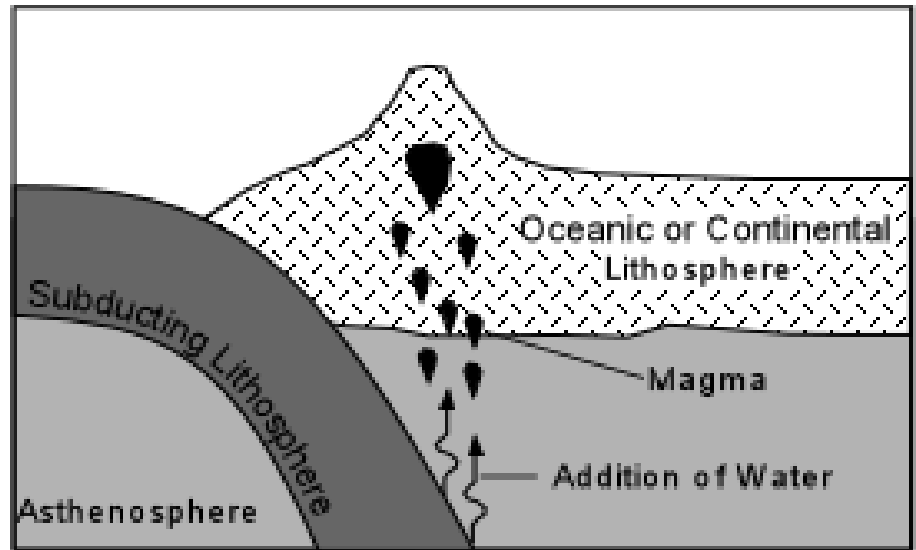
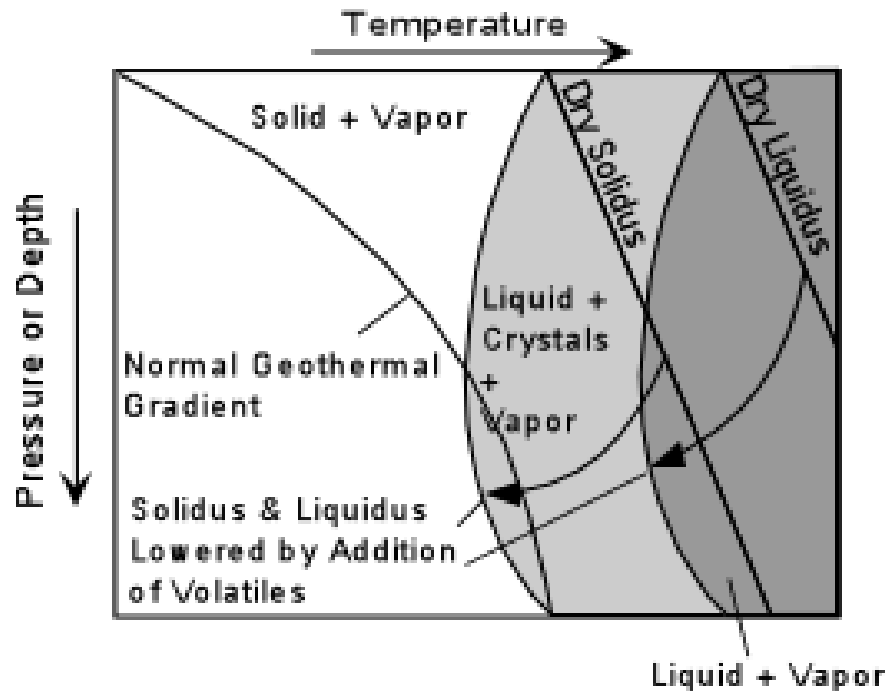
3) Melting by chemical changes



- Are volcanism
- Liberation of water via dehydration reactions of minerals in the subducted plate
- Addition of water to the plate above – which partially melts.

3) Melting by chemical changes

Water in the melt decreases the viscosity and may favor diapirism.

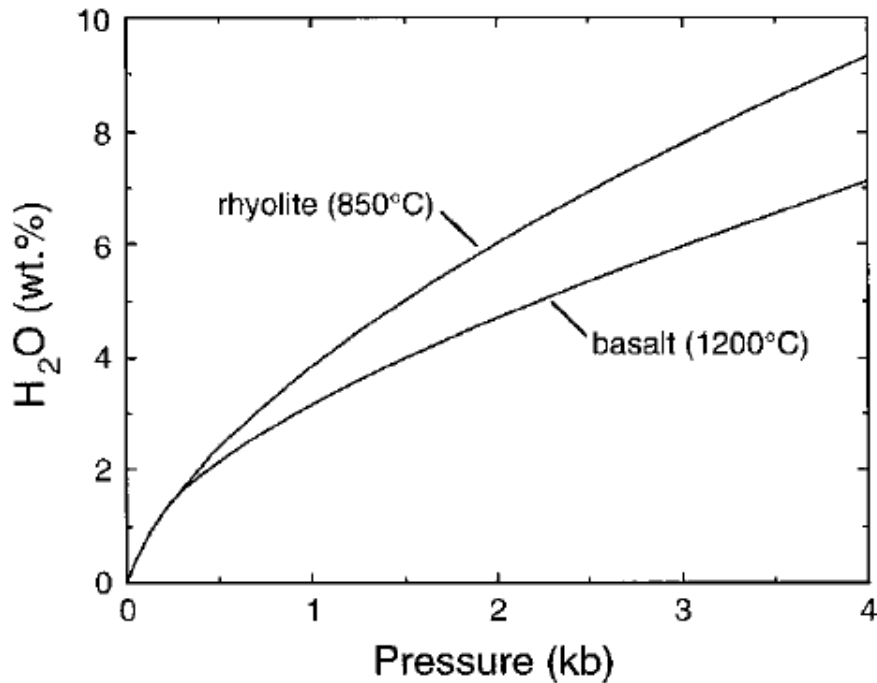


Solubility of Volatiles in Magmas

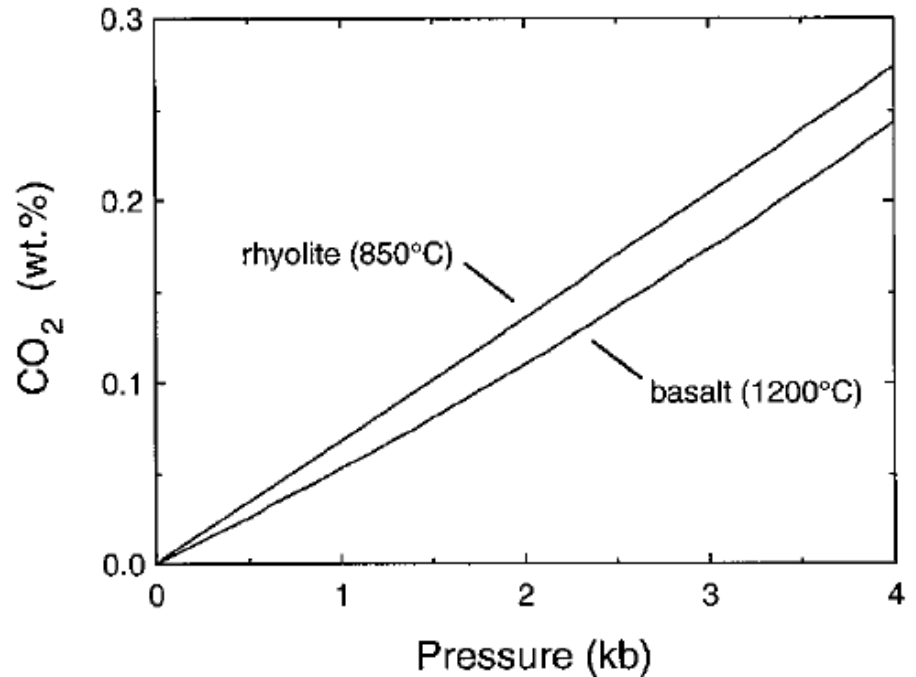
Solubility: max. amount of volatiles that can dissolve under given P, T, X

→ H₂O is 50-100 x more soluble than CO₂ !!

Water solubility in silicate melts

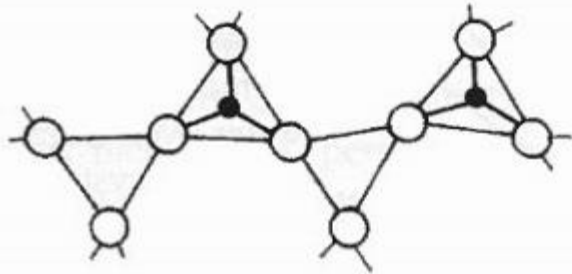


Carbon dioxide solubility in silicate melts



Effect of Water: Depolymerization of Silicate Melts

Si-O polymer in
anhydrous melt

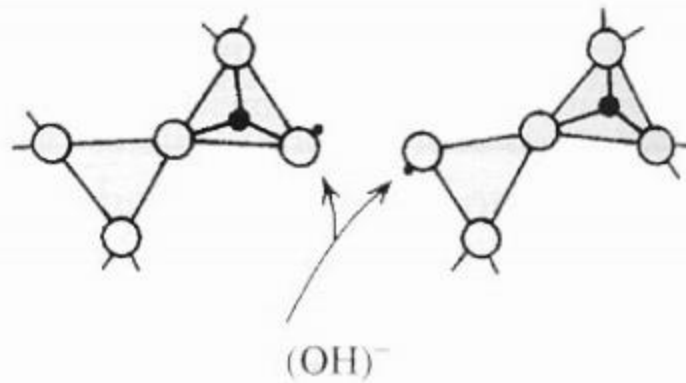


+

Water
molecule

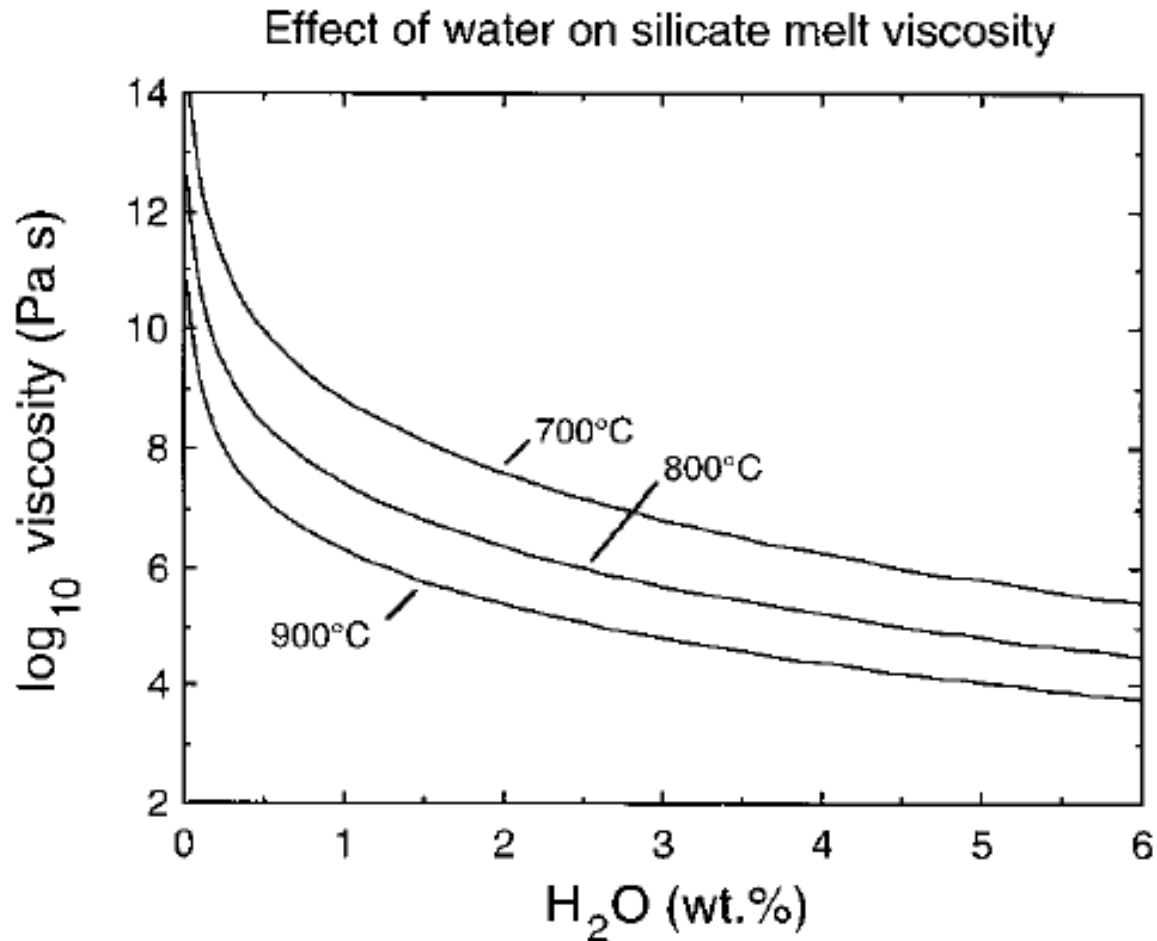


Broken Si-O polymer
in hydrous melt



Viscosity: effects of water

- As magma ascents, it loses water (to bubbles) and becomes more viscous
- Decrease the activation energy and the Si-O bonds



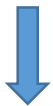
Why study volatile species?

→ Play a fundamental role in forcing magma to ascend, and erupt

For example:
typical percentage by
mass might be 0.1%



equivalent to 90%
bubbles in magma!



Volume increase !!

Exsolved volatile species

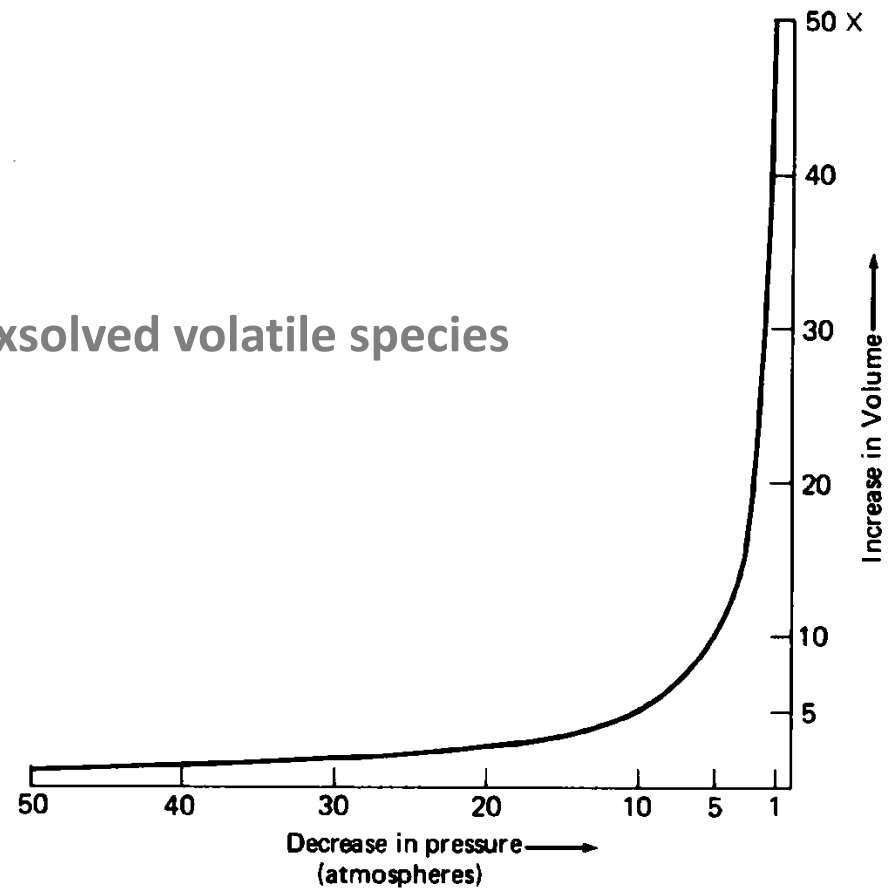
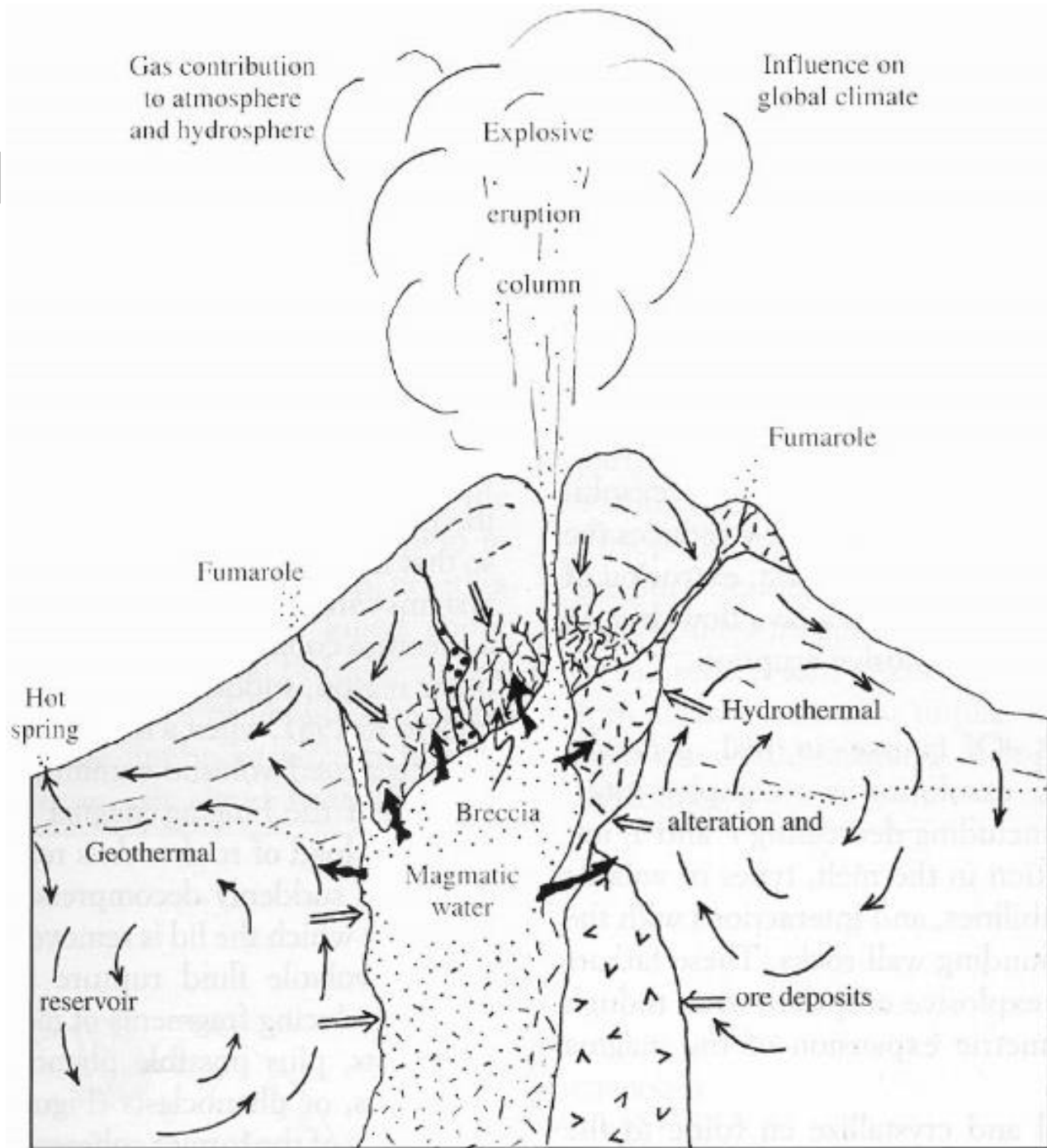
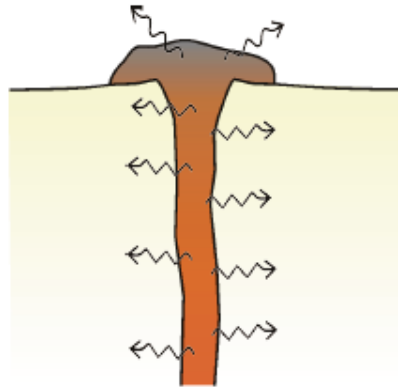


Figure 3.4. Graph showing the approximate volume of volcanic gases at a constant high temperature and varying pressure. For each 10 meters of depth below sea level, or about 4 meters of depth below ground level, pressure increases by 1 atmosphere. For example, volcanic gas bubbles in magma at a depth of 36 meters below ground surface (10 atmospheres) would expand approximately 10 times in volume as they approach the surface (1 atmosphere).

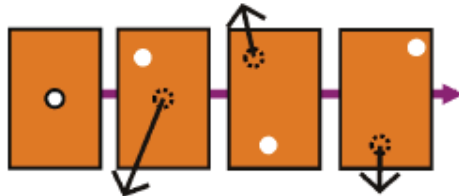
Volatiles and Eruptions



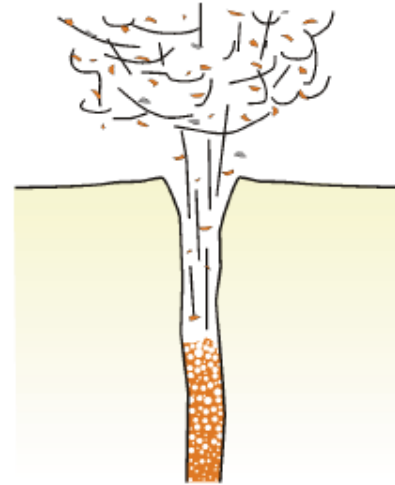
Volatiles influence eruptive style



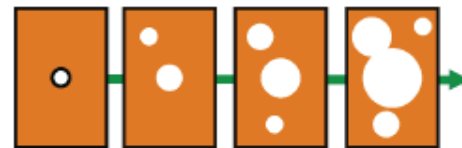
Open-system
degassing



- gas is removed from the system as it is exsolved from the melt

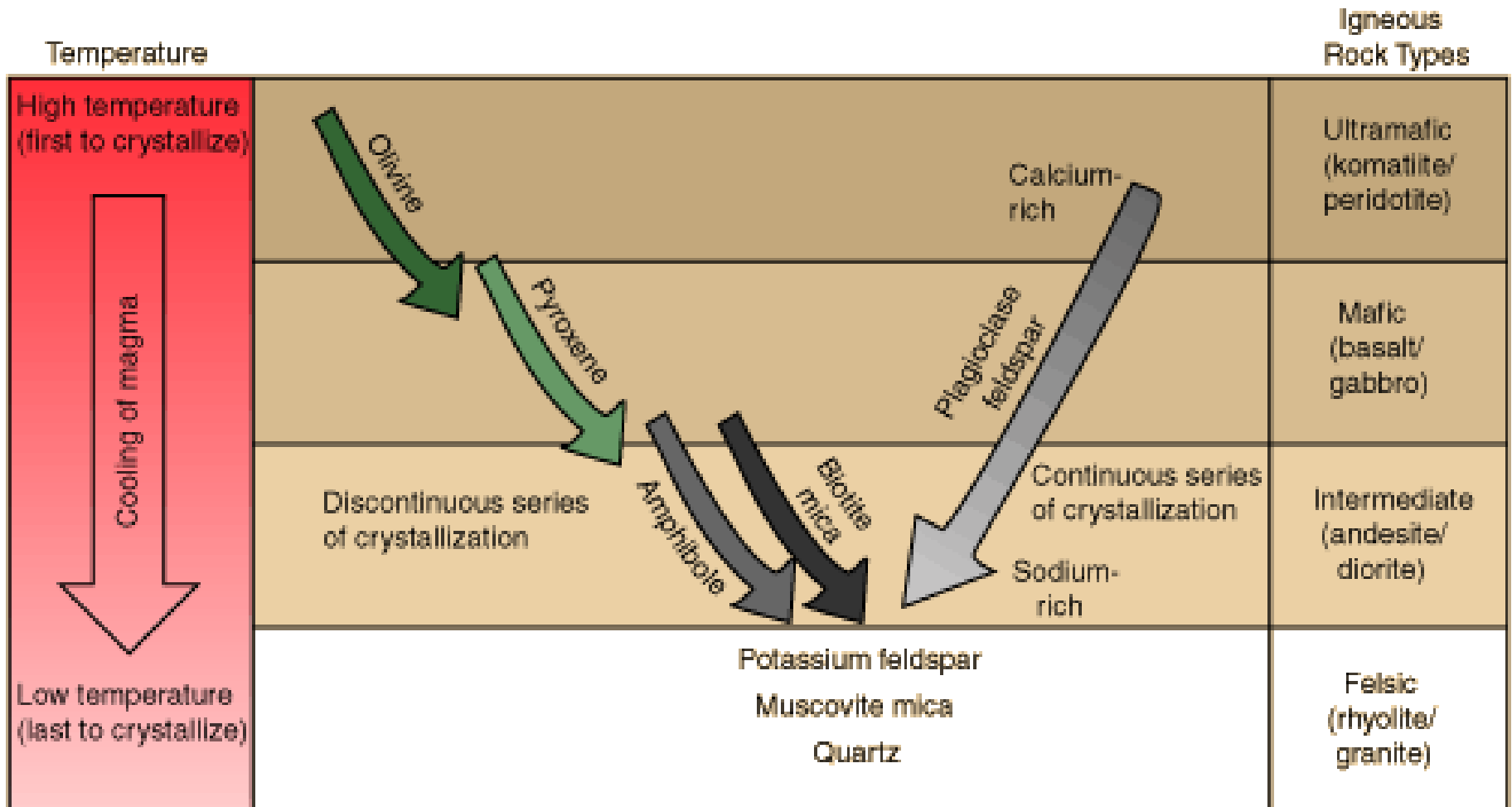


Closed-system
volatile exsolution

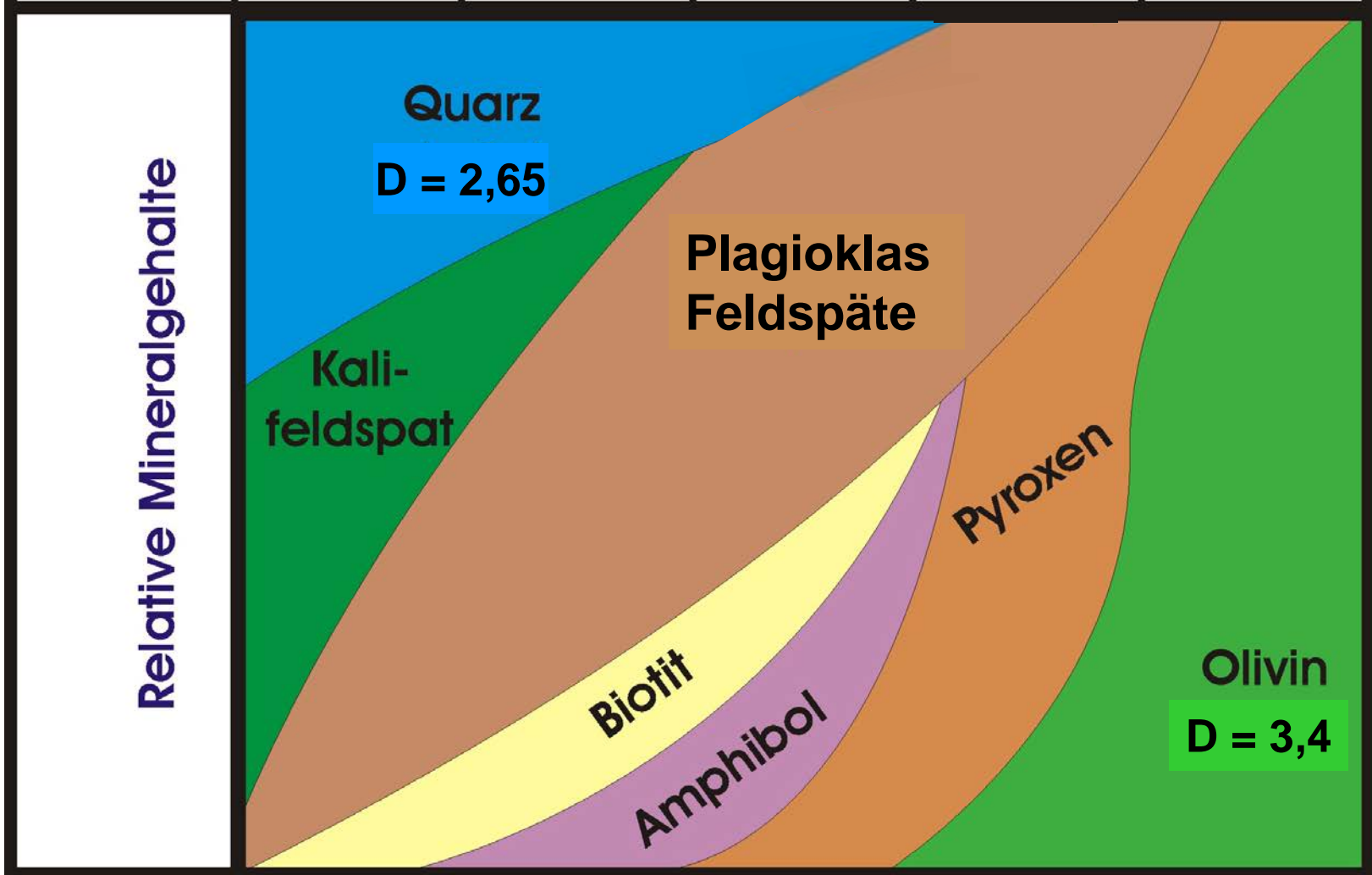


- exsolved gas remains in contact with the melt

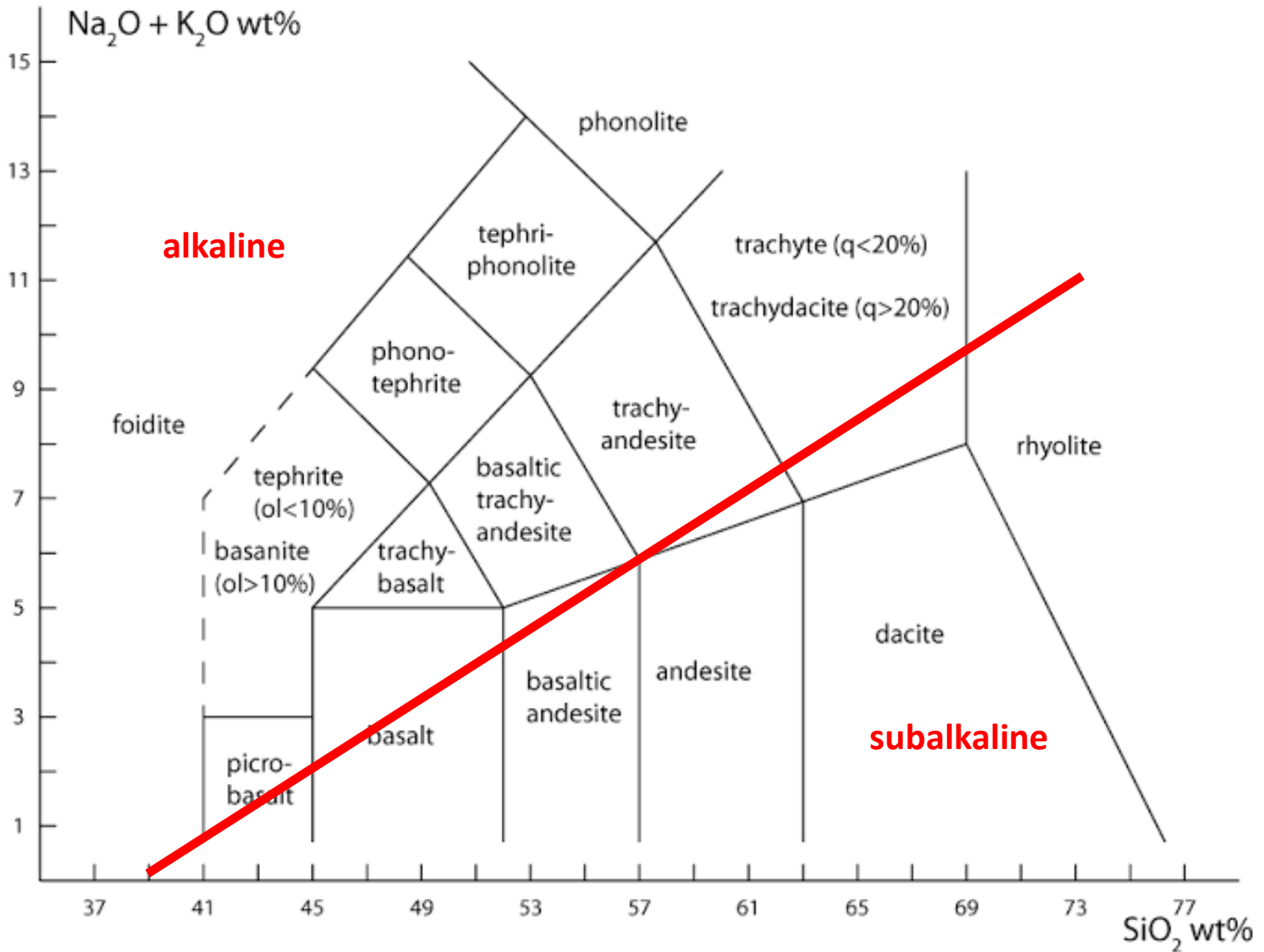
Bowen's Reaction Series



Intrusiv	Granit	Grano- diorit	Diorit	Gabbro	Peridotit
Extrusiv	Rhyolith	Dacit	Andesit	Basalt	-



Chemical classification of igneous rocks (TAS-Diagram)



Metamorphose

Isochemische Umwandlung des Mineralbestandes von Gesteinen durch Druck- und Temperaturänderungen unter Beibehaltung des festen Zustands (**Lösungs-Fällungs-Reaktion**) und Wachstum neuer, P- und T-angepasster Minerale.

Temperaturbereich $> 220 \pm 20 \text{ }^\circ \text{C}$ bis $640 \text{ }^\circ \text{C}$ (beginnende Anatexis)

Metamorphite = Gesteine der Metamorphose

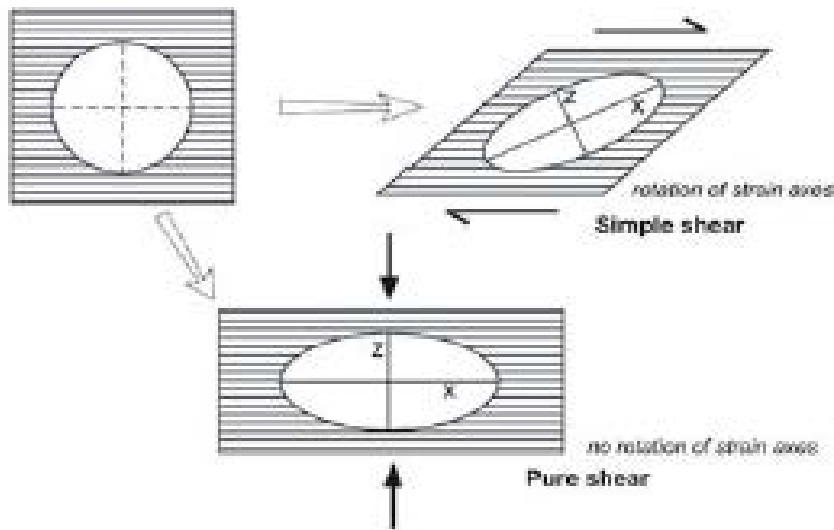
Faktoren der Prägung metamorpher Gesteine:

- Druck (P) und Temperatur (T)
- Zeit (t)
- Zusammensetzung der fluiden Phase
- Deformation

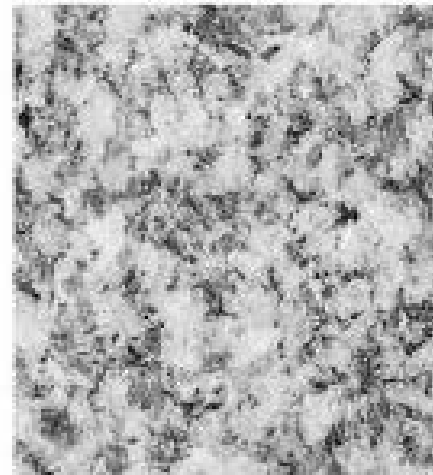
Wie entsteht Schieferung/Foliation in Metamorphiten?

Schieferung = Ausbildung von Trennflächen im Gestein

Ursache: Wachstum von blättrigen und stängeligen Mineralen in Richtung des minimalen Stresses

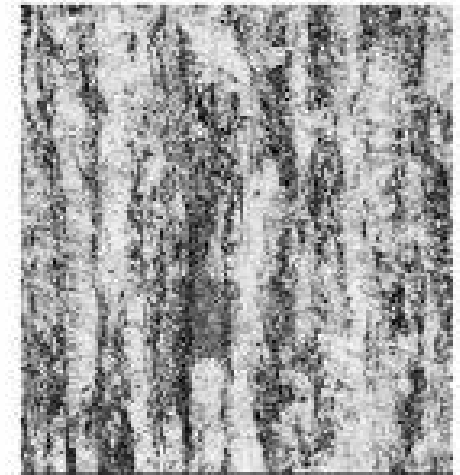


Ungestört



vorher

Gerichteter Druck



nachher

Mineralveränderungen bei der Metamorphose

Kornvergrößerung durch Korngrenzwanderung:

- Kalk → Marmor
- Sandstein → Quarzit

Texturänderung:

- Glimmerschiefer

Umkristallisation durch Deformation:

- Granit → Gneis

Isochemische Strukturänderung (Phasenumwandlung):

- Calcit → Aragonit

Mineralreaktionen:

- Muskovit + Biotit + Quarz →
Fe-Granat + Kalifeldspat + Fluid

Metamorphose-Typen

Regionalmetamorphose (Mitteldruckmetamorphose):

gleicher Anstieg von Druck und Temperatur (Normaltyp)

Druckbetonte Metamorphose (Hochdruckmetamorphose):

Niedrige Temperaturen und hoher Druck

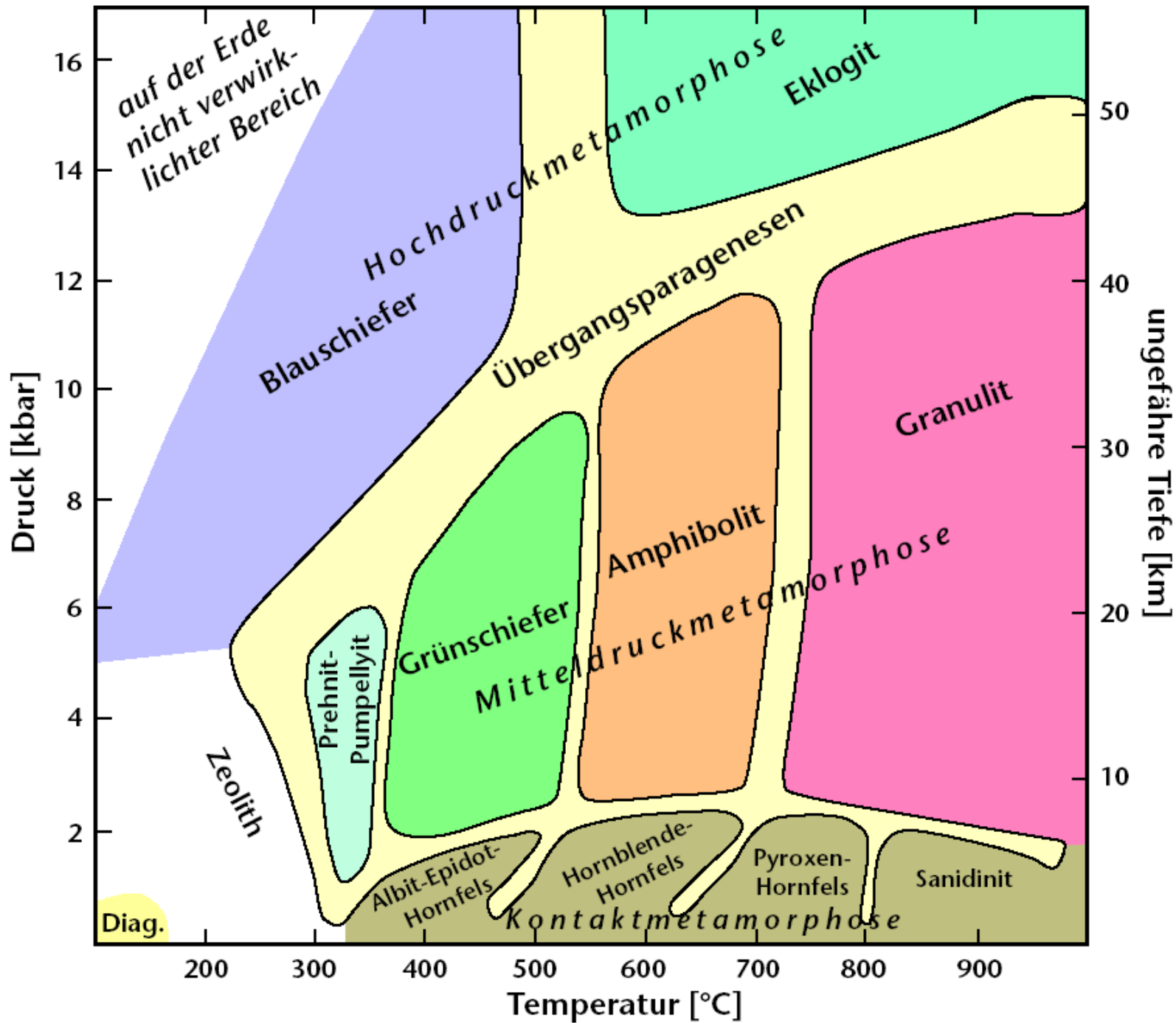
Temperaturbetonte Metamorphose (Kontaktmetamorphose):

Gesteinsumwandlung im heißen Kontaktbereich zu Magmatiten

Metasomatose (Sonderfall):

Veränderung des Chemismus des Metamorphits durch bedeutende Stoffzufuhr bzw. Stoffabfuhr.

z.B. im hydrothermalen Kreislauf an mittelozeanischen Rücken (Ozeanboden-Metamorphose).



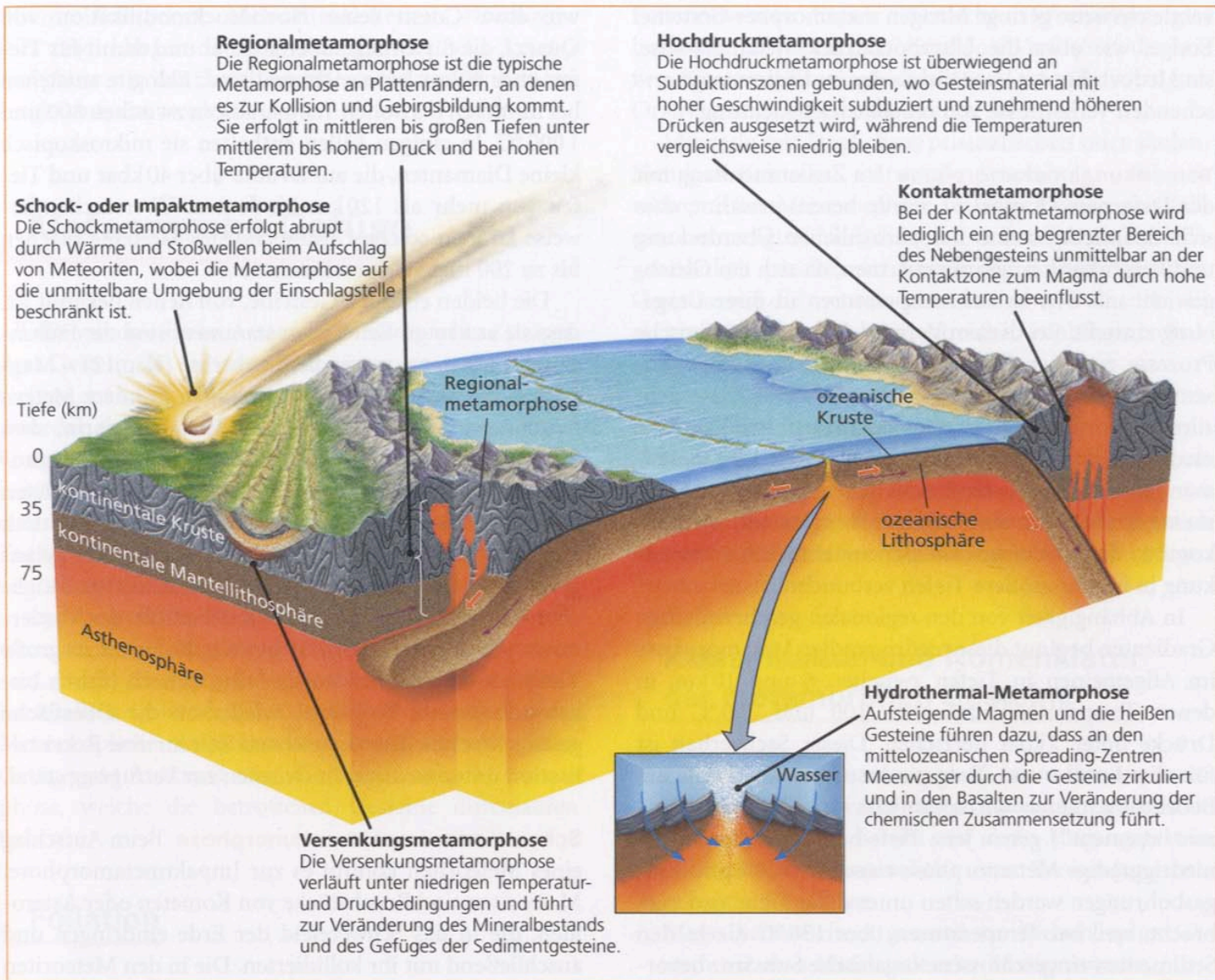


Abb. 6.3 Die Interaktion von Lithosphäre und Asthenosphäre führt zur Bildung metamorpher Gesteine.

Stark vereinfachte Tabelle der häufigsten
metamorphen Gesteine

Die Korngröße ist hauptsächlich abhängig von der Temperatur und der Deformation!

Metamorphosegrad	Zonengliederung	Ausgangssedimente/-gesteine							
	nach Mineralfazies der Regionalmetamorphose	Sedimente und Sedimentgesteine						Magmatite (Erstarrungsgesteine)	
		Ton	kalkiger Tonschlamm	Kalk		Quarzsand	organische Substanzen	Granit	Basalt
beginnend	Diagenese	Tonstein*	Mergel	Kalk	Dolomit	Quarzsandstein	Bitumen Kohle		
	Zeolithfazies	Tonschiefer*	Kalk-Tonschiefer	Kalkmarmor (oft mit kleinen Glimmern)	Dolomitmarmor (oft mit klein. Glimmern)	Quarzit (oft mit kleinen Glimmern)	Graphit	Granit	Diabas
niedrig	Grünschieferfazies	Phyllit*	Kalkphyllit						Grünschiefer
mittel	Epidot-Albitfazies	Glimmerschiefer* (oft mit Granat)	Kalkglimmerschiefer Silikatmarmor					Orthogneis	Amphibolit
hoch	Amphibolitfazies	Paragneis	Para-Amphibolit (z.B. Hornblendengarbenschiefer)						
sehr hoch	Granulitfazies	Granulit						Eklogit	

* Tonstein: sehr feinkörnig, Minerale mit Lupe kaum erkennbar (veränderlich fest).
 Phyllit: feinkörnig, Minerale mit der Lupe erkennbar, oft verfalltet.
 Glimmerschiefer: Minerale mit freiem Auge leicht erkennbar.

Metamorphose



Fluid-Rock Interaction: Palagonitization

- rinds of variable thickness on every mafic glass surface exposed to aquatic fluids.
- formed by dissolution of glass with contemporaneous precipitation of insoluble material at the glass–fluid interface.
- The process of palagonitization is accompanied by extensive mobilization of all elements involved in the alteration process, resulting in the depletion or enrichment of certain elements.
- Extent, direction & rate of element mobility and the palagonitization process itself depend on a number of different, complex interacting properties:
 - (1) temperature,
 - (2) time,
 - (3) structure of the primary material,
 - (4) reactive surface area of the primary material,
 - (5) structure of the precipitating secondary phases
 - (6) growth rates of the secondary phases,
 - (7) fluid properties such as fluid flow rates, pH, Eh, ionic strength, and oxygen fugacity.

Fluid-Rock Interaction: Palagonitization

- Process of glass palagonitization is a two-stage process:
 - 1) glass dissolution
 - 2) palagonite precipitation

→ these 2 processes have different controlling mechanisms, as well as complex feedback mechanisms.
- Exact reaction mechanisms of palagonitization so far remain controversial
- 4 general theories for the reaction kinetics of glass dissolution:
 1. “Precipitate–layer hypotheses”, according to which the primary phase is protected by a precipitate layer. Alteration is thus controlled by diffusion through this precipitate layer.
 2. “Surface-reaction hypotheses”, according to which the alteration rate is controlled by reactions occurring at the primary phase–fluid interface.
 3. “Leached-layer hypotheses”, in which diffusion through a cation-depleted layer controls the release of other cations deeper in the primary material. At more advanced stages, a steady state is developed between dissolution and development of the leached layer.
 4. “Hydrated-layer hypotheses”, according to which a hydrated layer develops before dissolution of the primary phase. Alteration is thus controlled by diffusion of fluids into the primary phase.

Fluid-Rock Interaction: Palagonitization



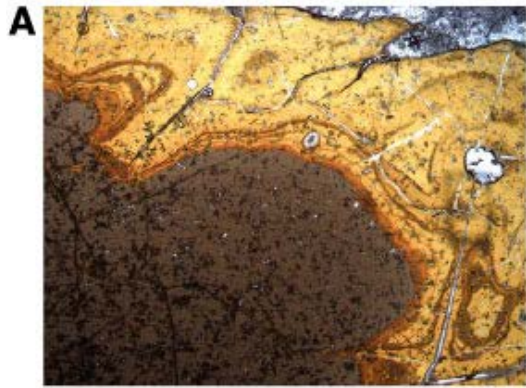
Fluid-Rock Interaction: Palagonitization



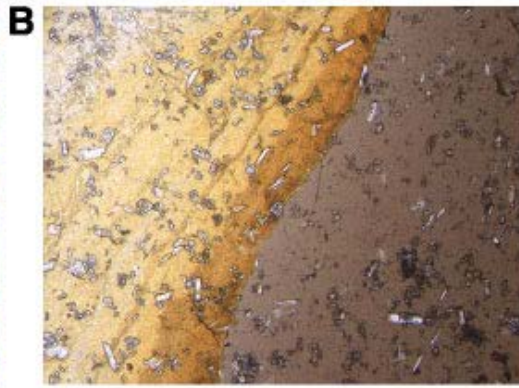
Fluid-Rock Interaction: Palagonitization



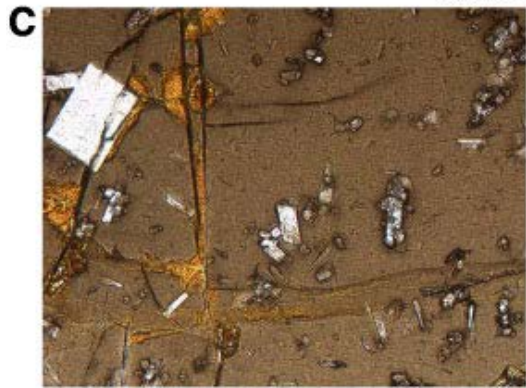
Fluid-Rock Interaction: Palagonitization



1.0 mm



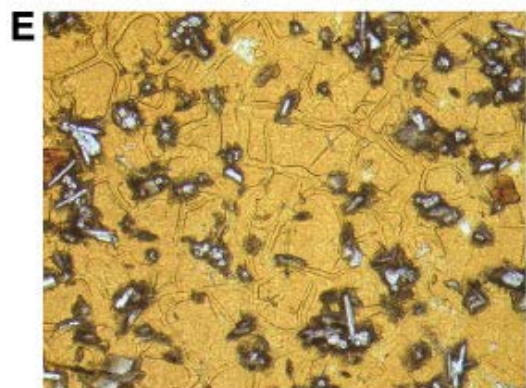
1.0 mm



0.5 mm



0.1 mm



0.5 mm



0.1 mm

Features of a hyaloclastite:

A. A palagonitic rim (yellow) embayed along cracks into fresh basalt glass .

B. Layered palagonite rim (left) next to fresh glass. Note the sharp boundary. **C.**

Detail of fresh quenched glass at the edge of a breccia shard showing small

plagioclase euhedra and tiny acicular plagioclase crystals, some of them intergrown with

cpx. A fracture lined with palagonite cuts vertically through the section. **D.** Individual

tabular crystals of plagioclase and plagioclase-cpx intergrowths coated with dark-brown

spherulitic material near the edge of a glass shard.

E. Palagonite replacing glass with acicular needles of plagioclase and stellate plagioclase-cpx

intergrowths. Most crystals are coated with a thin rim of brown spherulitic

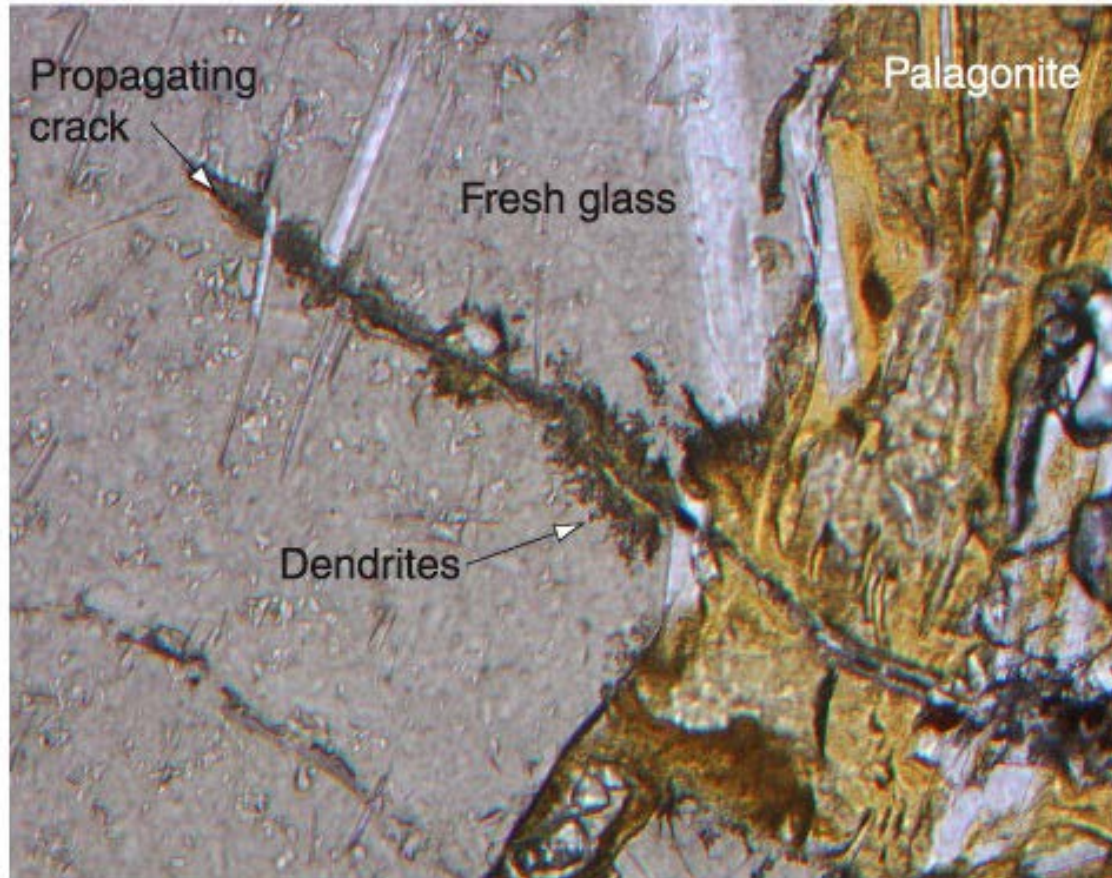
material. Note the fracture pattern in the altered glass.

F. Detail of a palagonitized glass shard showing crystal intergrowths and an altered skeletal olivine replaced by orange secondary minerals.

Fluid-Rock Interaction: Palagonitization

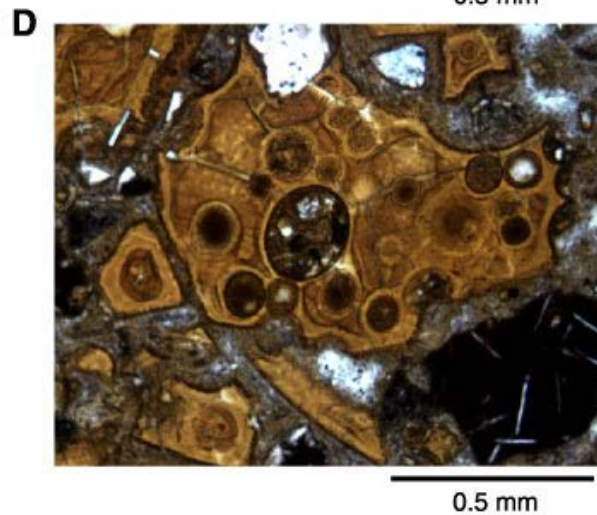
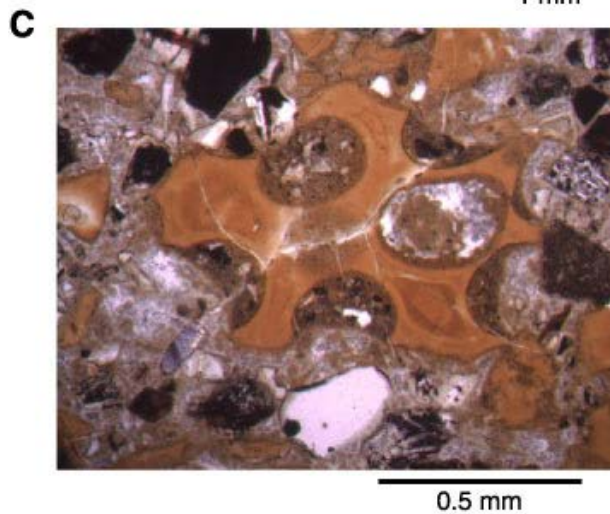
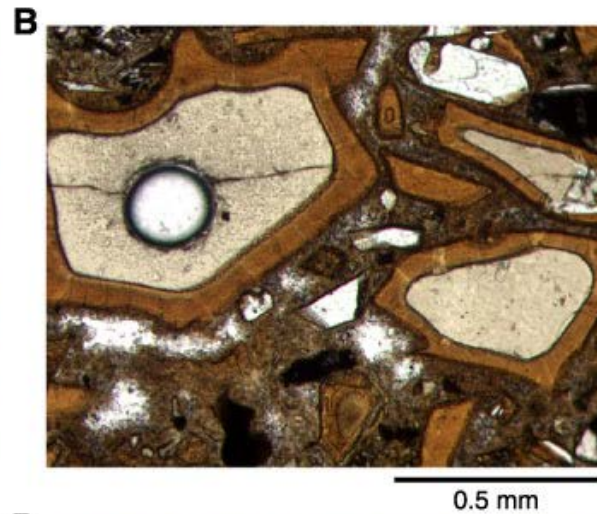
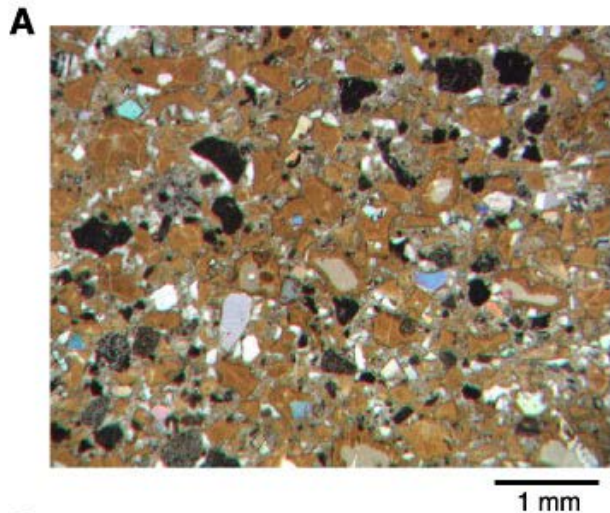
Basaltic glass altered to yellowish brown-orange palagonite.

Note the early stages of palagonitization surrounded by dendrites along the crack, aligned perpendicularly to the palagonitization front.



0.5 mm

Fluid-Rock Interaction: Palagonitization



Thin sections of palagonitic basaltic glass shards in a palagonitized crystal vitric tuff (plane-polarized light).

A. Palagonitized crystal vitric tuff texture.

B. Glass fragments with palagonitic rims.

C. Completely palagonitized vesicular glass shard with matrix material in vesicles.

D. Palagonitized glass shard containing spherulites and filled vesicles. Individual vesicles are rimmed with palagonite

Metamorphic petrology

Serpentinization



Serpentinite
(Troodos ophiolite, Cyprus)

Photo: Siim Sepp (www.sandatlas.org)

Serpentinite & Serpentine

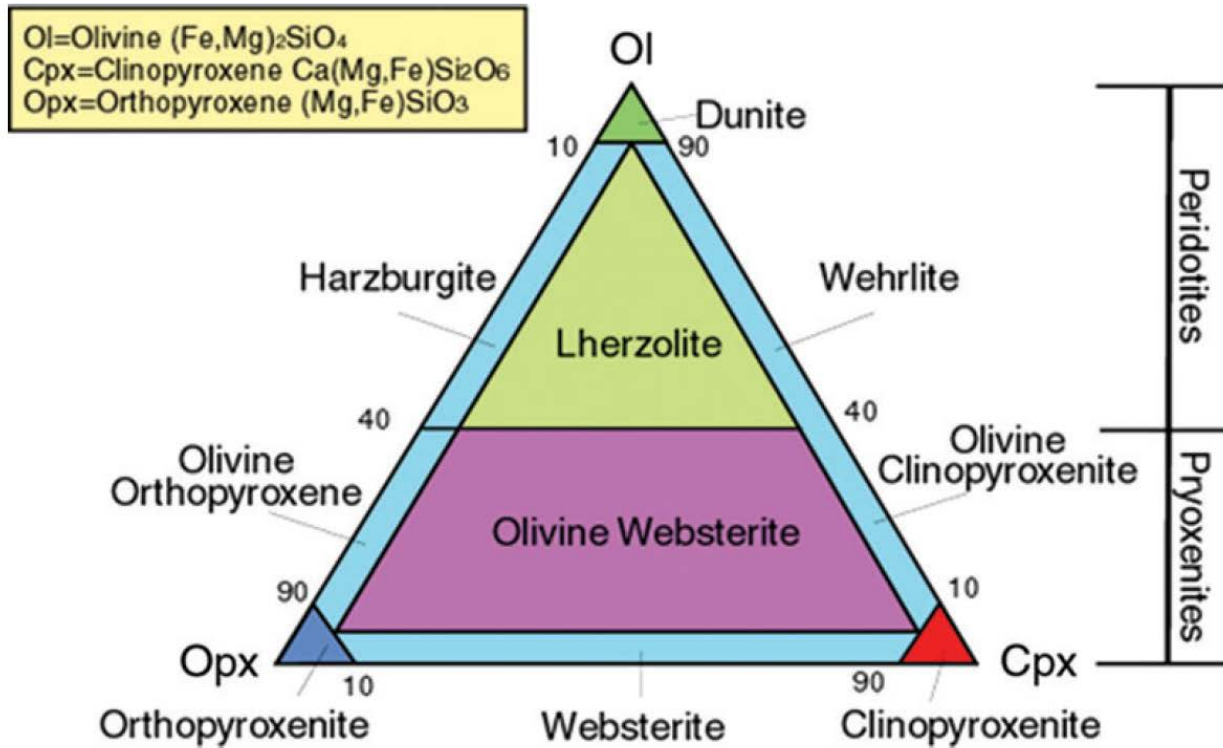
Serpentinite

- Ultramafic, generally massive, aphanitic rocks
- Composition: mostly *serpentine minerals*; accessory magnetite, brucite, other Mg-silicates, Ca-Al-silicates
- Protoliths: *ultramafic rocks* with abundant Mg-rich olivines and/or pyroxenes (peridotite, dunite, pyroxenite), rare protoliths: metasomatized gabbro, dolomite
- Many different fabrics and colors – mostly shades of yellow & green up to black

Serpentine

- family of *silicate minerals* rich in magnesium and water.
 - light to dark, yellowish-greenish-black, greasy looking and feel slippery.
- Serpent rock (latin: serpentinus) due to color and flaky, mottled appearance

Classification of ultramafic rocks



Classification of ultramafic rocks based on Le Maitre (2002).

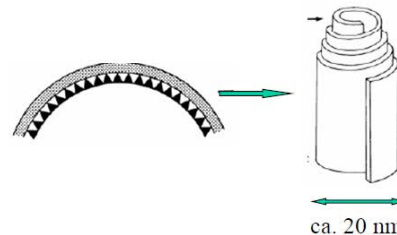
Serpentine minerals

Serpentine mineral subgroup: $\text{Mg}_3\text{Si}_2\text{O}_5(\text{OH})_4$

- Density: 2.2 – 2.9 g/cm³
- Hardness: 2.5 – 4
- Limited substitution of Fe^{2+} and Fe^{3+} , Al^{3+} for Mg^{2+} and Si^{4+}
- **3 Serpentine minerals**, with small but persistent compositional variations (-> no polymorphism!):
 - **Antigorite** (mkl., lamellated, platy habit, green)
 - **Lizardite** (trig., flaky, platy habit, green, most common serpentine mineral)
 - **Chrysotile** (rh, fibrous habit, asbestos, pale colours: white-yellow-greenish)



Antigorit- „Wellblech“



Chrysotilfaser

Serpentinization

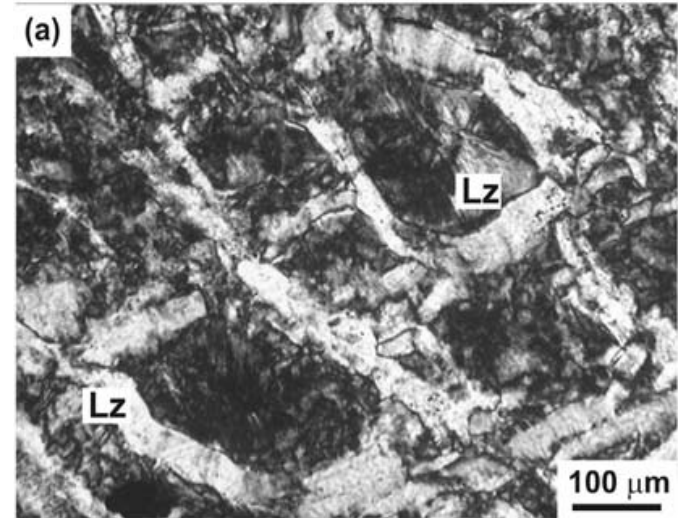
Serpentinization

Transformation of the minerals in *ultramafic rocks* by *hydrous alteration* and/or *metamorphism* to serpentine minerals.

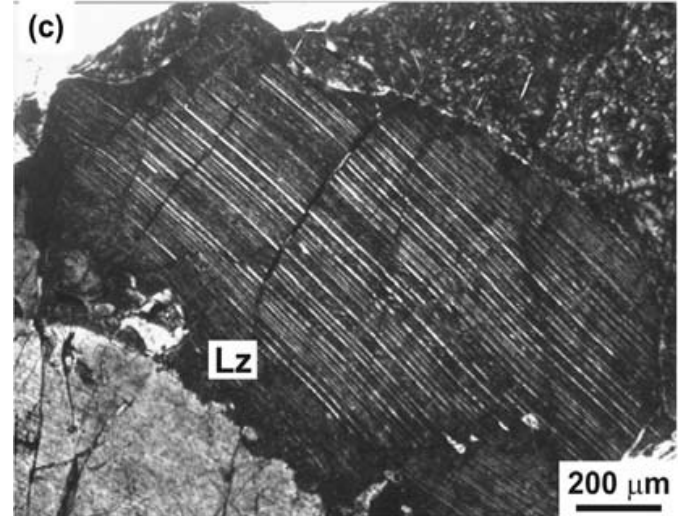
- Occuring in(sub)-greenschist-facies, blueshist-facies, amphibolit-facies
- Anhydrous Mg-, Fe-rich silicate minerals (pyroxene, olivine) form hydrous silicate minerals (serpentine) plus some other possibilities like brucite and magnetite.
- The degree to which a mass of ultramafic rock undergoes serpentinization depends on the starting rock composition and on whether or not fluids transport Ca, and other elements away during the process.
- Serpentine replacement of olivine grains begins by hydration reactions along cracks → **mesh texture** after complete serpentinization
- Serpentine replacement of pyroxenes creates a “**bastite texture**”
- Relict textures can be removed by deformation processes

Serpentinite microstructures

Lizardite with mesh structure after peridotitic olivine:
the mesh rim consists of apparent fibres oriented perpendicularly to the mesh boundaries; the mesh core mainly consists of fine grained random lizardite.
Crossed Polarized Light (XPL).



“Bastite” structure after peridotitic orthopyroxene
consisting of lizardite (Lz). The original clinopyroxene exsolutions are still visible, although totally replaced by lizardite with different optical orientation.
Crossed Polarized Light (XPL)



Serpentinization

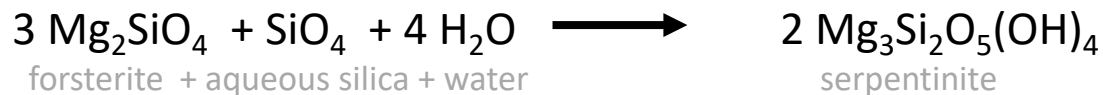
- In case of no change in proportion of chemical constituents during serpentinization
 - density decrease of 20% from 3.3 → 2.65 g/cm³
 - volume increase
 - Volume increase could be avoided if some original components can be transported away after/during serpentinization (e.g. MgO, SiO₂)
- Far reaching geological implications
- Both possibilities were controversially discussed for many decades – up to today!
- volume changes on larger scale obliterated by ubiquitous shear zones
 - > deformation due to expansion or tectonics hard/impossible to discriminate
 - subtle tendency towards volume increase due to petrological indications
 - > Still an open system -> transport of Ca into adjacent rock (metasomatized into Ca-rich, silica-poor minerals as epidote group minerals)

Serpentinization reactions

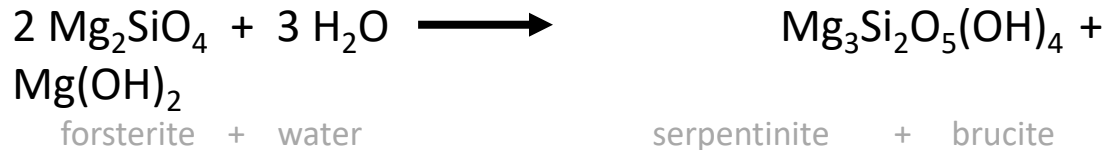
Serpentine and serpentinite is formed from olivine via several reactions, some are complementary:

1) exchange of silica between forsterite and fayalite to form serpentine and magnetite:

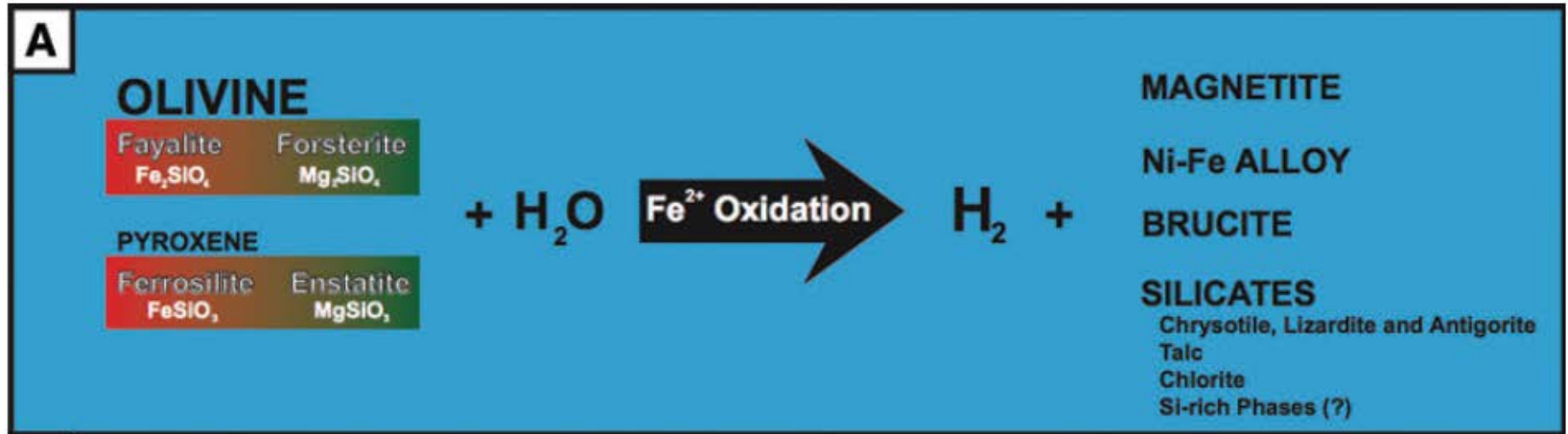
→ reactions are highly exothermic → generation of heat



2) hydration of olivine with water only to yield serpentine and brucite:



Serpentinization reactions

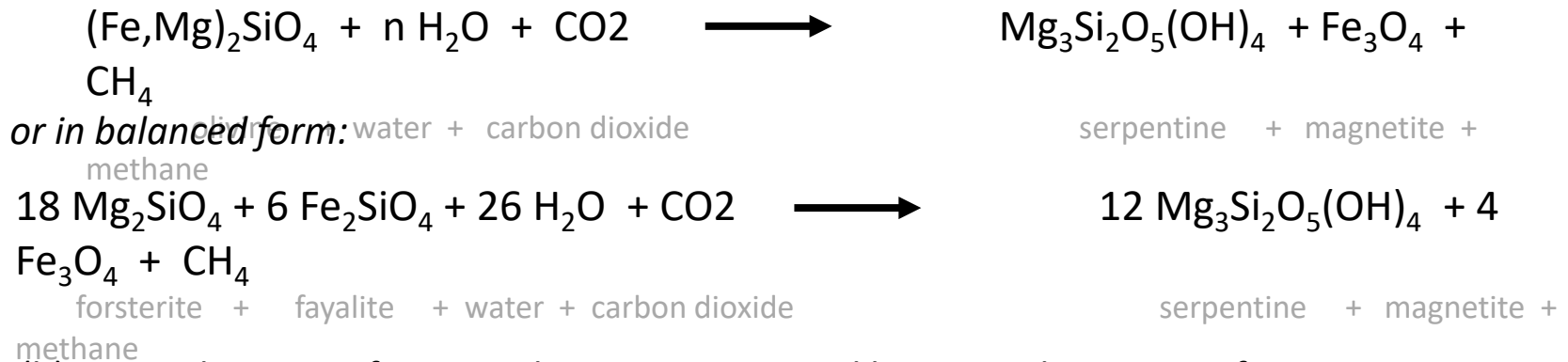


Poorly soluble reaction products (aqueous silica, dissolved magnesium ions) might be transported in solution out of the serpentinized zone by diffusion or advection.

Serpentinization reactions

3) In presence of CO₂, serpentinization may form magnesite or generate methane:
 -> serpentinization may produce some hydrocarbon gases within the oceanic crust.

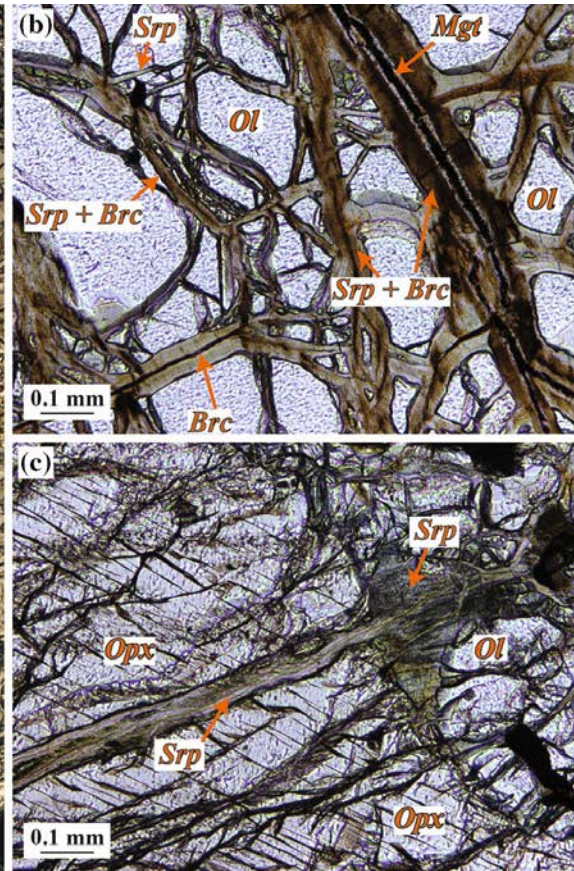
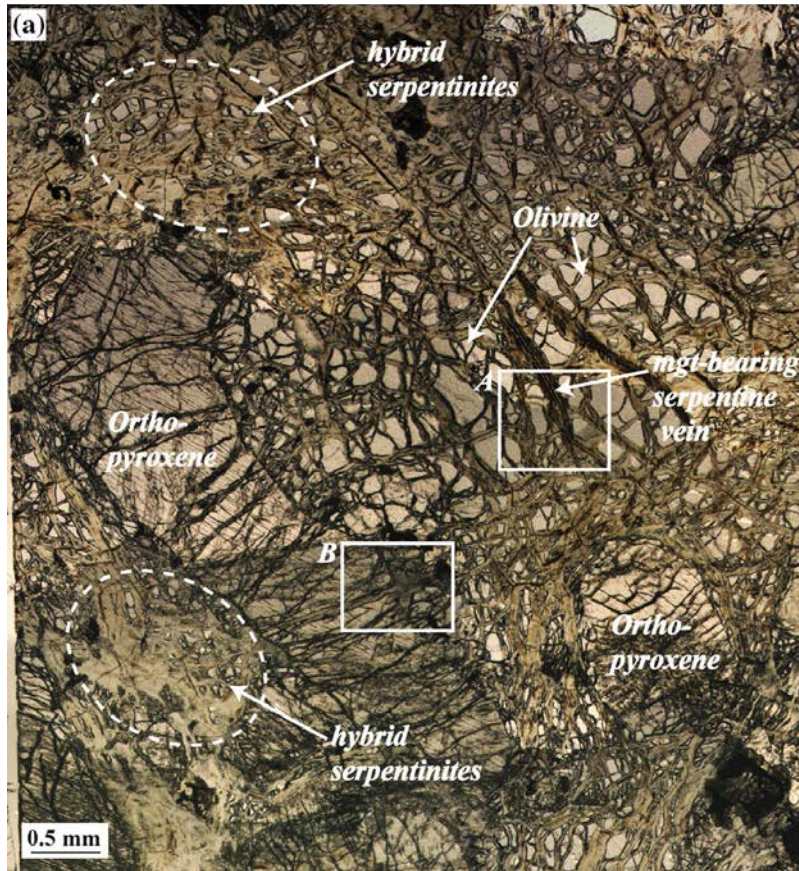
(a) Favored reaction for Mg-poor olivine or insufficient CO₂ to promote talc formation:



(b) Favored reaction for Mg-rich compositions and low partial pressure of CO₂:



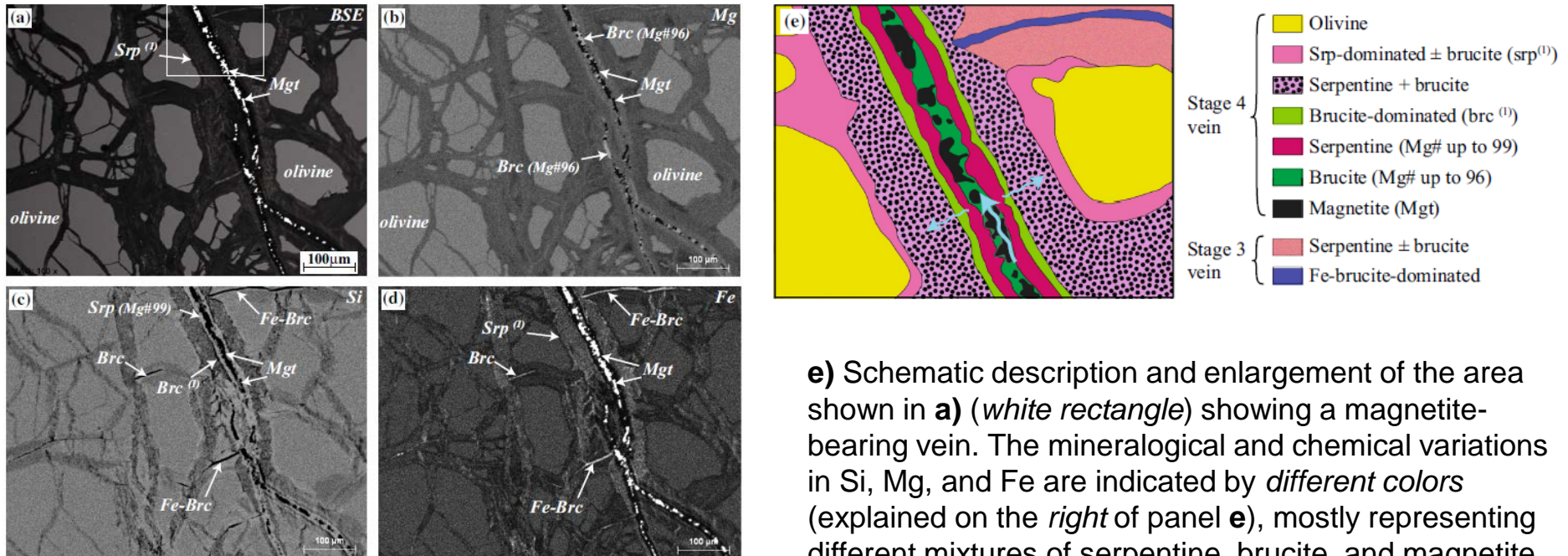
Serpentinization reactions and textures



partly replaced opx and ol, where replacement of ol by serpentinite is more advanced than replacement of opx.

(From: Schwarzenbach et al. 2016, Contrib Mineral Petrol)

Serpentinization reactions & textures



Element distribution maps of olivine-hosted veins:

- a)** BSE image,
- b)** element distribution map of Mg,
- c)** element distribution map of Si,
- d)** element distribution map of Fe.

e) Schematic description and enlargement of the area shown in **a)** (white rectangle) showing a magnetite-bearing vein. The mineralogical and chemical variations in Si, Mg, and Fe are indicated by different colors (explained on the right of panel **e**), mostly representing different mixtures of serpentine, brucite, and magnetite. The pale blue arrows in **e)** indicate fluid flow

(From: Schwarzenbach et al. 2016, Contrib Mineral Petrol)

Occurrence of Serpentinities

- Serpentinities are probably very widespread in the mantle, but not nearly as common in the upper parts of the crust.
- In the upper crust they occur mostly where ultramafic rocks occur:

(a) Ophiolite complexes:

+ Intact slabs of ophiolite and mélangé associations

Some large intact slabs were emplaced at hot bodies

- > significant dynamo-thermal metamorphism in underlying metamorphic sole
- > inverted metamorphic zonation

+ Mountain belts (cold Ophiolite complexes)

- Alpine peridotites & serpentinites
- Tectonical emplacement as typically cold bodies

(b) at / near the seafloor

- fast spreading ridges -> High-T and low-T serpentinization at detachment faults
- slow- to ultraslow-spreading ridges → Low-T seafloor serpentinization (e.g. Atlantic Massif at the Mid-Atlantic Ridge)

Ophiolite Sequence

- An ophiolite sequence consists of:
 - deep sea sediments
 - basaltic pillow lavas,
 - sheeted dykes,
 - gabbros,
 - peridotites.
- The name ophiolite means “snakestone” from “ophio” (snake) and “lithos” (stone).
 - named for the green, snake-like serpentine minerals formed in altered ocean crust and mantle.

OPHIOLITE SEQUENCE



Pillow Basalts: these formations are the result of the rapid cooling of hot, fluid magma that comes into contact with water.

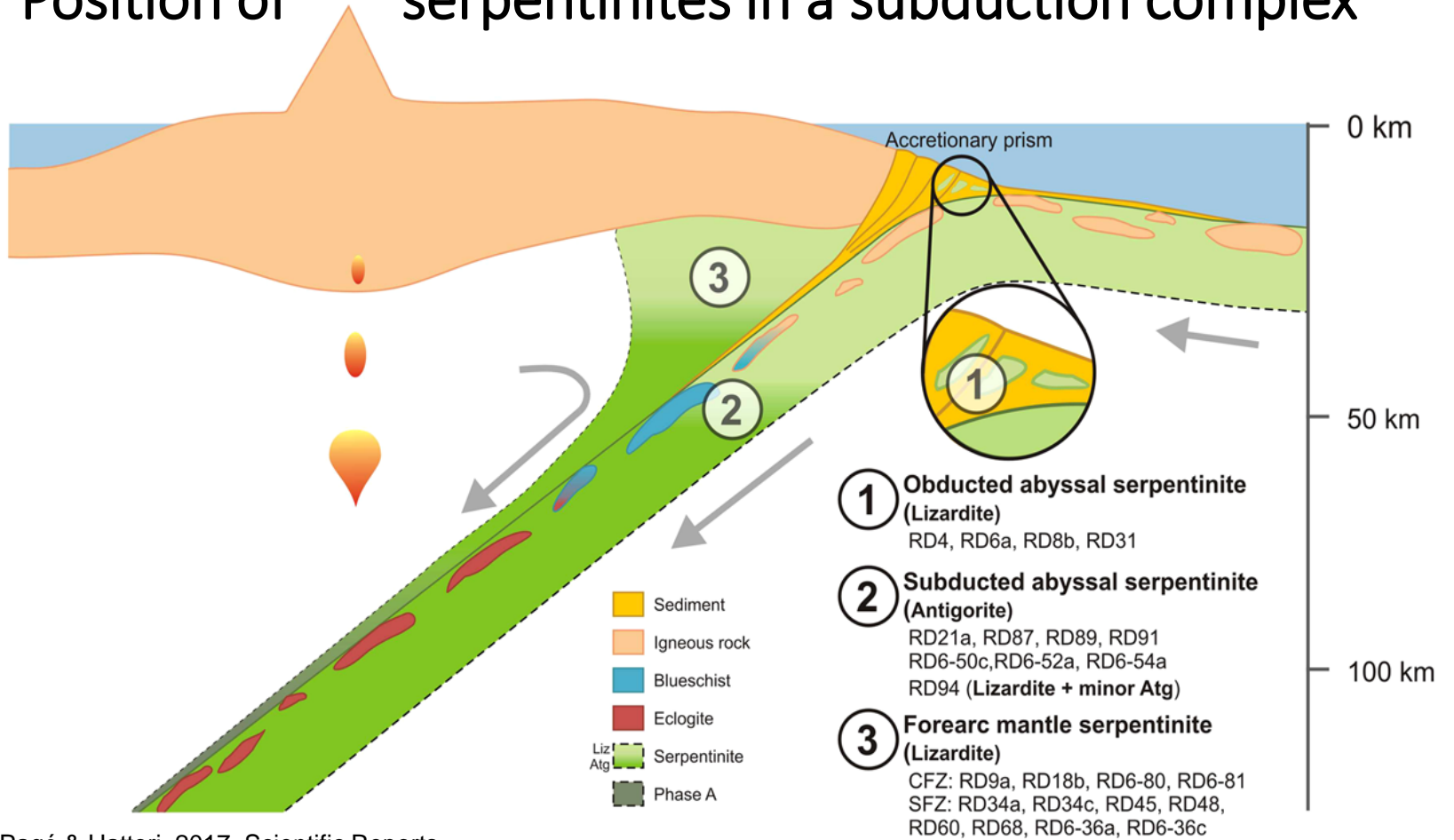
Sheeted Dyke Complex: consist of swarms of basaltic dykes, the feeder channels for the overlying pillow basalts.

Gabbros: usually banded or layered resulting from the crystallisation in the magma chamber at the base of the crust.

Peridotites: this section represents the lower part of the mantle and has usually been hydrated to serpentinites

The diagram illustrates a typical ophiolite sequence based on the ophiolites from Oman, which is where the accompanying photographs were taken. (photos from: "The Mid-Oceanic Ridges: Mountains below the sea", A. Nicolas)

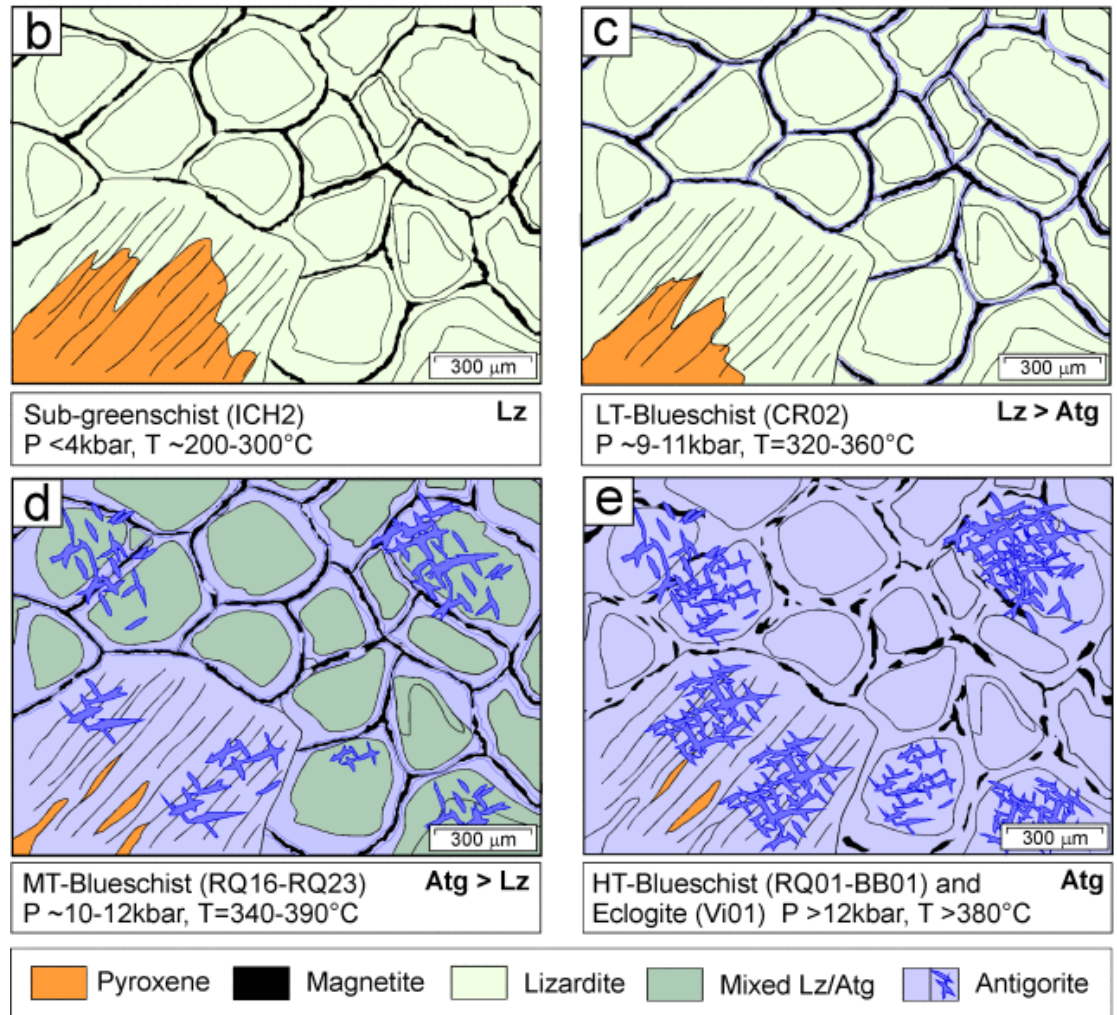
Position of serpentinites in a subduction complex



From: Pagé & Hattori, 2017, Scientific Reports

Progressive transition from Lizardite-chrysotile to antigorite paragenesis under a HP metamorphic gradient

- (b) Sub-greenschist conditions: only lizardite is present.
- (c) LT-blueschist: antigorite appears along the lizardite grain boundaries via a dissolution–precipitation process.
- (d) MT-blueschist: antigorite becomes the major phase. The veins of antigorite at the lizardite grain boundaries widen and the grain cores are mixed lizardite/antigorite.
- (e) HT-blueschist: antigorite becomes the sole serpentine variety. Antigorite develops infra-millimetric blades superimposed over the original mesh texture.



From: Schwartz et al. 2012, Lithos

Phase diagram serpentine minerals

Lz, lizardite; Atg, antigorite; Chr, chrysotile; Fo, forsterite; Tlc, talc; Brc, brucite.

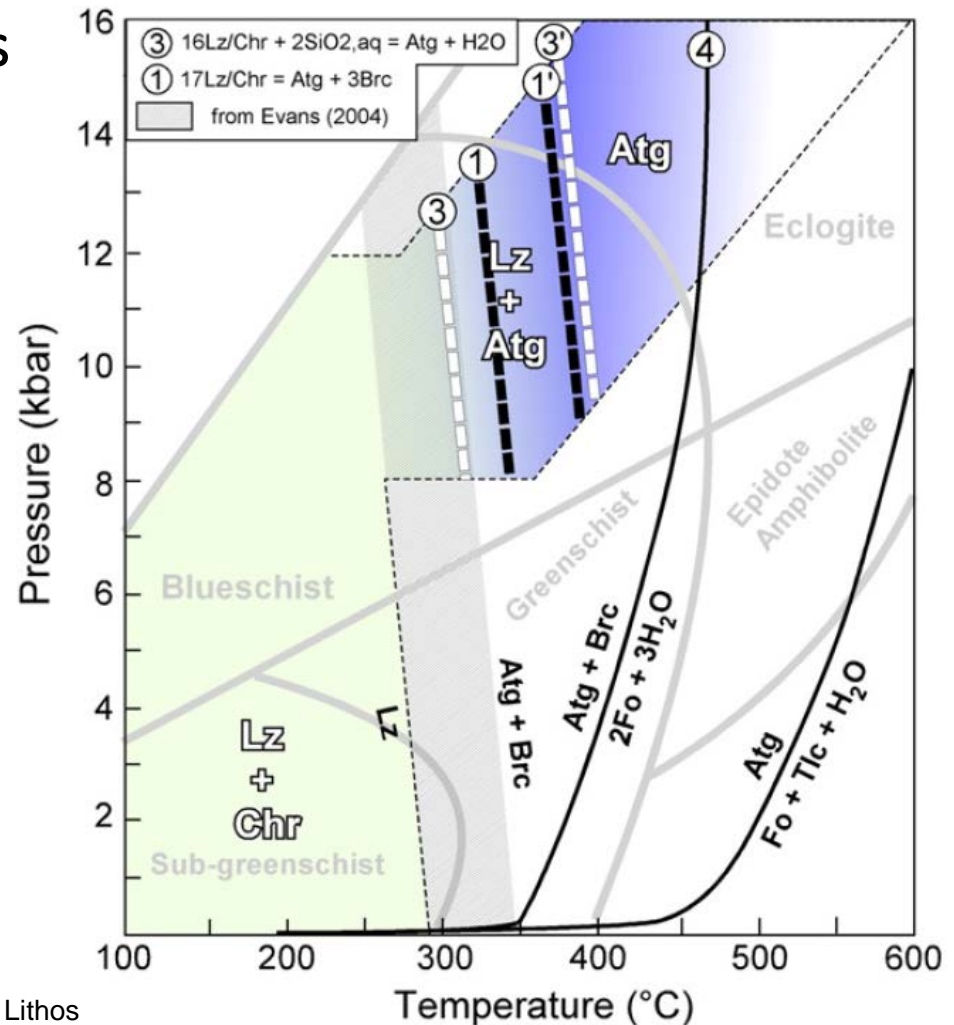
(1) and (3) correspond to the onset of the reactions
 (1') and (3') correspond to the end of the reactions
 with the complete consumption of Lz.

Natural stability field domain of coexisting Lz and Atg
 is restricted to $\sim 320^\circ\text{C} < T < 390^\circ\text{C}$.

Between 320 and 390 °C, the Atg develops through
 Reaction (3) in the presence of SiO₂-rich fluids by
 dissolution–precipitation processes.

At 390 °C and above, Lz is entirely replaced by Atg.

Above 460 °C, Reaction (4) results in the onset of
 crystallization of olivine.



From: Schwartz et al. 2012, Lithos

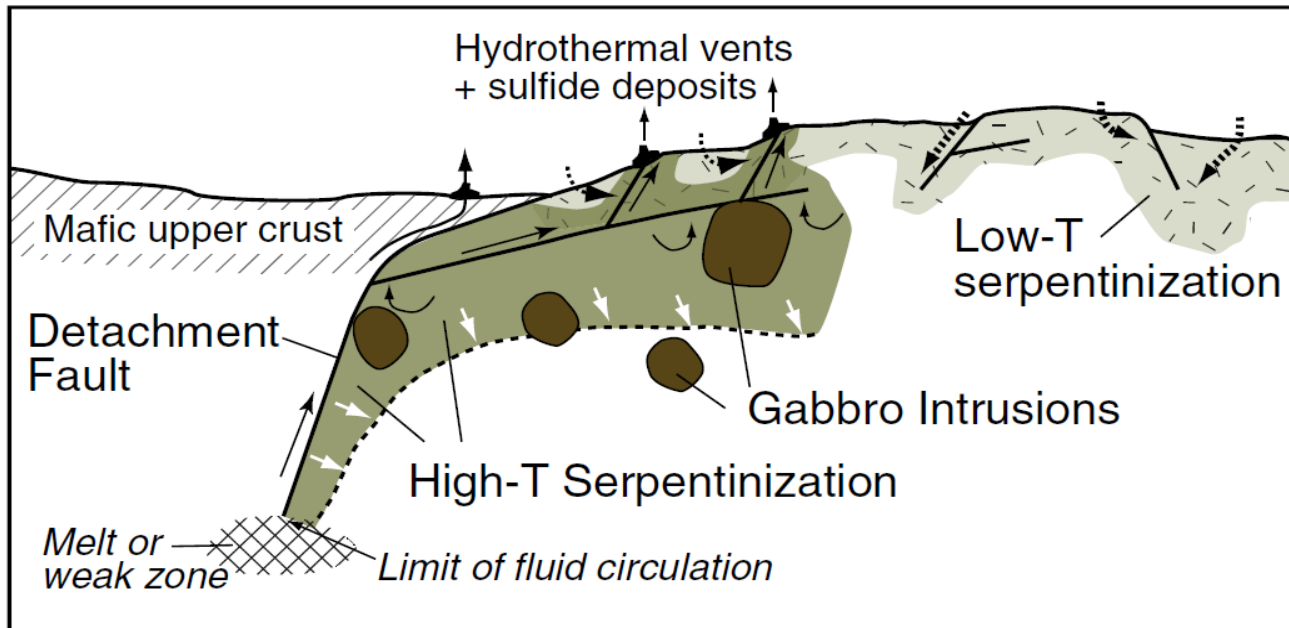
Serpentinization processes at fast-spreading ridges

Process in extensional tectonics -> Fluid circulation is focused along **detachment faults**.

-> **High-T serpentinization** (white arrows) proceeds as fluids penetrate into footwall

-> Gabbro intrusions drive hydrothermal fluid circulation (black arrows)

→ further high-T serpentinization and generation of sulfide deposits at seafloor vents.



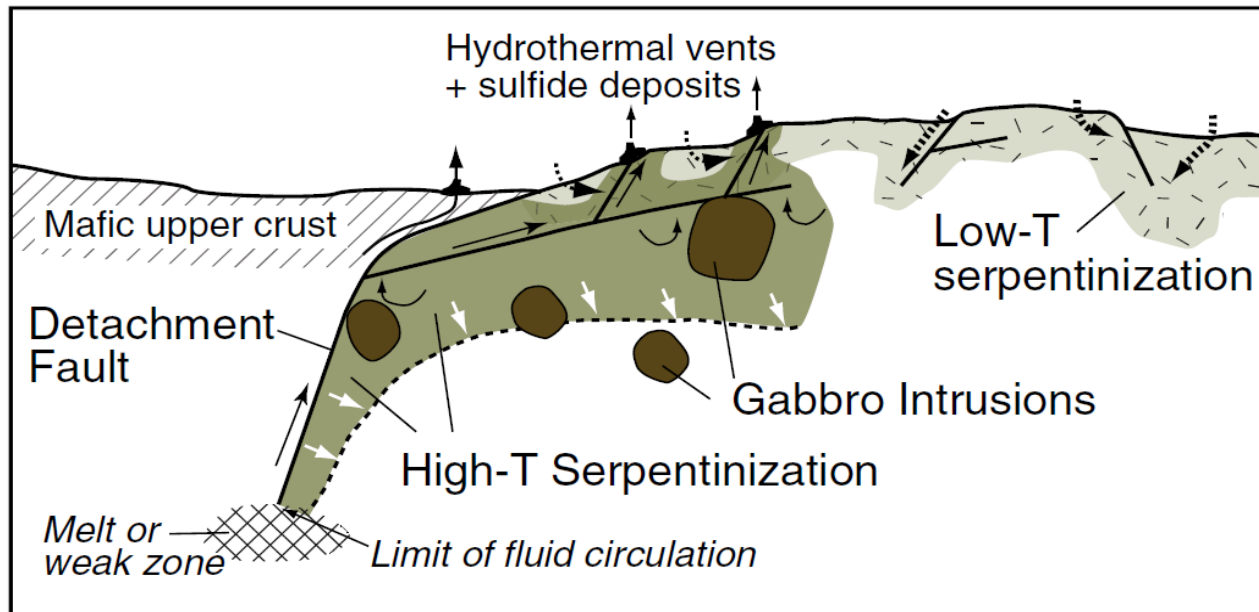
Taken from: Alt, J.C., et al., Lithos (2013)

Serpentinization processes at fast-spreading ridges

Low-T serpentinization (light shading) is driven by cooling of the lithosphere and is associated with faulting, fracturing and exposure of peridotite at the seafloor.

-> Can occur superimposed on high-T serpentinization

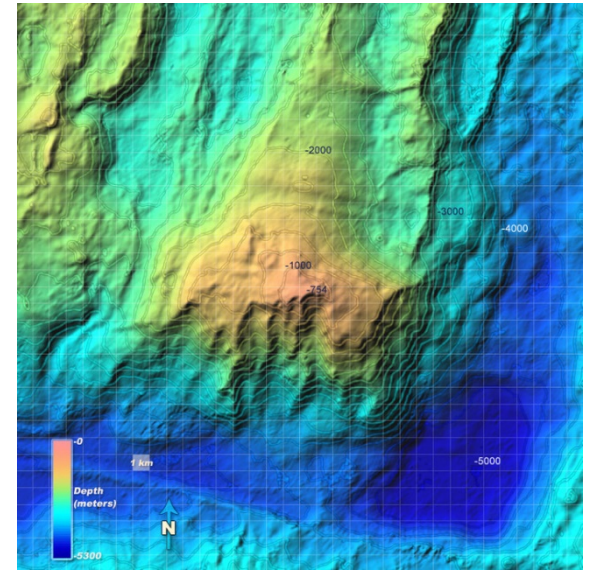
-> often accompanied by the formation of carbonates & sulfides through microbial reduction of marine sulfate within serpentinites



Taken from: Alt, J.C., et al., Lithos (2013)

Lost City Hydrothermal Field

- Serpentine-hosted hydrothermal field with an remarkable submarine ecosystem in which geological, chemical, and biological processes are intimately interlinked
- located 15 km west of the spreading axis of the Mid-Atlantic Ridge at 30°N, near the summit of the Atlantis Massif.



The Atlantis Massif rises ~14,000 feet above the surrounding seafloor and is formed by long-lived faulting

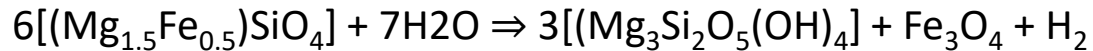
Highly deformed serpentinites directly underlie Lost City. This image was taken with the robotic vehicle Hercules during the NOAA-UW expedition. The wreckfish is ~ 1 m in length.

Image courtesy of University of Washington and the Lost City Team, IFE, URI-IAO and NOAA.

Lost City Hydrothermal Field

- Serpentinization reactions in the subsurface produce Ca-enriched high-pH fluids (pH = 9-11) that have temperatures between 40°C to 91°C.
- Serpentinization reaction within the Atlantis Massif creates reducing environments marked by high H₂ concentrations, which are well suited to abiotic hydrocarbon production.

The general reaction is:



This small Beehive structure vents the highest temperature (91°C), highest pH fluids (11) at Lost City. This image was taken with Alvin in 2003 during the NSF-funded expedition. Lasers are 10 cm apart.



Trace Elements – Major Elements

No rigorous definition of a trace element, but typically 11 elements are described as major elements because they form more than 99 wt% of most igneous rocks;

- the relative abundance of major elements determines the proportions of rock-forming minerals such as feldspar, quartz, micas, olivine, pyroxenes and amphiboles.
- major elements (ME) in order of increasing atomic number: O, Na, Mg, Al, Si, P, K, Ca, Ti, Mn and Fe.

→ all other elements typically occur in lower abundance, <0.1 wt.%, and are described as Trace Elements

Trace Elements – Major Elements

Periodic Table of the Elements
and Ground-State Electronic Configurations

Group →

Period ↓

1	IA 1 H $1s^1$																	2 He $1s^2$
2	3 Li $[\text{He}]2s^1$	4 Be $[\text{He}]2s^2$											5 B $2s^2 2p^1$	6 C $2s^2 2p^2$	7 N $2s^2 2p^3$	8 O $2s^2 2p^4$	9 F $2s^2 2p^5$	10 Ne $2s^2 2p^6$
3	11 Na $[\text{Ne}]3s^1$	12 Mg $[\text{Ne}]3s^2$											13 Al $3s^2 3p^1$	14 Si $3s^2 3p^2$	15 P $3s^2 3p^3$	16 S $3s^2 3p^4$	17 Cl $3s^2 3p^5$	18 Ar $3s^2 3p^6$
4	19 K $[\text{Ar}]4s^1$	20 Ca $[\text{Ar}]4s^2$	21 Sc $3d^1 4s^2$	22 Ti $3d^2 4s^2$	23 V $3d^3 4s^2$	24 Cr $3d^5 4s^1$	25 Mn $3d^5 4s^2$	26 Fe $3d^6 4s^2$	27 Co $3d^7 4s^2$	28 Ni $3d^8 4s^2$	29 Cu $3d^{10} 4s^1$	30 Zn $3d^{10} 4s^2$	31 Ga $4s^2 4p^1$	32 Ge $4s^2 4p^2$	33 As $4s^2 4p^3$	34 Se $4s^2 4p^4$	35 Br $4s^2 4p^5$	36 Kr $4s^2 4p^6$
5	37 Rb $[\text{Kr}]5s^1$	38 Sr $[\text{Kr}]5s^2$	39 Y $4d^1 5s^2$	40 Zr $4d^2 5s^2$	41 Nb $4d^4 5s^1$	42 Mo $4d^5 5s^1$	43 Tc $4d^6 5s^1$	44 Ru $4d^7 5s^1$	45 Rh $4d^8 5s^1$	46 Pd $4d^{10}$	47 Ag $4d^{10} 5s^1$	48 Cd $4d^{10} 5s^2$	49 In $5s^2 5p^1$	50 Sn $5s^2 5p^2$	51 Sb $5s^2 5p^3$	52 Te $5s^2 5p^4$	53 I $5s^2 5p^5$	54 Xe $5s^2 5p^6$
6	55 Cs $[\text{Xe}]6s^1$	56 Ba $[\text{Xe}]6s^2$	57 La $5d^1 6s^2$	72 Hf $5d^2 6s^2$	73 Ta $5d^3 6s^2$	74 W $5d^4 6s^2$	75 Re $5d^5 6s^2$	76 Os $5d^6 6s^2$	77 Ir $5d^7 6s^2$	78 Pt $5d^9 6s^1$	79 Au $5d^{10} 6s^1$	80 Hg $5d^{10} 6s^2$	81 Tl $6s^2 6p^1$	82 Pb $6s^2 6p^2$	83 Bi $6s^2 6p^3$	84 Po $6s^2 6p^4$	85 At $6s^2 6p^5$	86 Rn $6s^2 6p^6$
7	87 Fr $[\text{Rn}]7s^1$	88 Ra $[\text{Rn}]7s^2$	89 Ac $6d^1 7s^2$	104 Unq	105 Unp	106 Unh	107 Uns											

* 58 Ce $4f^1 5d^1 6s^2$	59 Pr $4f^3 6s^2$	60 Nd $4f^4 6s^2$	61 Pm $4f^5 6s^2$	62 Sm $4f^6 6s^2$	63 Eu $4f^7 6s^2$	64 Gd $4f^7 5d^1 6s^2$	65 Tb $4f^9 6s^2$	66 Dy $4f^{10} 6s^2$	67 Ho $4f^{11} 6s^2$	68 Er $4f^{12} 6s^2$	69 Tm $4f^{13} 6s^2$	70 Yb $4f^{14} 6s^2$	71 Lu $4f^{14} 5d^1 6s^2$
† 90 Th $6d^2 7s^2$	91 Pa $5f^2 6d^1 7s^2$	92 U $5f^3 6d^1 7s^2$	93 Np $5f^4 6d^1 7s^2$	94 Pu $5f^6 7s^2$	95 Am $5f^7 7s^2$	96 Cm $5f^7 6d^1 7s^2$	97 Bk $5f^8 6d^1 7s^2$	98 Cf $5f^{10} 7s^2$	99 Es $5f^{11} 7s^2$	100 Fm $5f^{12} 7s^2$	101 Md $5f^{13} 7s^2$	102 No $5f^{14} 7s^2$	103 Lr $5f^{14} 6d^1 7s^2$

Isotope Geochemistry

Two principal applications of radiogenic isotope geochemistry:

1) *Geochronology*

uses the constancy of the rate of radioactive decay

→ Dating method

2) *Tracer studies*

Uses the differences in the ratio of the radiogenic daughter isotope to other isotopes of an element. (as e.g. in biology)

→ Origin of volatiles, minerals & rocks

Isotope Geochemistry

TABLE 4.1: Geologically Useful Long-Lived Radioactive Decay Schemes

Parent	Decay Mode	λ	Half-life	Daughter	Ratio
^{40}K	β^+ , e.c, β^-	$5.543 \times 10^{-10} \text{y}^{-1}$	$1.28 \times 10^9 \text{yr}$	^{40}Ar , ^{40}Ca	$^{40}\text{Ar}/^{36}\text{Ar}$
^{87}Rb	β^-	$1.42 \times 10^{-11} \text{y}^{-1}$	$4.8 \times 10^{10} \text{yr}$	^{87}Sr	$^{87}\text{Sr}/^{86}\text{Sr}$
^{138}La	β^-	$2.67 \times 10^{-12} \text{y}^{-1}$	$2.59 \times 10^{11} \text{yr}$	^{138}Ce , ^{138}Ba	$^{138}\text{Ce}/^{142}\text{Ce}$, $^{138}\text{Ce}/^{136}\text{Ce}$
^{147}Sm	α	$6.54 \times 10^{-12} \text{y}^{-1}$	$1.06 \times 10^{11} \text{yr}$	^{143}Nd	$^{143}\text{Nd}/^{144}\text{Nd}$
^{176}Lu	β^-	$1.94 \times 10^{-11} \text{y}^{-1}$	$3.6 \times 10^{10} \text{yr}$	^{176}Hf	$^{176}\text{Hf}/^{177}\text{Hf}$
^{187}Re	β^-	$1.64 \times 10^{-11} \text{y}^{-1}$	$4.23 \times 10^{10} \text{yr}$	^{187}Os	$^{187}\text{Os}/^{188}\text{Os}$, ($^{187}\text{Os}/^{186}\text{Os}$)
^{190}Pt	α	$1.54 \times 10^{-12} \text{y}^{-1}$	$4.50 \times 10^{11} \text{yr}$	^{186}Os	$^{186}\text{Os}/^{188}\text{Os}$
^{232}Th	α	$4.948 \times 10^{-11} \text{y}^{-1}$	$1.4 \times 10^{10} \text{yr}$	^{208}Pb , ^4He	$^{208}\text{Pb}/^{204}\text{Pb}$, $^3\text{He}/^4\text{He}$
^{235}U	α	$9.849 \times 10^{-10} \text{y}^{-1}$	$7.07 \times 10^8 \text{yr}$	^{207}Pb , ^4He	$^{207}\text{Pb}/^{204}\text{Pb}$, $^3\text{He}/^4\text{He}$
^{238}U	α	$1.551 \times 10^{-10} \text{y}^{-1}$	$4.47 \times 10^9 \text{yr}$	^{206}Pb , ^4He	$^{206}\text{Pb}/^{204}\text{Pb}$, $^3\text{He}/^4\text{He}$

Note: the branching ratio, i.e. ratios of decays to ^{40}Ar to total decays of ^{40}K is 0.117. ^{147}Sm and ^{190}Pt also produce ^4He , but a trivial amount compared to U and Th.

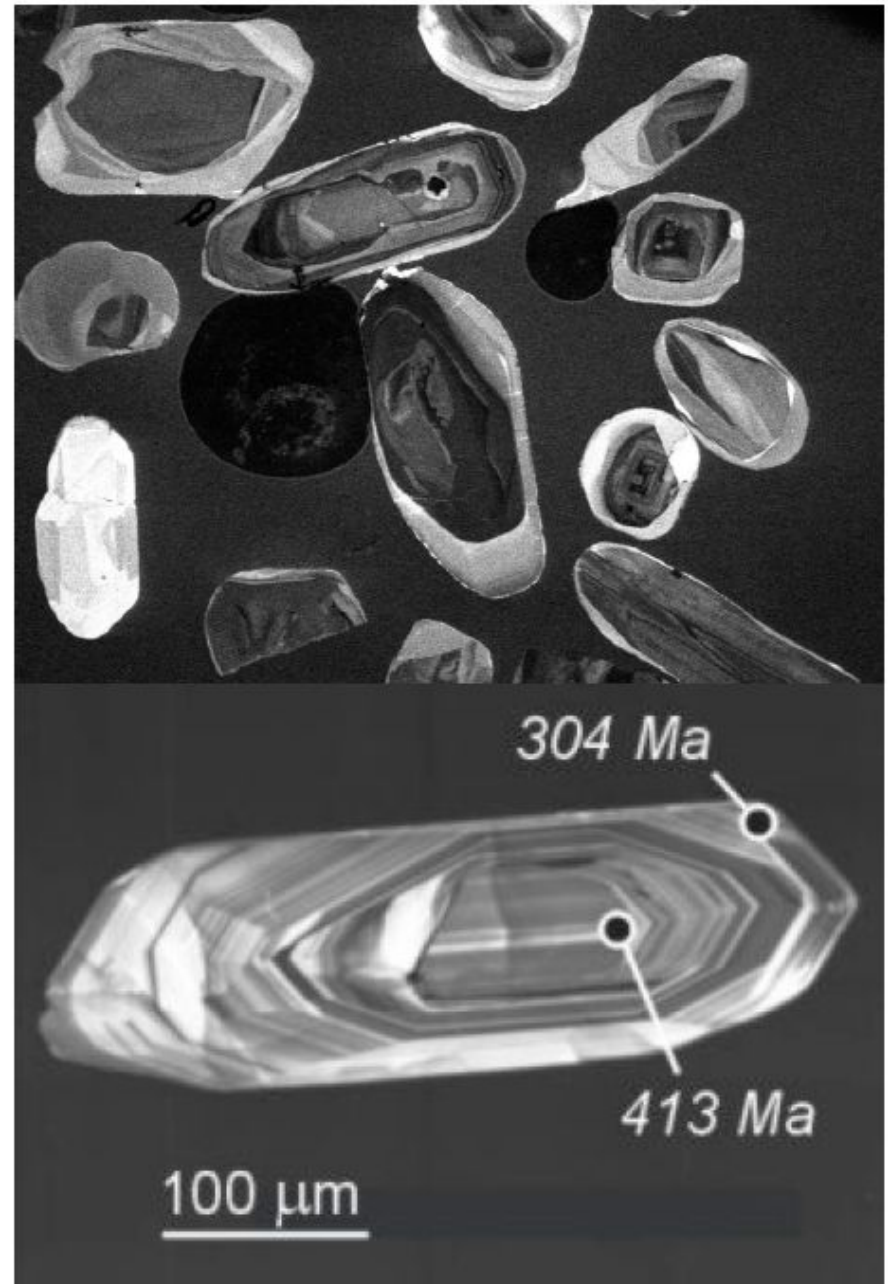
Isotope Geochemistry

Prerequisite:

stable minerals!!

No exchange of parent or
daughter elements with
surrounding

→ zircon



Archean-eon craton were found in the area of the Nuvvuagittuq greenstone belt in northern Quebec.



- Different ages determined: ca. 3,7 billion years and ca. 4,3 billion years.
- Dispute so far unsolved...
- Evidence for fossils of microorganisms discovered in these rocks, which would be the oldest trace of life yet discovered on Earth.

Age determination of Nuvvuagittuq Greenstone Belt

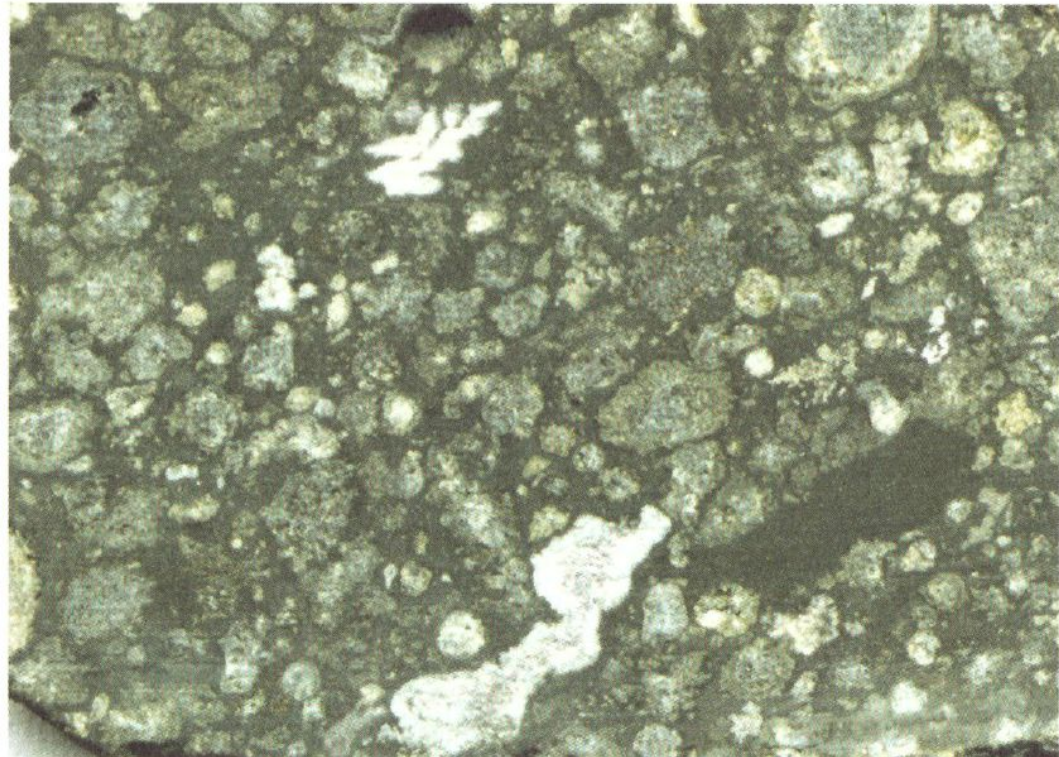
- U-Pb dating on zircons → minimum of 3.7 billion years old.
Done 2007 on zircons found within granitic intrusions that cut portions of the belt, and therefore, are younger than the features it cuts.
-> This measurement is widely accepted.
-> It alone does not provide a maximum age.
- Sm-Nd dating and Nd isotope fractionation in 2012 → age of 4.3 billion years
-> dating of intruding gabbros and measuring neodymium isotope fractionation in less-deformed members of a sub-unit.
->The age of 4.3 billion years would make the NGB the oldest known rocks on Earth.
- Detrital zircons from quartz–biotite schists → max age of 3780 Ma.
→ This study states that the age of 4.3 billion years reflects isotope ratios inherited from Hadean crust that was melted to form the parent rocks of the NGB.

Chondrites („stone meteorites“)

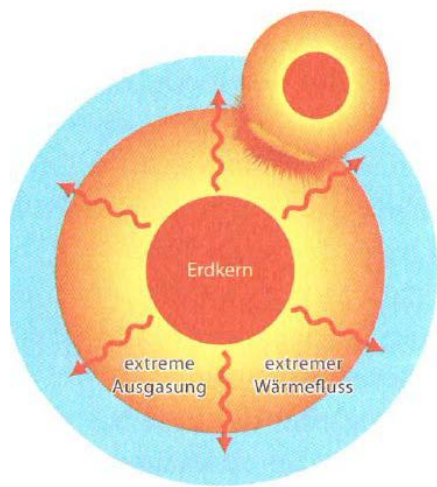
- provides important clues for understanding the origin and age of the Solar System
- formed during accretion in the early Solar System to form primitive asteroids
- Dating using $^{206}\text{Pb}/^{204}\text{Pb}$ gives an estimated age of $4,566.6 \pm 1.0$ Ma
- chondrules, millimetre-sized spherical objects that originated as freely floating, molten or partially molten droplets in space; most chondrules are rich in the silicate minerals olivine and pyroxene. To lesser extend also: Ca minerals and Al, metallic Fe-Ni and sulfides, Phyllosilicates, Magnetite, ..

Abb. 2-10 |

Der kohlige Meteorit Allende (Durchmesser etwa 10 cm) ist aus mm-großen Silikat-kügelchen (Chondren) aufgebaut (Basilico Fresco/Wikipedia).

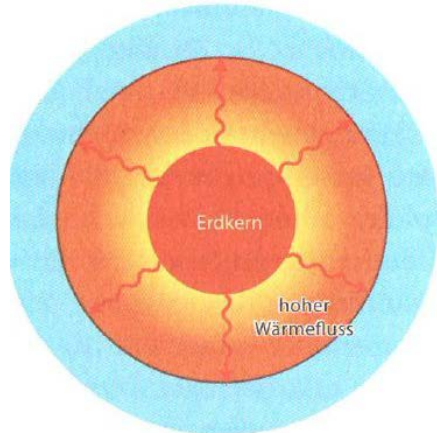


The early stages of the Early Earth



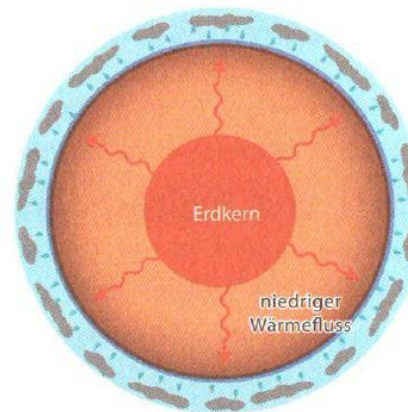
30–60 Millionen Jahre nach Entstehung der Protoerde

- 1 Giant Impact führte zur Aufheizung und Zerrüttung des Erdmantels (Oberflächentemperatur $\sim 2000^\circ\text{C}$).
- 2 Extreme H_2O - und CO_2 - Ausgasung.
- 3 Bildung einer sehr dichten Protoatmosphäre aus H_2O , CO_2 und gasförmigen Metallen (Druck $\sim 300\text{--}500$ Bar).



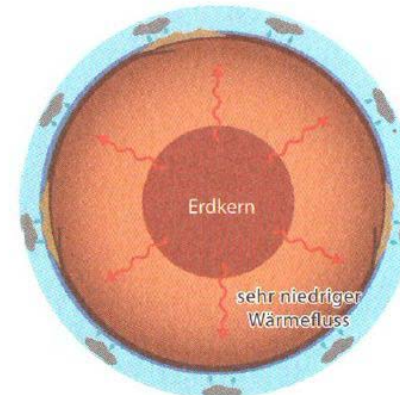
70–100 Millionen Jahre nach Entstehung der Protoerde

- 4 Langsame Abkühlung (Oberflächentemperatur $\sim 1000^\circ\text{C}$); Kondensation und Erstarren der M Bildung einer dünnen peridotitischen Kruste.
- 5 Sehr dichte Protoatmosphäre aus H_2O und C ($P_{\text{H}_2\text{O}} > 200$ Bar und $P_{\text{CO}_2} \sim 50\text{--}200$ Bar).



160–400 Millionen Jahre nach Entstehung der Protoerde

- 6 Weitere Abkühlung (Oberflächentemperatur $< 200^\circ\text{C}$) Kondensation von Wasser, Ausregnen des Ozeans.
- 7 Residuale Atmosphäre aus CO_2 und wenig H_2O ($P_{\text{CO}_2} \sim 50\text{--}200$ Bar).



Jünger als 400 Millionen Jahre nach Entstehung der Protoerde

- 8 Beginn der Plattentektonik, erste Proto-Kontinente Einsetzen des Kohlenstoffkreislaufs durch Basaltverwitterung; erste Karbonatbildung; CO_2 - und H_2O -Recycling in den Mantel durch Subduktion (Oberflächentemperaturen $\sim 20\text{--}150^\circ\text{C}$);
- 9 Residuale Atmosphäre aus CO_2 ($P_{\text{CO}_2} \sim 5\text{--}20$ Bar).

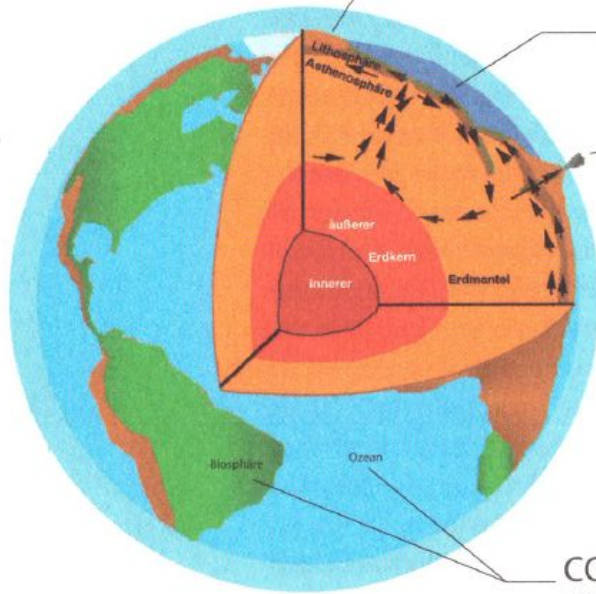
Silikat-Karbonat-Kreislauf

Verwitterung von Silikaten
 $\text{CaSiO}_3 + 2\text{CO}_2 + \text{H}_2\text{O} \rightarrow \text{Ca}^{2+} + 2\text{HCO}_3^- + \text{SiO}_2$

Kalkbildung
 $\text{Ca}^{2+} + 2\text{HCO}_3^- \rightarrow \text{CaCO}_3 + \text{CO}_2 + \text{H}_2\text{O}$

Subduktion und Vulkanismus
 $\text{CaCO}_3 + \text{SiO}_2 \rightarrow \text{CaSiO}_3 + \text{CO}_2$

CO_2 -organischer Kohlenstoffkreislauf
 $\text{CO}_2 + \text{H}_2\text{O} \rightarrow \text{CH}_2\text{O} + \text{O}_2$

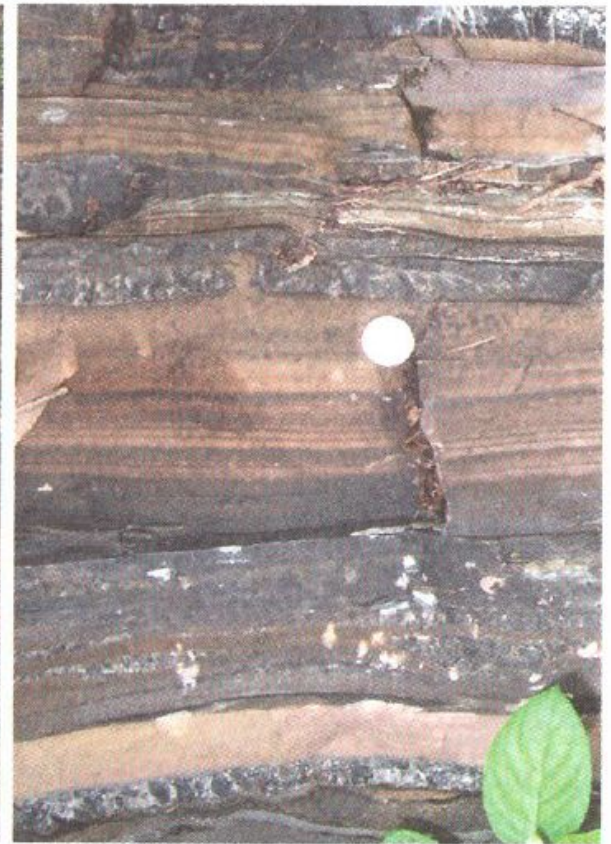
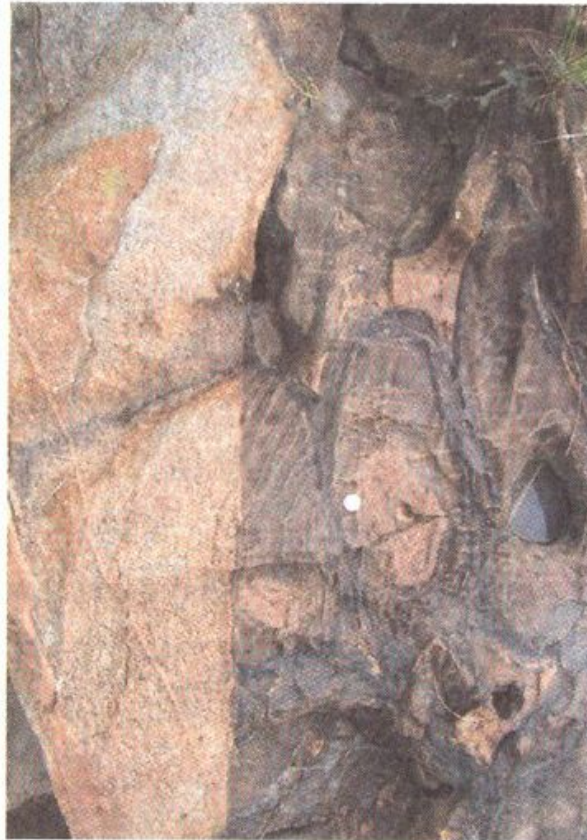


Prerequisite for silicate-carbonate-cycle: Plate tectonics

Mantel) ausgetauscht. Voraussetzung für den **Silikat-Karbonat-Kreislauf** ist die Plattentektonik. Mit deren Beginn setzte auch der Silikat-Karbonat-Kreislauf ein. Der hohe CO_2 -Gehalt der Atmosphäre verursachte einen «sauren Regen» und damit eine hohe Verwitterungsrate an der Erdoberfläche, bei der Kalziumsilikat (CaSiO_3) mit CO_2 reagiert. Dabei entstehen Kalzium- (Ca^{2+}) und Hydrogenkarbonationen (HCO_3^-) und Kieselsäure (SiO_2). Ca^{2+} und HCO_3^- werden über die Flüsse in die Ozeane transportiert und reagieren dort zu Kalk (CaCO_3), CO_2 und H_2O . Bei der Subduktion reagiert der subduzierte Kalk mit Kieselsäure und bildet wieder Kalziumsilikat und CO_2 , das teilweise über den Vulkanismus wieder in die Atmosphäre eingebracht wird. In der Bilanz sind diese Reaktionen ausgeglichen. Allerdings verlaufen die Teilreaktionen in verschiedenen erdgeschichtlichen Abschnitten unterschiedlich schnell ab, was zu starken Schwankungen im CO_2 -Gehalt der Atmosphäre führt und damit entweder ein **Treibhaus-** oder ein **Eiszeitklima** fördert. Langfristig ist der Transport in den

Abb. 4-3 |

Links: Archaische Pillow-Lava aus dem Barberton-Grünsteingürtel von Südafrika. Die Entgasungskanäle belegen eine Entstehung im Flachwasser. Mitte: Kontakt von TTG zu Pillowlaven aus dem Barberton-Grünsteingürtel. Rechts: Sedimentäre Cherts aus dem Barberton-Grünsteingürtel in Südafrika (Photos: Armin Zeh, Frankfurt).



Die ältesten bislang datierten Gesteine stammen alle aus Nordamerika (verändert nach Eisbacher 1996 aus Walter 2014): Der Nuvvuagittuq Greenstone Belt, aus der Superior Provinz (möglicherweise ~ 4,3 Mia. Jahre) und der Acasta-Gneis (~ 4 Mia. Jahre), beide aus Kanada, sowie der Amitsoq-Gneis mit dem Isua-Grünsteingürtel (~ 3,9 Mia. Jahre) aus Südgrönland.

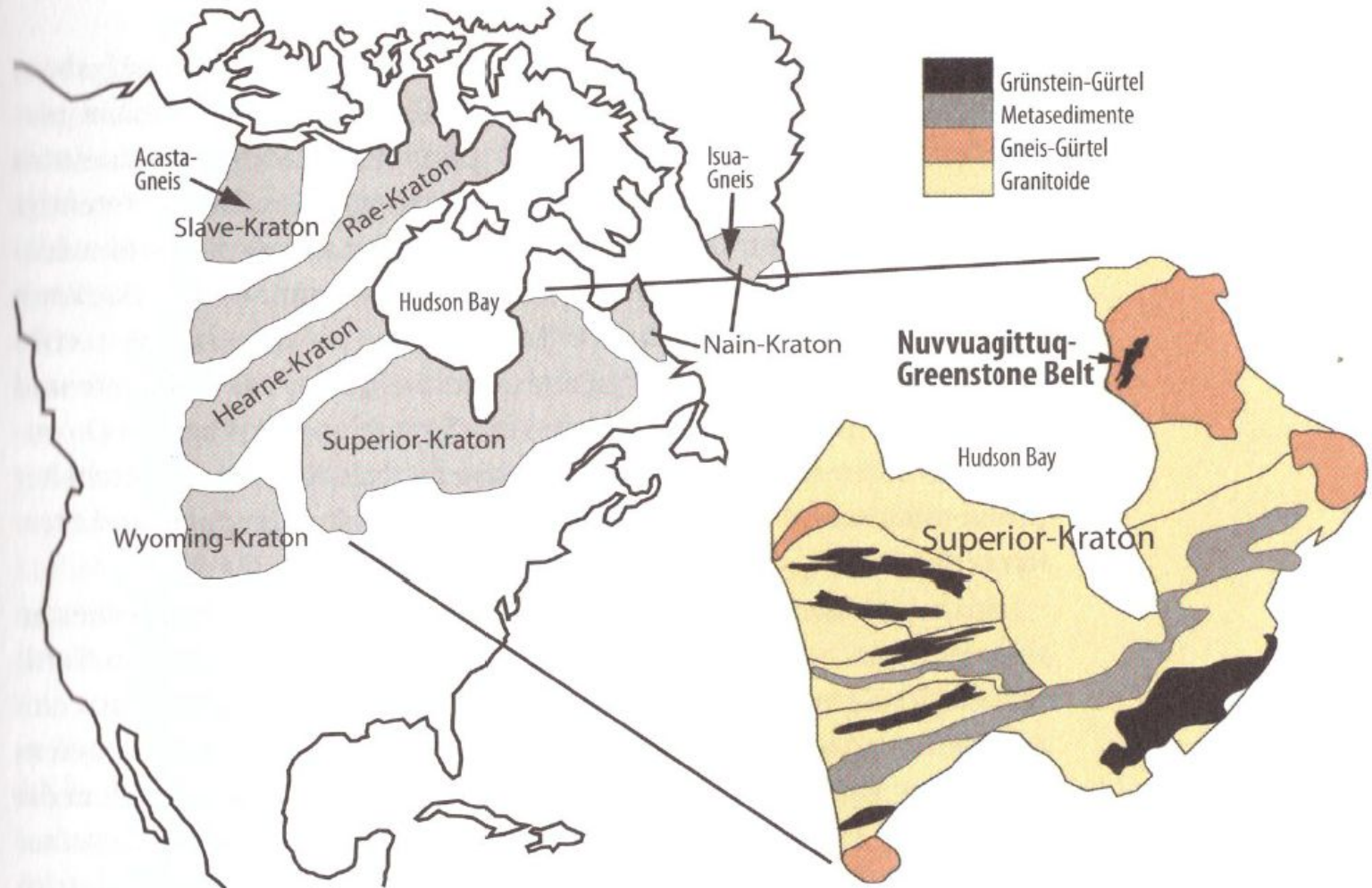
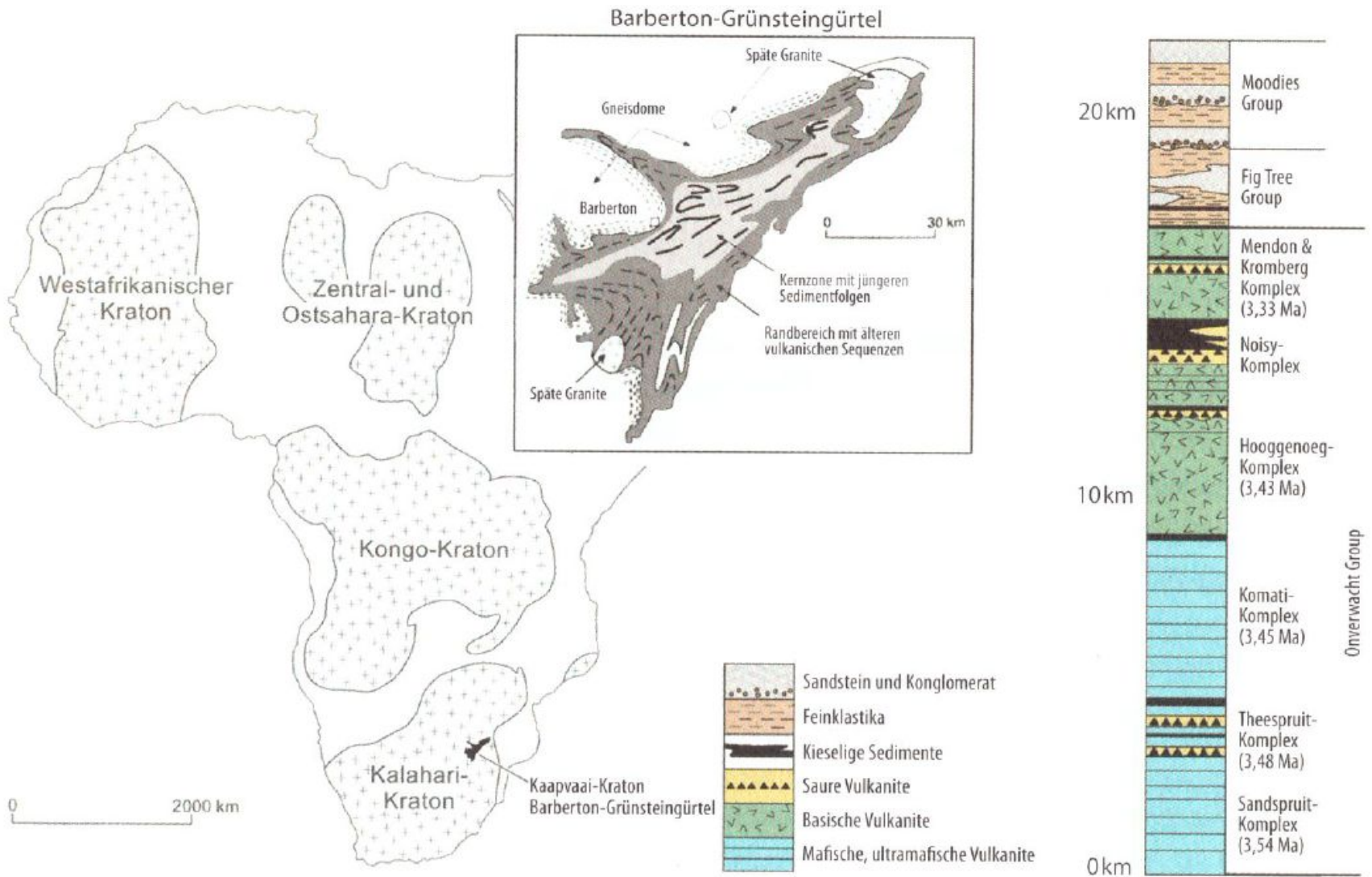


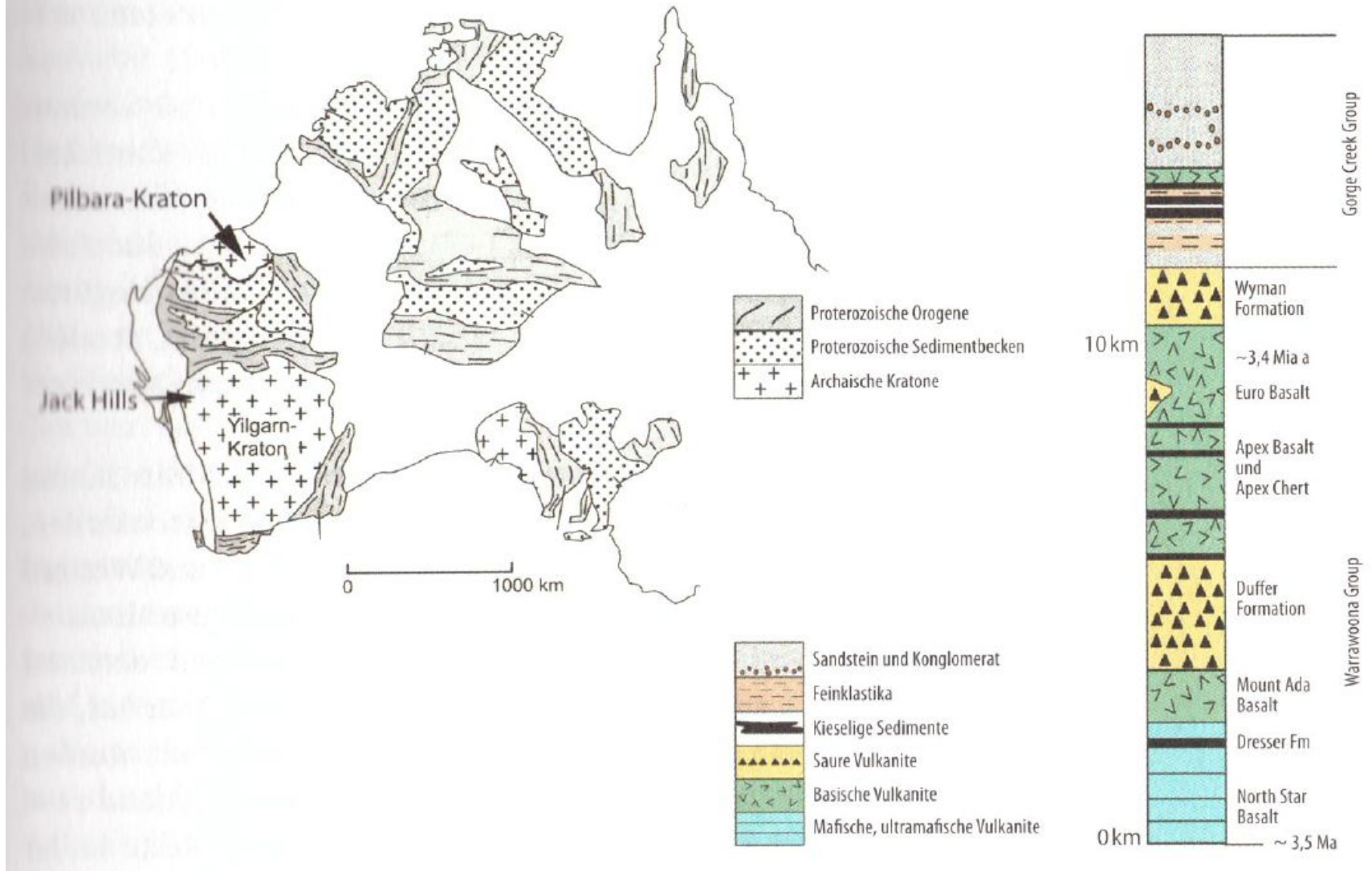
Abb. 4-5

Afrika wird aus mehreren archaischen Kratonen aufgebaut. (modifiziert nach Walter 2014, Stanley 2001 und Furnes et al. 2013).



Die Kratone in Australien (modifiziert nach Walter 2014 und Stanley 2001).

Abb. 4-6



Neoproterozoikum

sehr hohe Raten der oxischen Photosynthese durch Eucaryota und Metabionta $\text{CO}_2 + \text{H}_2\text{O} \xrightarrow{\text{Licht}} \text{CH}_2\text{O} + \text{O}_2$

Sehr wenig CH_4 , wenig CO_2 , viel O_2

Resultat: neoproterozoische Eiszeit

Spätes Paläoproterozoikum und Mesoproterozoikum

Anstieg der Solarstrahlung und der CO_2 -Konzentration durch Karbonatbildung. Resultat: keine Eiszeit

Frühes Paläoproterozoikum

Maximum der Krustenbildung, intensive Verwitterung, oxische Photosynthese: $\text{CO}_2 + \text{H}_2\text{O} \xrightarrow{\text{Licht}} \text{CH}_2\text{O} + \text{O}_2$

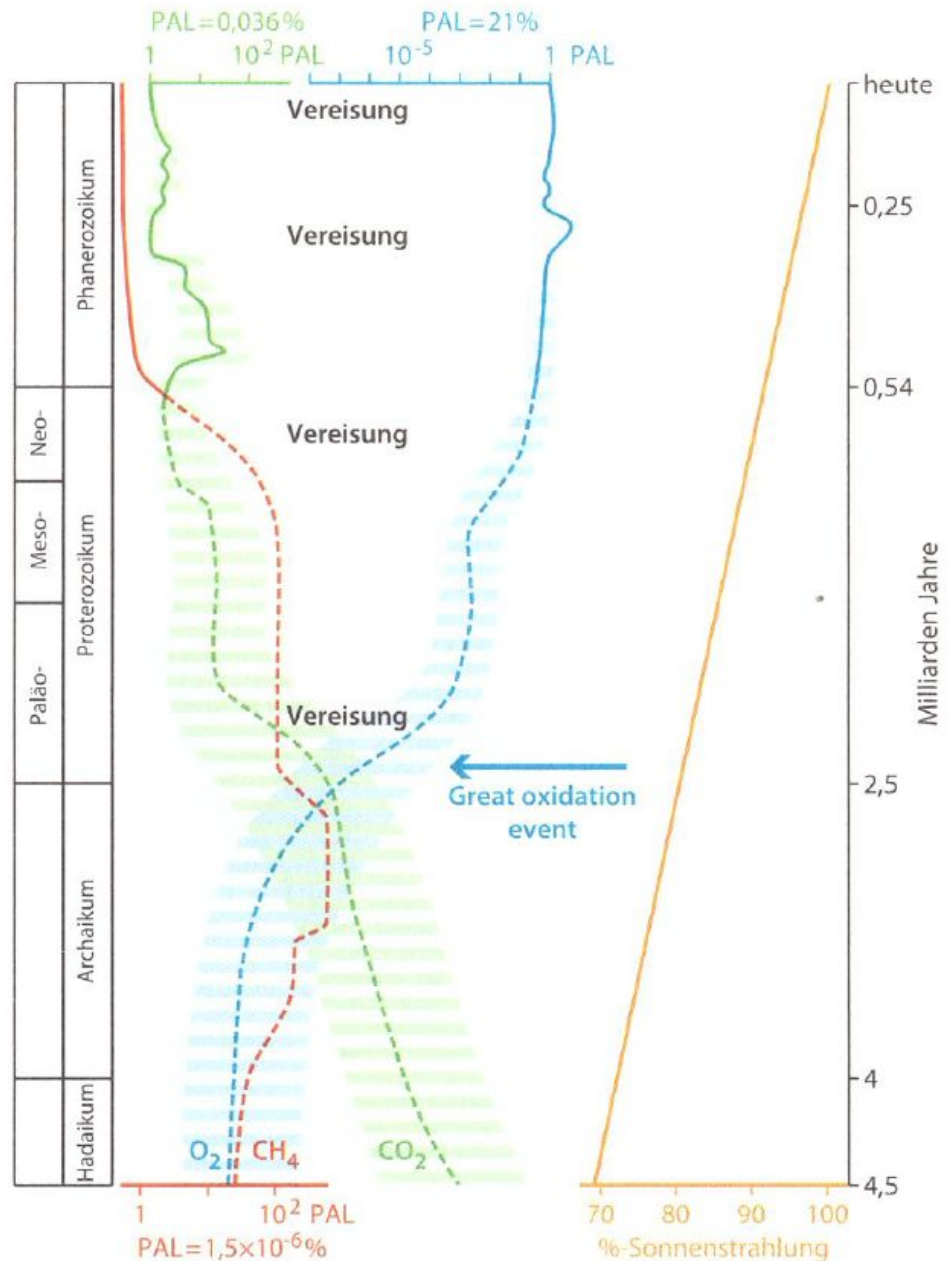
Wenig CH_4 , wenig CO_2 führen zur huronischen Eiszeit

Archaikum

anoxische Photosynthese: $\text{CO}_2 + 2\text{H}_2\text{S} \xrightarrow{\text{Licht}} \text{CH}_2\text{O} + \text{H}_2\text{O} + 2\text{S}$

Methanogenese: $\text{CH}_2\text{O} \longrightarrow \text{CO}_2 + \text{CH}_4$

Methan als sehr effektives Treibhausgas verhindert eine Eiszeit.



Annual Review of Earth and Planetary Sciences

Earth's Continental Lithosphere Through Time

Chris J. Hawkesworth,^{1,2} Peter A. Cawood,^{2,3}
Bruno Dhuime,^{1,4} and Tony I.S. Kemp⁵

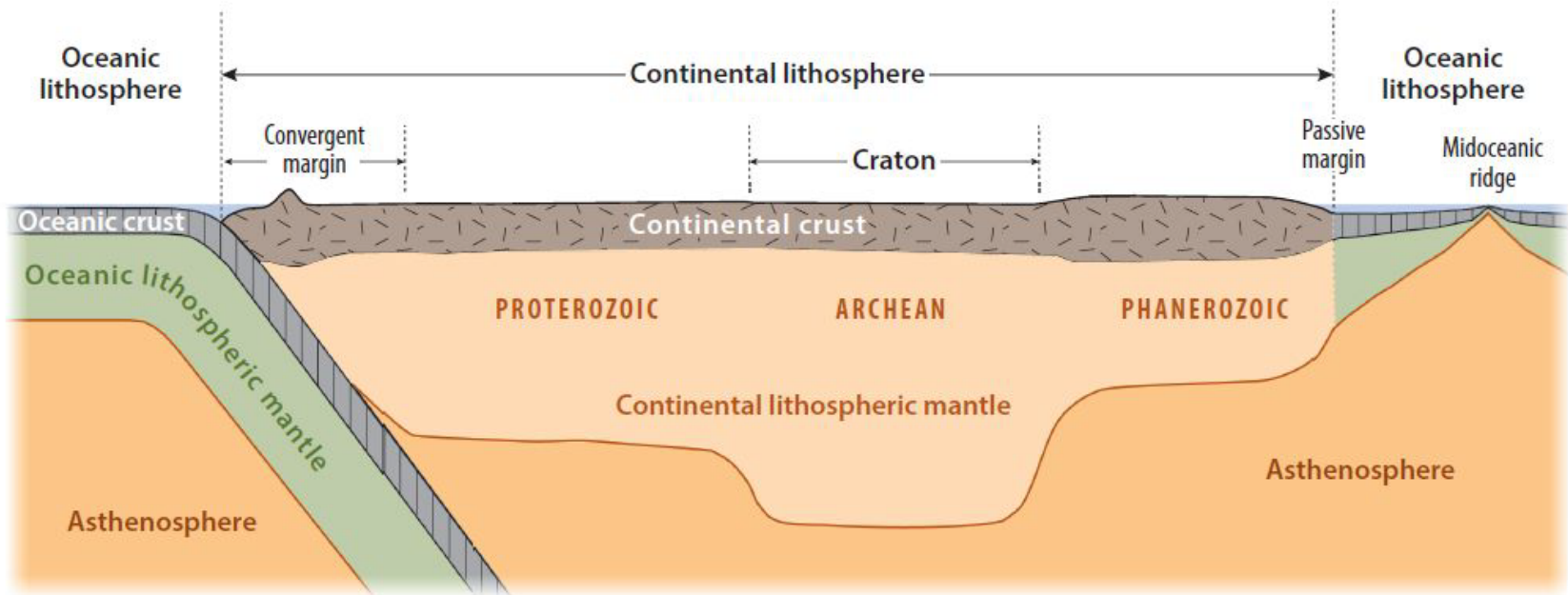
¹School of Earth Sciences, University of Bristol, Bristol BS8 1RJ, United Kingdom;
email: c.j.hawkesworth@bristol.ac.uk, B.Dhuime@bristol.ac.uk

²School of Earth and Environmental Sciences, University of St. Andrews, St. Andrews KY16
9AL, United Kingdom

³School of Earth, Atmosphere & Environment, Monash University, Melbourne, VIC 3800,
Australia; email: peter.cawood@monash.edu

⁴CNRS-UMR 5243, Géosciences Montpellier, Université de Montpellier, 34095 Montpellier
Cedex 05, France

⁵School of Earth Sciences, University of Western Australia, Perth, WA 6009, Australia;
email: tony.kemp@uwa.edu.au



Crystallization age

Age of crystallization of a mineral or rock from a melt

Model age

Age at which new crust is generated from the mantle

Depleted mantle

Mantle depleted through extraction of one or more basaltic melts

Crust generation

Formation of new crust; extracted from the mantle

Crust recycling (and destruction)

Return of crust to the mantle

Crust reworking

Intracrustal remobilization, involving erosion and sedimentation, and/or (re)melting of preexisting crustal rocks

Growth of crust

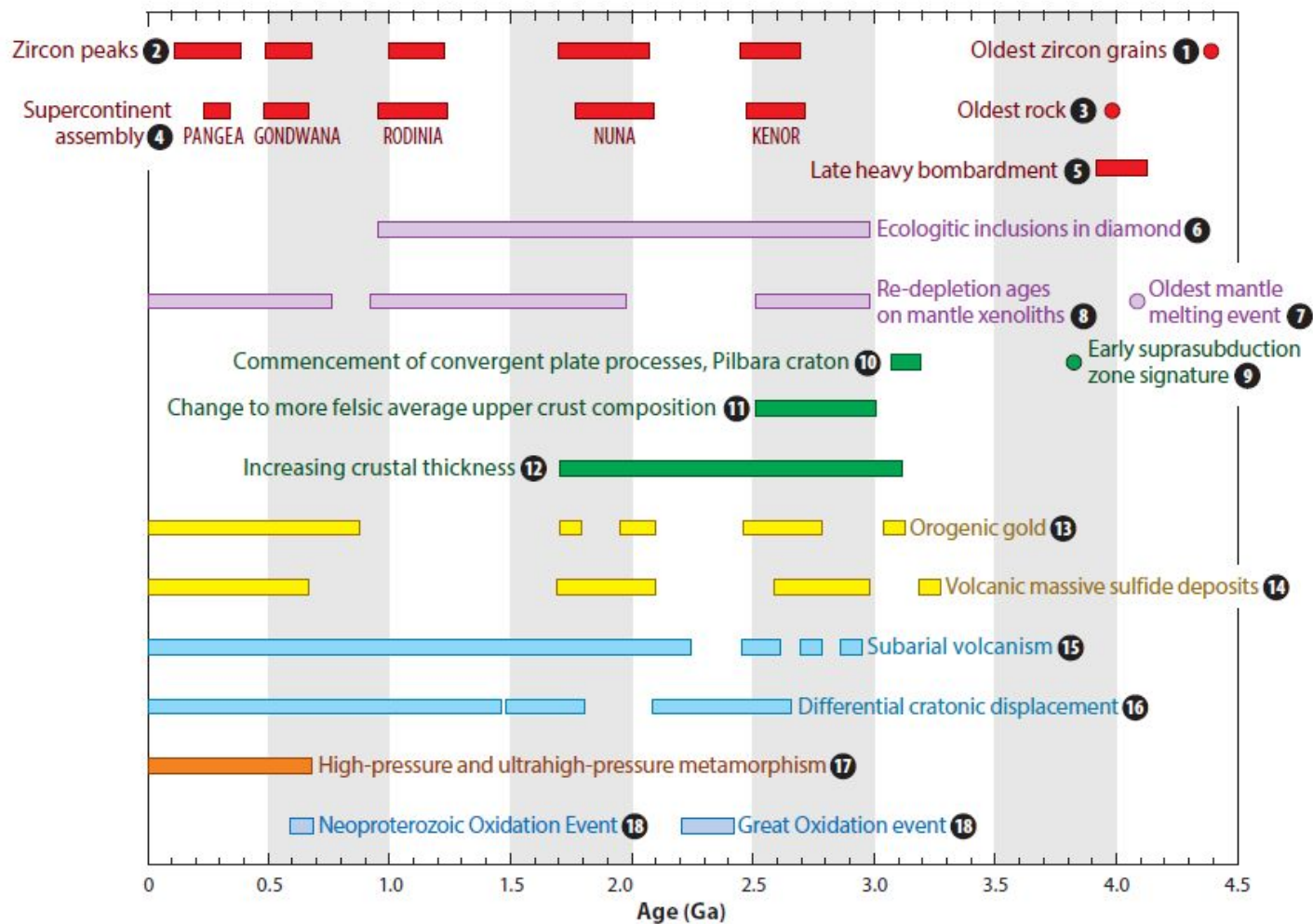
The volume of new crust less the amount lost by recycling

Supercontinents

Assembly of large volumes of continental crust, i.e., redistribution of continental crust on Earth's surface

Figure 1

Schematic cross section of types of continental lithosphere emphasizing the thick stable nature of Archean cratons, accompanied by a glossary of some of the terms used. Thickness of lithosphere beneath Archean regions is of the order of 200–250 km, and that of the oceanic lithosphere is up to 100 km (after Cawood et al. 2013).



- ① Wilde et al. 2001
- ② Voice et al. 2011 and references therein
- ③ Bowring & Williams 1999
- ④ Adapted from Campbell & Allen 2008
- ⑤ Marchi et al. 2014
- ⑥ Shirey & Richardson 2011
- ⑦ Malitch & Merkle 2004
- ⑧ Figure 5 and references
- ⑨ Jenner et al. 2009, O'Neil et al. 2011, and Turner et al. 2014

- ⑩ Smithies et al. 2007 and Van Kranendonk et al. 2007
- ⑪ Keller & Schoene 2012 and Tang et al. 2016
- ⑫ Dhuime et al. 2015
- ⑬ Goldfarb et al. 2001
- ⑭ Mosier et al. 2009
- ⑮ Kump & Barley 2007, Shields 2007, Cawood et al. 2013, and Flament et al. 2013
- ⑯ Cawood et al. 2006, Evans & Pisarevsky 2008
- ⑰ Brown 2006, 2007, 2014
- ⑱ Campbell & Squire 2010, Farquhar et al. 2013 and references therein

Source: Hawkesworth et al. *Ann Rev EPS* (2017)

Figure 2

Ages (*circles*) and age ranges (*bars*) of major events and cycles preserved in Earth history. Sources of the data are indicated in the figure key: (1) The oldest terrestrial fragments, zircons from the Jack Hills; (2) the age range of principal peaks in U-Pb crystallization ages; (3) the oldest rocks, Slave craton; (4) the approximate age range of supercontinent assembly; (5) the late heavy bombardment; (6) the age range of eclogitic inclusions in diamonds; (7) the oldest Os model ages from detrital osmiridium grains, Witwatersrand Basin; (8) Re-depletion age ranges for peridotite xenoliths (see also **Figure 5**); (9) the ~3.8 Ga Nuvvuagittuq greenstone belt, Superior craton, and 3.85 Ga metabasalts from Isua, Greenland, are similar to modern subduction-related islands; (10) the pre-3.2 Ga rock units from Pilbara craton are associated with vertical tectonics, and rocks younger than 3.1 Ga are inferred to have formed by plate subduction processes; (11) the shift from predominantly mafic crustal compositions prior to 3.0 Ga to increasingly felsic compositions by 2.5 Ga; (12) the secular increase in time-integrated Rb/Sr ratios between 3.1 Ga and 1.7 Ga, indicative of a doubling in average continental crustal thickness from ca. 20 km to ca. 40 km; (13) the main pulses of orogenic gold deposition; (14) the main pulses of volcanic-hosted massive sulfide deposits; (15) subaerial large igneous province magmatism increases from 3.0 to 2.5 Ga, corresponding with the increase in $^{87}\text{Sr}/^{86}\text{Sr}$ ratios of seawater consistent with the emergence and weathering of continental crust; (16) the significant difference between the relative paleopositions of the Kaapvaal and Superior cratons at 2.68 Ga and 2.07 Ga and Baltica and Australia between 1.77 Ga and 1.5 Ga; (17) the high-pressure and ultrahigh-pressure metamorphism, which are limited to rock units dated at <0.7 Ga; and (18) the increases in atmospheric oxygen values during the Great Oxidation Event and the Neoproterozoic Oxidation Event.

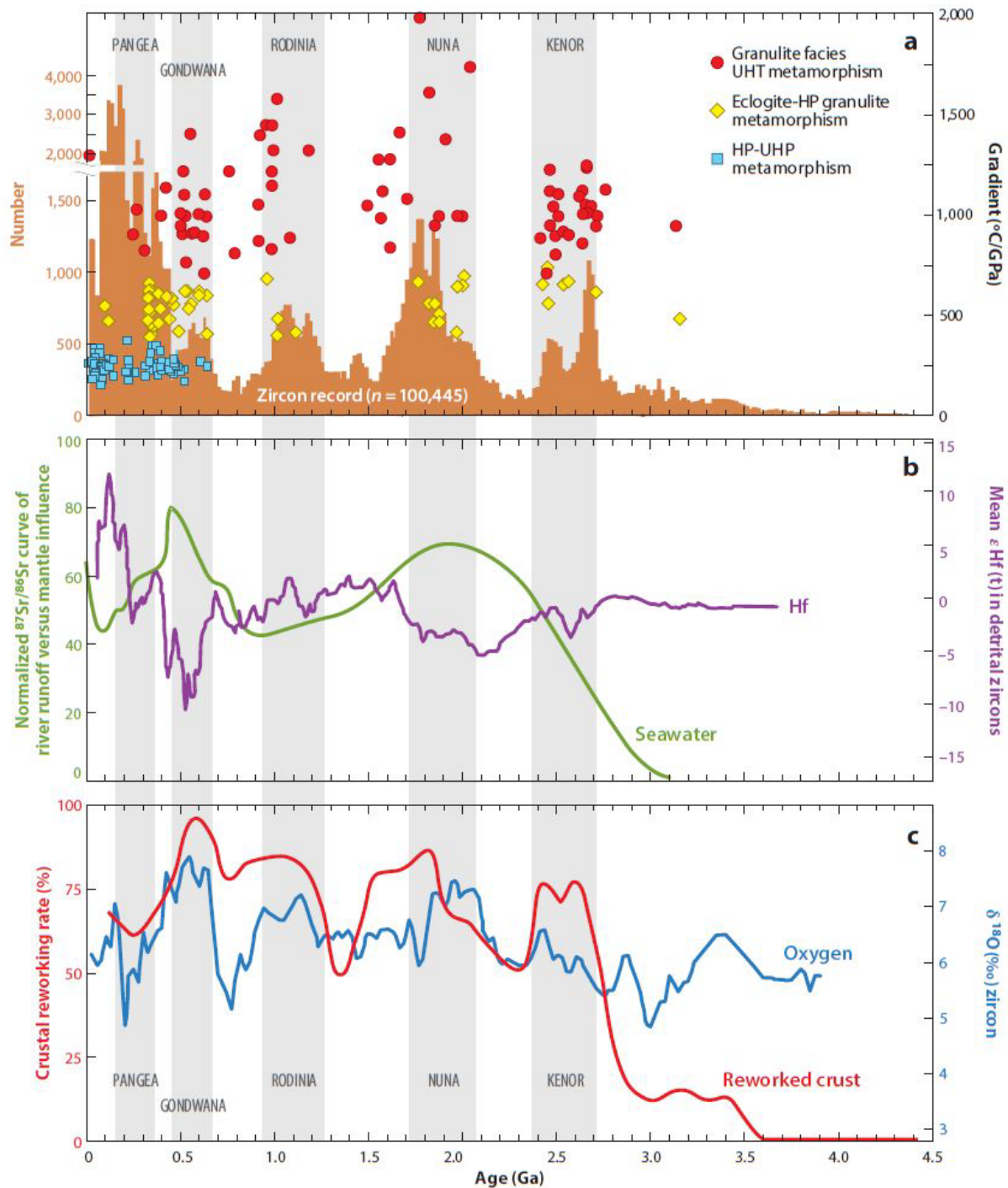


Figure 3

(a) Histogram of over 100,000 detrital zircon analyses showing peaks in U-Pb crystallization ages over the course of Earth history (Voice et al. 2011), which are similar to the ages of supercontinent assembly. Also shown is the apparent thermal gradient at the age of peak metamorphism for the three main types of extreme metamorphic belts (Brown 2007, 2014). (b) Normalized seawater $^{87}\text{Sr}/^{86}\text{Sr}$ curve (Shields 2007), and the running mean of initial ϵHf in $\sim 7,000$ detrital zircons from recent sediments (Cawood et al. 2013). (c) The red curve represents changes in the degrees of reworking of the continental crust through time, calculated from the distributions of the proportions of reworked crust and new crust, calculated from Hf isotope variations in zircons (Dhuime et al. 2012). The blue curve is the moving average distilled from compilation of $\sim 3,300$ $\delta^{18}\text{O}$ analyses of zircon versus U-Pb ages (Spencer et al. 2014). Abbreviations: HP, high-pressure; UHP, ultrahigh-pressure; UHT, ultrahigh-temperature. ϵHf is a measure of the deviation of the Hf isotope ratios of a sample from that of a chondritic reservoir, taken to be the bulk earth, as expressed in

$$\epsilon\text{Hf} = \left[\frac{(^{176}\text{Hf}/^{177}\text{Hf})_{\text{sample}} - (^{176}\text{Hf}/^{177}\text{Hf})_{\text{Chon}}}{(^{176}\text{Hf}/^{177}\text{Hf})_{\text{Chon}}} \right] \times 10,000.$$

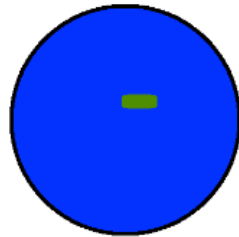
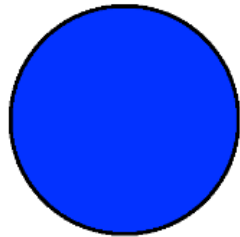
Source: Hawkesworth et al. *Ann Rev EPS* (2017)

THE SUPERCONTINENT CYCLE

The supercontinent cycle refers to the periodic aggregation of most of the extant continental lithosphere into a single entity. Several supercontinents are recognized: Pangea in the Mesozoic, Pannotia (including Gondwana) in the late Neoproterozoic, Rodinia in the early Neoproterozoic, and Columbia (including Nuna) in the Paleoproterozoic. In the Archean, fundamental differences between some of the better-known cratons suggest it is unlikely the extant continental lithosphere was ever aggregated into a single Archean supercontinent. Notwithstanding, most Archean cratons preserve evidence of rifted margins of Proterozoic age, which suggests they were once fragments of several larger entities or supercratons.

Source: Brown et al. *Ann Rev EPS* (2020)

Supercontinent cycle - simplified



Vaalbara
~3 Gya



Ur
~3 Gya



Kenorland
~2.72 Gya



Columbia/Nuna
~2 Gya



Rodinia
~1 Gya



Pannotia
~550 Mya



Pangaea
~300 Mya



Laurasia & Gondwana
~200 Mya



Earth
Present

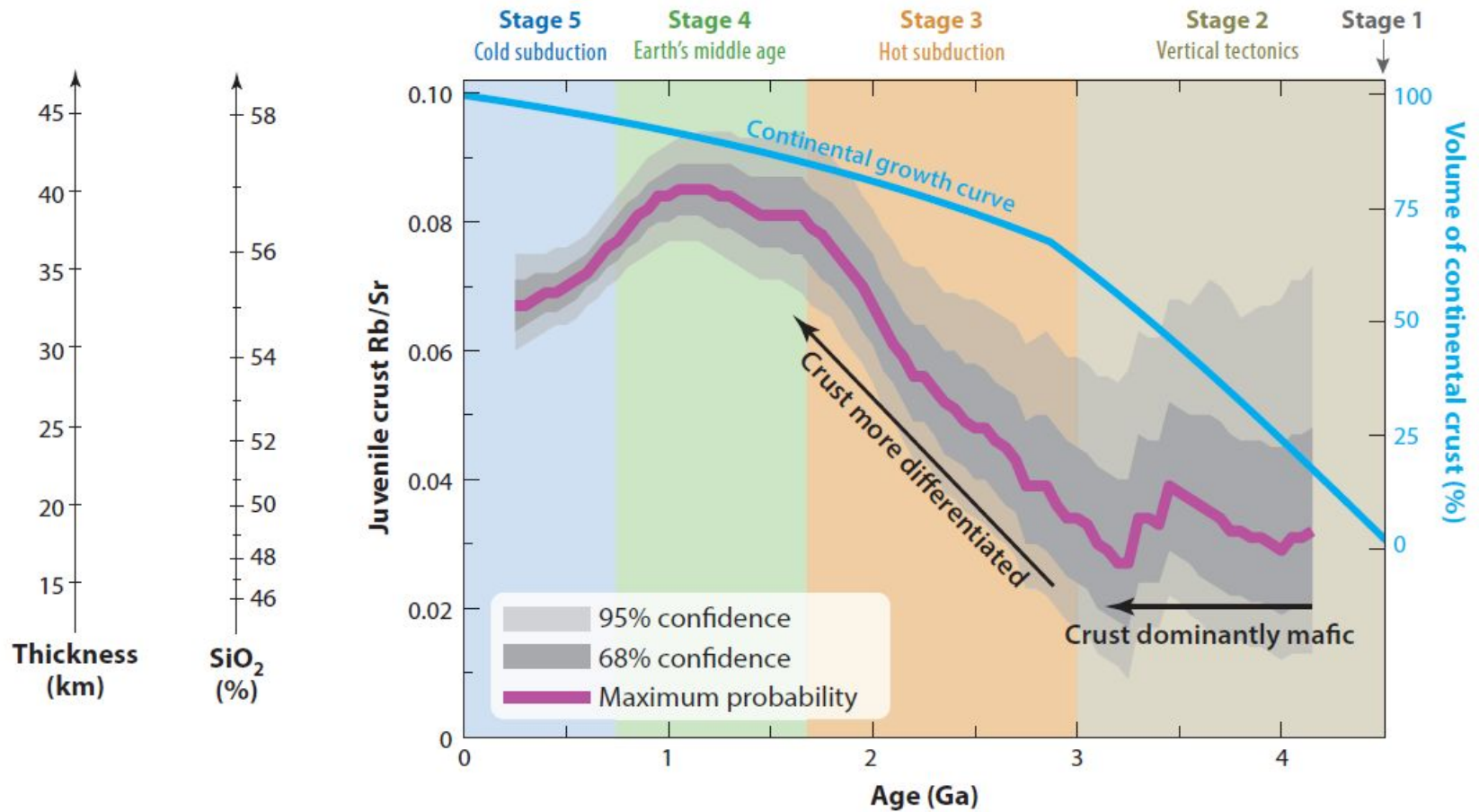


Figure 7

The estimated Rb/Sr ratios of juvenile continental crust plotted against the age of crust formation for ~13,000 whole-rock analyses (Dhuime et al. 2015). Rb/Sr increases with both whole-rock silica content and crustal thickness at the site of magma generation. The calculated volumes of continental crust from Dhuime et al. (2012) are presented for comparison. Stages of Earth evolution: Stage 1 is the early accretion of Earth, which may have persisted for 5–10 Myr (Elkins-Tanton 2008); stage 2 is dominated by vertical tectonics; stage 3 is dominated by hot subduction; stage 4 is Earth's middle age; and stage 5 is characterized by cold subduction.

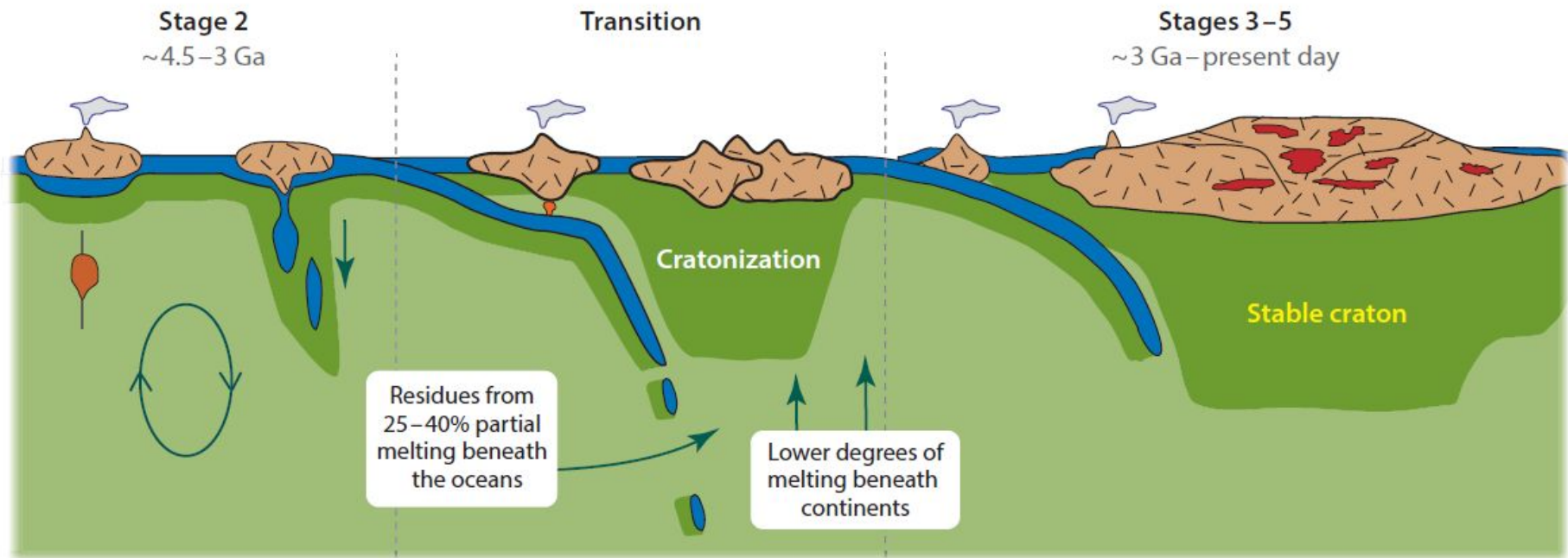


Figure 9

Schematic depiction of changing tectonic processes controlling the evolution of the lithosphere from an early Earth dominated by nonplate processes (stage 2) to one in which plate tectonics is the main mechanism for the generation and recycling of lithosphere (stages 3–5). These changes are a response to the secular cooling of the mantle and the consequent increase in lithospheric strength and rigidity. The mantle xenolith record suggests that they represent residues (from relatively shallow partial melting of hot mantle beneath the oceans), which subsequently accreted beneath continents. In contrast, the mafic crust that is the source of Archean tonalite-trondhjemite-granodiorites has relatively low Lu/Hf and Sm/Nd ratios, implying lower degrees of partial melting.

Annual Review of Earth and Planetary Sciences

Plate Tectonics and the Archean Earth

Michael Brown,¹ Tim Johnson,^{2,3}
and Nicholas J. Gardiner^{4,5}

¹Laboratory for Crustal Petrology, Department of Geology, University of Maryland,
College Park, Maryland 20742, USA; email: mbrown@umd.edu

²School of Earth and Planetary Sciences, The Institute for Geoscience Research (TIGeR), Space
Science and Technology Centre, Curtin University, Perth, Western Australia 6845, Australia

³State Key Laboratory of Geological Processes and Mineral Resources, China University of
Geosciences, Wuhan, Hubei Province 430074, China

⁴School of Earth and Environmental Sciences, University of St Andrews, St Andrews KY16 9AL,
United Kingdom

⁵School of Earth, Atmosphere and Environment, Monash University, Victoria 3800, Australia

Plate Tectonics and the Archean Earth

Michael Brown,¹ Tim Johnson,^{2,3}
and Nicholas J. Gardiner^{4,5}

Abstract

If we accept that a critical condition for plate tectonics is the creation and maintenance of a global network of narrow boundaries separating multiple plates, then to argue for plate tectonics during the Archean requires more than a local record of subduction. A case is made for plate tectonics back to the early Paleoproterozoic, when a cycle of breakup and collision led to formation of the supercontinent Columbia, and bimodal metamorphism is registered globally. Before this, less preserved crust and survivorship bias become greater concerns, and the geological record may yield only a lower limit on the emergence of plate tectonics. Higher mantle temperature in the Archean precluded or limited stable subduction, requiring a transition to plate tectonics from another tectonic mode. This transition is recorded by changes in geochemical proxies and interpreted based on numerical modeling. Improved understanding of the secular evolution of temperature and water in the mantle are key targets for future research.

Plate Tectonics and the Archean Earth

- Higher mantle temperature in the Archean precluded or limited stable subduction, requiring a transition to plate tectonics from another tectonic mode.
- Plate tectonics can be demonstrated on Earth since the early Paleoproterozoic (since c. 2.2 Ga), but before the Proterozoic Earth's tectonic mode remains ambiguous.
- The Mesoarchean to early Paleoproterozoic (3.2–2.3 Ga) represents a period of transition from an early tectonic mode (stagnant or sluggish lid) to plate tectonics.
- The development of a global network of narrow boundaries separating multiple plates could have been kick-started by plume-induced subduction.

Present-day plate boundaries

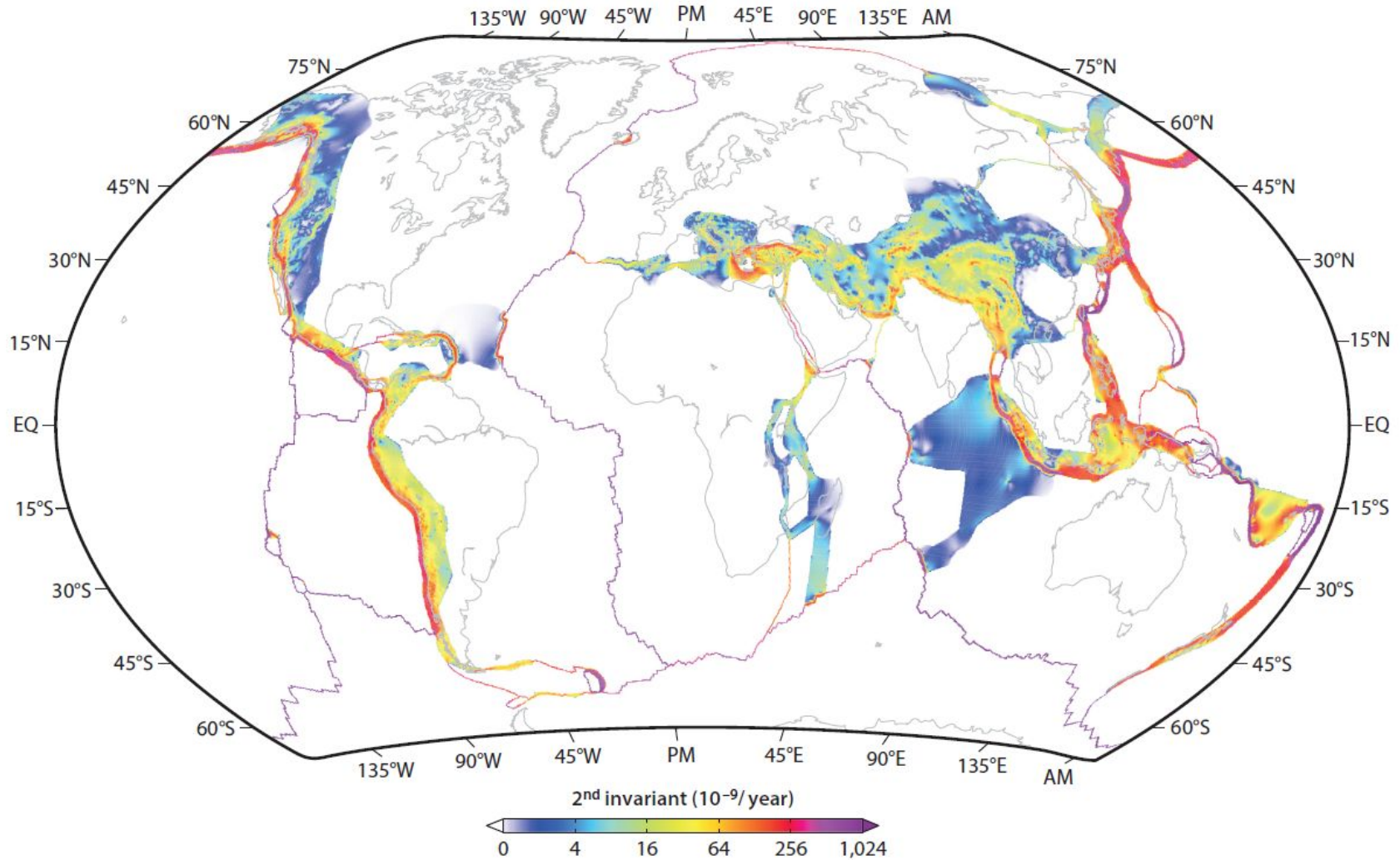


Figure 1

Map of present-day plate boundary deformation zones. White areas were assumed to be rigid plates, and the rigid body rotation of these plates was imposed as a boundary condition when solving for plate boundary strain rates from geodetic velocities. Figure adapted from Kreemer et al. (2014).

WATER IN THE EARTH

An additional complication is the critical control of water on the viscosity of the mantle. Unfortunately, how water has been distributed between the interior and surface of Earth through time is uncertain. Some have argued that present-day Earth's mantle may be highly outgassed, containing only a small fraction of its original water content. Others have suggested that Earth in the Hadean had abundant surface water and a dry mantle, implying that regassing of the mantle has dominated Earth evolution. However, recent research has demonstrated that a deep hydrous mantle reservoir has been present in Earth's interior since at least the Paleoarchean. This is another unsolved and highly contentious issue that is fundamental to the question of whether plate tectonics could have operated on the Archean Earth, but one that is beyond our scope here.

THE ARCHEAN ROCK RECORD

Plate tectonics has allowed us to make sense of almost all the large-scale features on Earth's surface. However, moving back in time, unambiguous recognition of volcanic arcs or their eroded remnants, or forearc sedimentary sequences, becomes increasingly difficult—particularly in the Archean, where field evidence is complex and ambiguous, and what remains of the crust is generally multiply deformed, fragmented, and metamorphosed. Because the rock record is limited and survivorship bias is a major concern, and Archean cratons generally do not preserve the uppermost levels of crust, where a record of subduction (for example, in the form of accretionary prisms and ophiolites) is more commonly preserved, evidence for the operation of plate tectonics in the Archean largely depends on geochemical indicators for subduction.

THE ARCHEAN ROCK RECORD

Survivorship Bias and the Geological Record in the Archean

- Rocks older than Paleoproterozoic in age (>3.6 Ga) are rare.
- Age distribution of detrital zircon grains and magmatic rocks shows a marked decline in the amount of preserved crust older than Neoproterozoic (>2.8 Ga).

→ To what extent is preserved crust older than Neoproterozoic is representative, in terms of either relative volume of rock types or the processes it records?

a) Is this crust the surviving remnants of a much larger volume that was destroyed?

b) was there only ever a small volume produced?

? How significant is the scarcity of Proterozoic crustal rocks and the almost complete absence of a Hadean rock record?

THE ARCHEAN ROCK RECORD

Key Features of Archean Geology

- Planetary differentiation is irreversible.
- Regardless of Earth's compositional and mineralogical structure immediately following the Moon-forming impact, the silicate Earth today is immeasurably more compositionally, mineralogically, and structurally complex.
- That Archean rocks are different from post-Archean geology is inevitable, irrespective of the tectonic mode in which they formed.

THE ARCHEAN ROCK RECORD

Key Features of Archean Geology

Lithological differences between pre- and post-Archean geology

- Archean continental is compositionally distinct from younger andesitic continental crust
- Furthermore, Archean upper crust may have been more mafic than post-Archean emergent crust
- Exposed Archean crust mostly comprises higher-grade gray gneiss terrains and lower-grade granite–greenstone belts with an archetypical dome-and-basin structure.
 - These probably represent the lower and upper levels of the ancient continental crust, respectively (Johnson et al. 2016), but they have also been interpreted as analogs of modern active continental arc margins and associated backarcs.
- Gray gneiss terrains are volumetrically dominated by sodic granitoids of the **tonalite–trondhjemite–granodiorite (TTG) series**. TTGs are compositionally similar to, but subtly different from, modern adakites that mostly form by partial melting of subducting hydrated oceanic crust.
Were TTGs also products of slab melting, or are other tectonic settings likely?

THE ARCHEAN ROCK RECORD

Key Features of Archean Geology

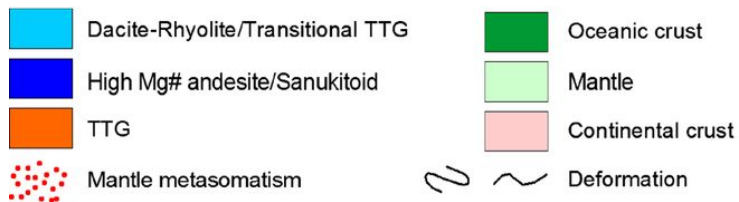
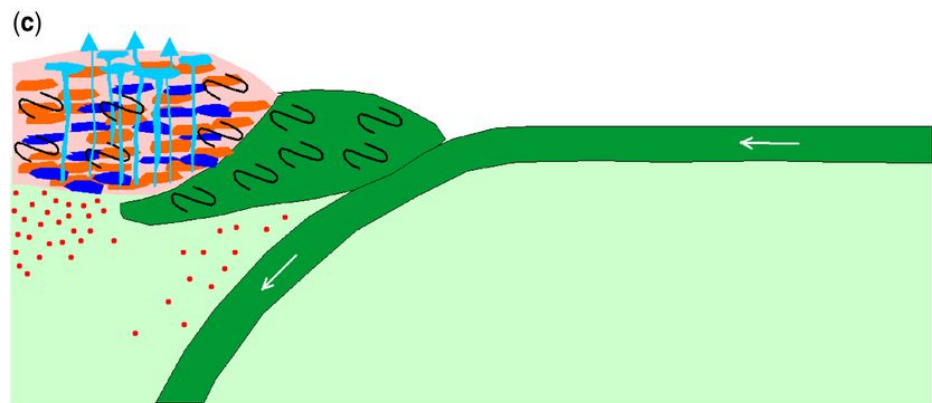
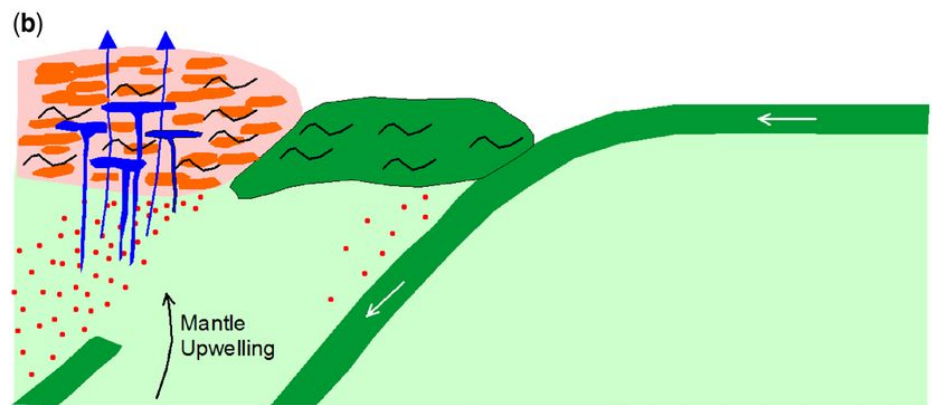
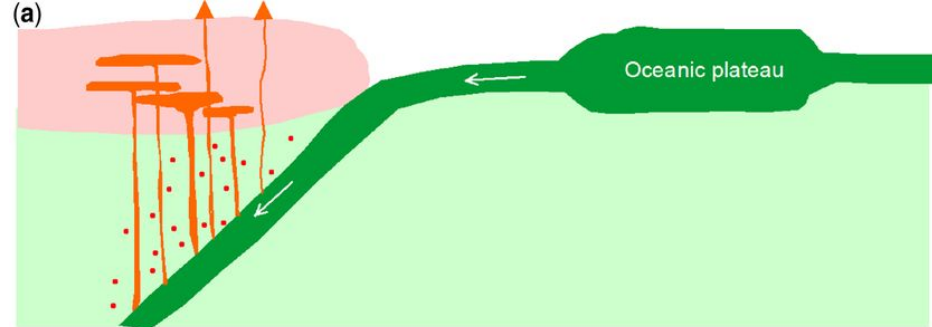
Lithological differences between pre- and post-Archean geology

tonalite–trondhjemite–granodiorite (TTG) series

THE TONALITE–TRONDHJEMITE–GRANODIORITE SUITE OF ROCKS

Archean rocks are generally found in cratons, which form the stable interiors of continents. Archean cratons are dominantly composed of gneisses derived from a variety of initial rock types, but mostly of igneous origin, many of which have been tectonically transposed during strong deformation, obscuring their original relationships. Within these gneisses, an important group of igneous rocks is the tonalite–trondhjemite–granodiorite (TTG) suite, which is largely confined to the Archean. TTGs are silica-rich ($\text{SiO}_2 > 64$ wt%, but commonly ~ 70 wt% or greater) rocks with high Al_2O_3 (15.0–16.0 wt%) and Na_2O (3.0–7.0 wt%) contents, low $\text{K}_2\text{O}/\text{Na}_2\text{O}$ (< 0.5) ratios, and low total ferromagnesian oxide (Fe_2O_3 total + MgO + MnO + $\text{TiO}_2 \leq 5$ wt%) contents. TTGs generally have fractionated rare earth element (REE) patterns and low heavy REE contents.

Neoproterozoic crustal growth by combined arc-plume action: evidence from the Kadiri Greenstone Belt, eastern Dharwar craton, India



Key Features of Archean Geology

Lithological differences between pre- and post-Archean geology

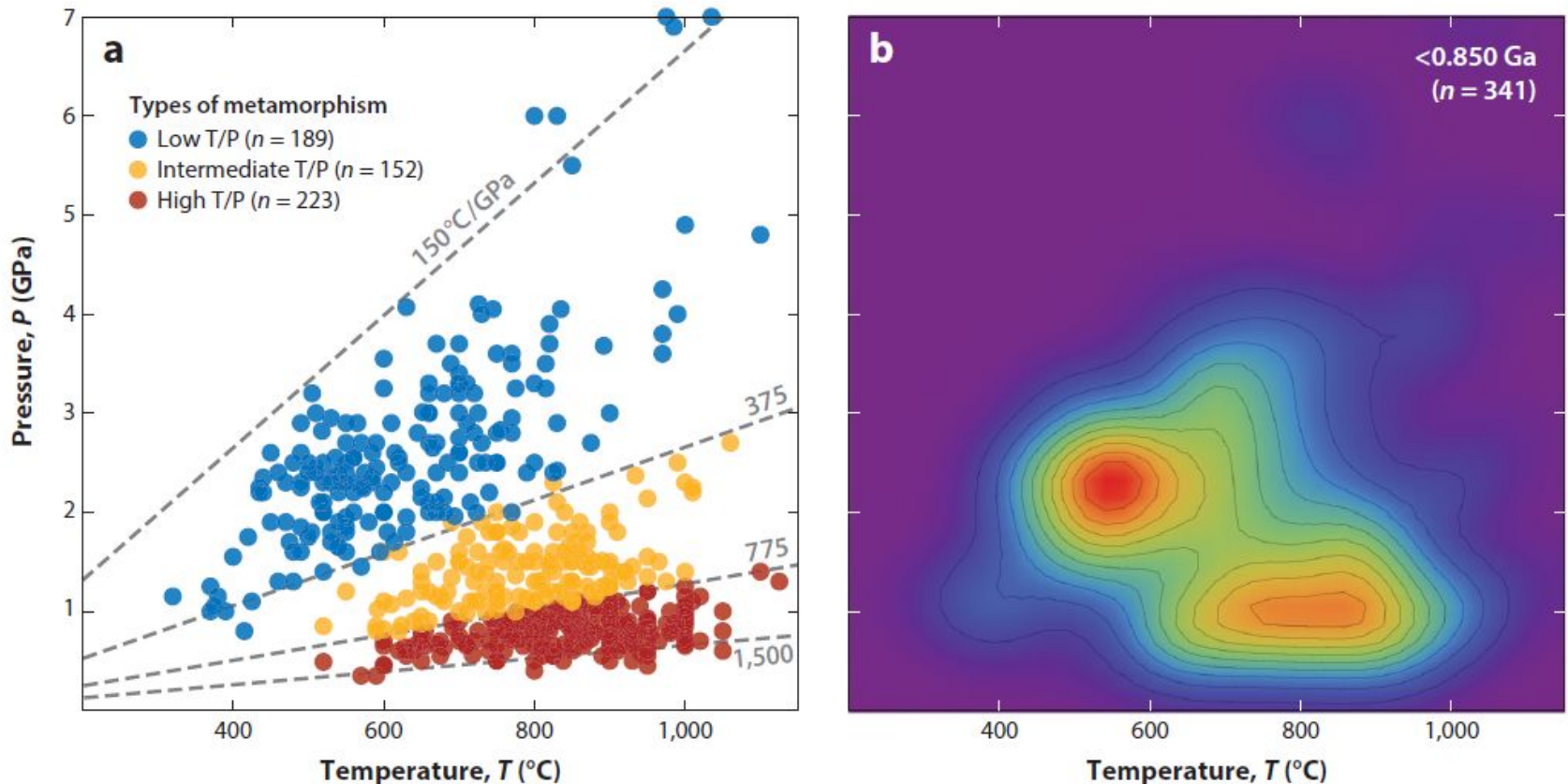
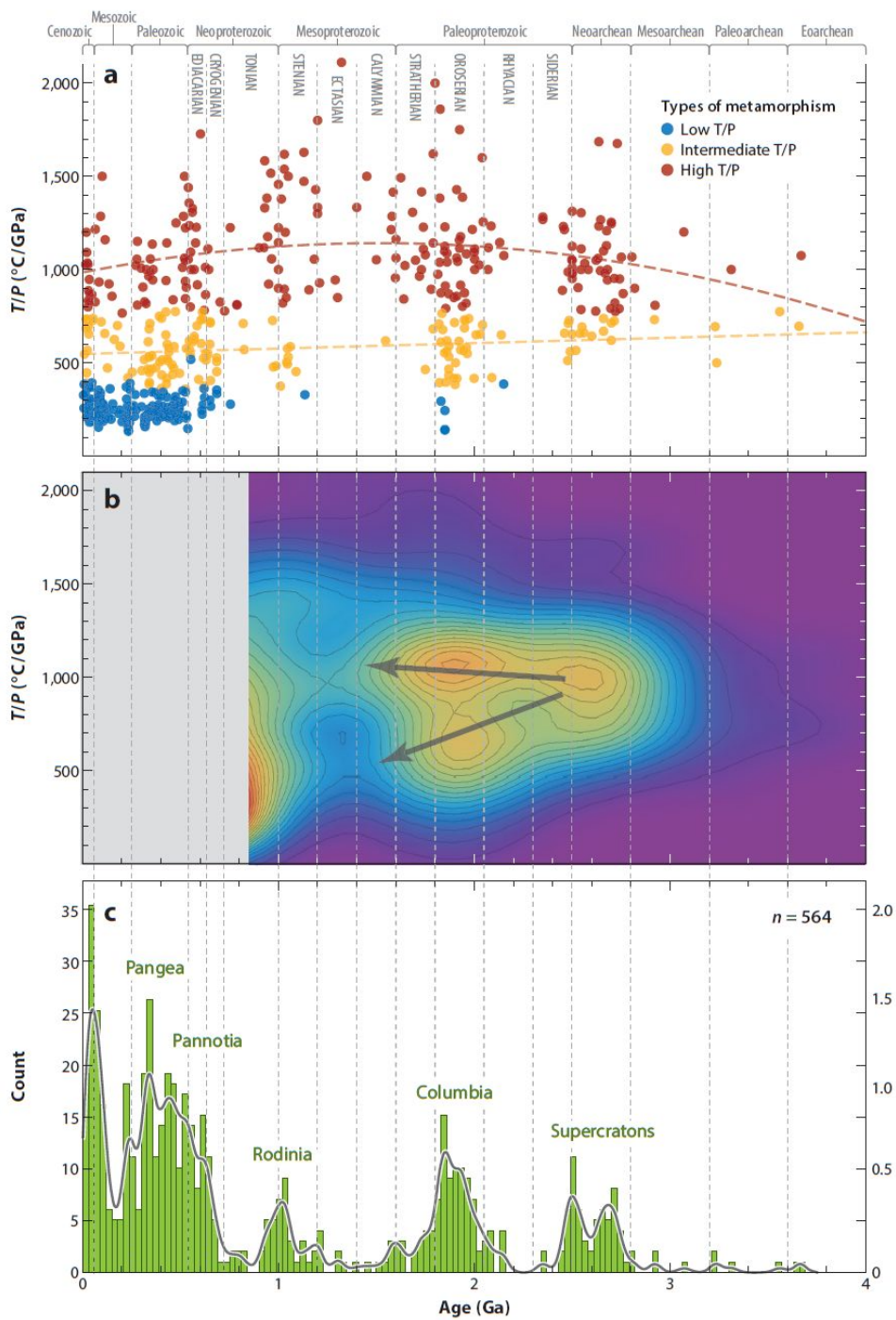


Figure 2

(a) Conditions of peak metamorphism for 564 localities with robust pressure (P), temperature (T), and age grouped by type, with representative thermal gradients (*thin gray dashed lines*). Three types of metamorphism are distinguished based on thermobaric ratios (T/P). (b) A plot of data < 850 Ma in age contoured for density (contours are smooth kernel density estimates for which the bandwidth was computed automatically using DensityPlot in Wolfram Mathematica) to emphasize the characteristic bimodality of crustal metamorphism since 850 Ma. Panel *a* data from Brown & Johnson (2019b). Figure adapted with permission from Brown & Johnson (2019a).



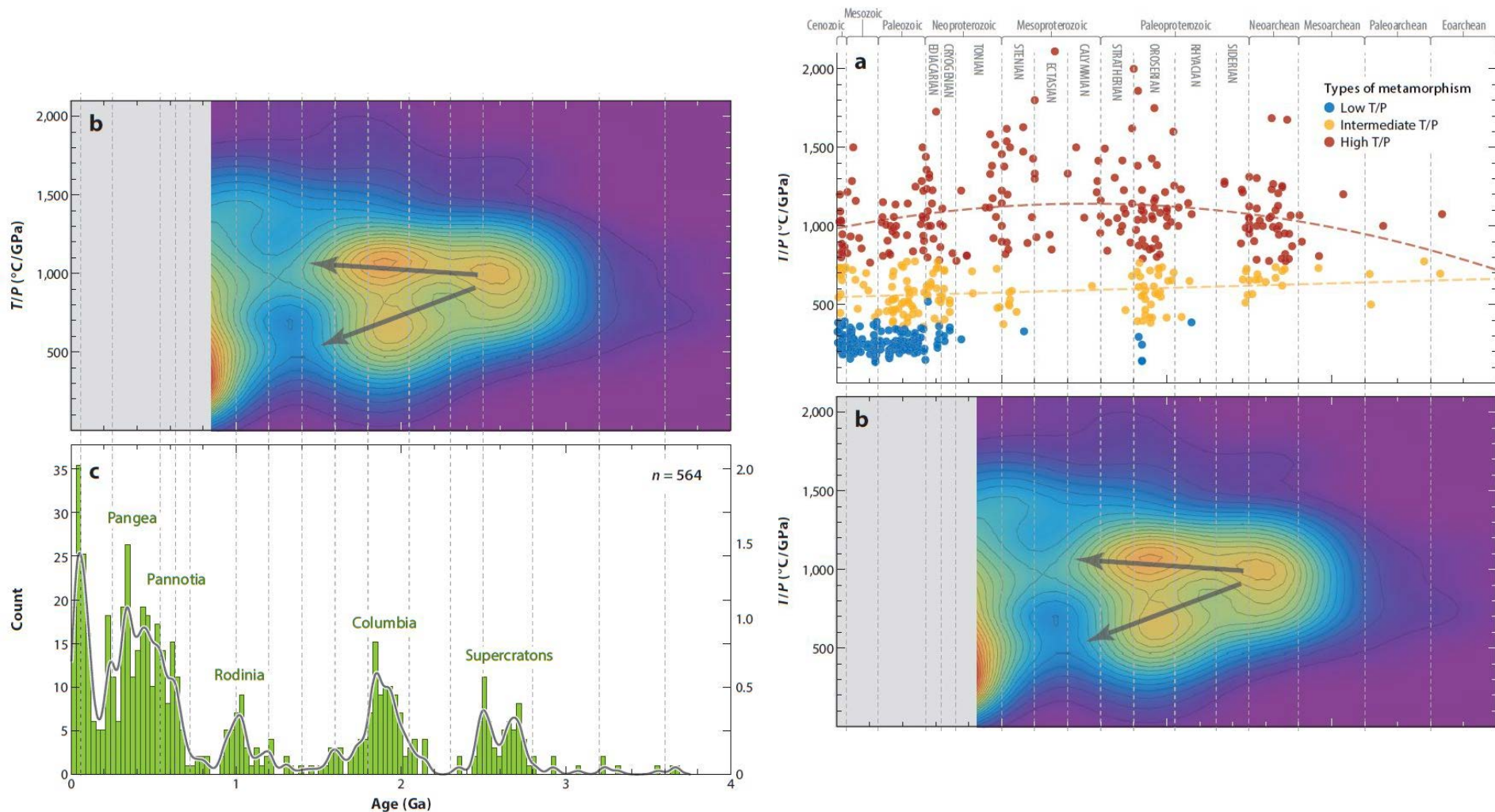


Figure 3 (Figure appears on preceding page)

(a) Metamorphic thermobaric ratios [temperature (T), pressure (P) (T/P)] for 564 localities grouped by type plotted against age. Three types of metamorphism are shown. The dashed lines show a second-order polynomial regression of the data for the high T/P (red) and a linear regression of the data for the intermediate T/P (orange) types, respectively. (b) T/P data for localities >850 Ma in age contoured for density (contours are smooth kernel density estimates for which the bandwidth was computed automatically using DensityPlot in Wolfram Mathematica) to emphasize the development of bimodality from the Neoproterozoic through the Proterozoic. (c) Histogram of ages and probability density function for metamorphism at 564 localities. Panels a and c adapted with permission from Brown & Johnson (2019a). Panel b adapted with permission from Brown & Johnson (2019c).

THE ARCHEAN ROCK RECORD

Key Features of Archean Geology

Lithological differences between pre- and post-Archean geology

- In addition to felsic domes, granite–greenstone belts comprise sequences of mainly (metamorphosed) basalt, with subordinate ultramafic to felsic volcanic rocks and various sedimentary rocks.
- A significant feature is the common occurrence of komatiites, high-magnesian ($\text{MgO} > 18 \text{ wt\%}$) lavas that are rare in the post-Archean rock record.
 - unusually high mantle temperatures required to form komatiites (ΔT_p of $+200\text{--}300^\circ\text{C}$)
 - commonly explained by invoking more vigorous plume activity promoted by higher temperatures at the core–mantle boundary.
- Majority of Archean lavas were erupted subaqueously, suggesting not much land had emerged before the late Archean–early Proterozoic
- If the development of significant topography in the Proterozoic reflects strengthening of the continental lithosphere, was the Archean lithosphere too weak to focus deformation and break into plates?

THE ARCHEAN ROCK RECORD

Key Features of Archean Geology

Petrogenesis of Archean Crust compared to present-day Crust

- **Modern arc basalts** have characteristic compositions reflecting partial melting, on average at ~100 km depth below the active magmatic arc, of depleted mantle that was hydrated and enriched in incompatible elements through interaction with fluids derived from subducted materials.

→ **Relative to MORB, arc basalts:**

- 1) are enriched in large ion lithophile elements (LILE);
- 2) show fractionated rare earth element (REE) patterns, with preferential incorporation of light REE (LREE) over heavy REE (HREE);
- 3) are depleted in high field strength elements, leading to pronounced negative anomalies in Nb, Ta, Zr, Hf, and Ti.

!! Although these characteristics are taken as a reliable proxy for subduction in many studies, they also occur in basalts derived from subduction-modified lithospheric mantle.

THE ARCHEAN ROCK RECORD

Key Features of Archean Geology

Petrogenesis of Archean Crust compared to present-day Crust

- fundamental questions:

- 1? do modern arc basalts really provide the key to the genesis of Archean basalts with similar compositional characteristics?
 - 2? are there plausible mechanisms by which hydrated crust can be recycled into the mantle other than by subduction?
- > Numerical modeling suggests that subduction and dripping of the lowermost crust and crustal overturns may represent plausible alternatives

THE ARCHEAN ROCK RECORD

Key Features of Archean Geology

Petrogenesis of Archean Crust compared to present-day Crust

- The so-called arc signature is also found in most TTGs, which show extreme REE fractionation, with high chondrite-normalized La/Yb ratios ($\text{La}_N/\text{Yb}_N > 15$) and preferential enrichment of Sr over Y ($\text{Sr}_N/\text{Y}_N > 20$) Notwithstanding that some TTGs may have formed through fractional crystallization the pronounced HREE and Y depletion in most TTGs (~80%) is interpreted to record partial melting of hydrated basaltic rocks (amphibolite) at depth within the stability field of garnet. Although garnet may indicate pressures >1.5 GPa based on experimental studies of amphibolite, its stability is highly sensitive to bulk rock Mg# [atomic $\text{Mg}/(\text{Mg} + \text{Fe}^{2+})$] and garnet may be stable at pressures as low as 0.7 GPa.
- This lower pressure is within the range of thickness for primary crust generated during the Archean, and melting this crust may not require subduction.

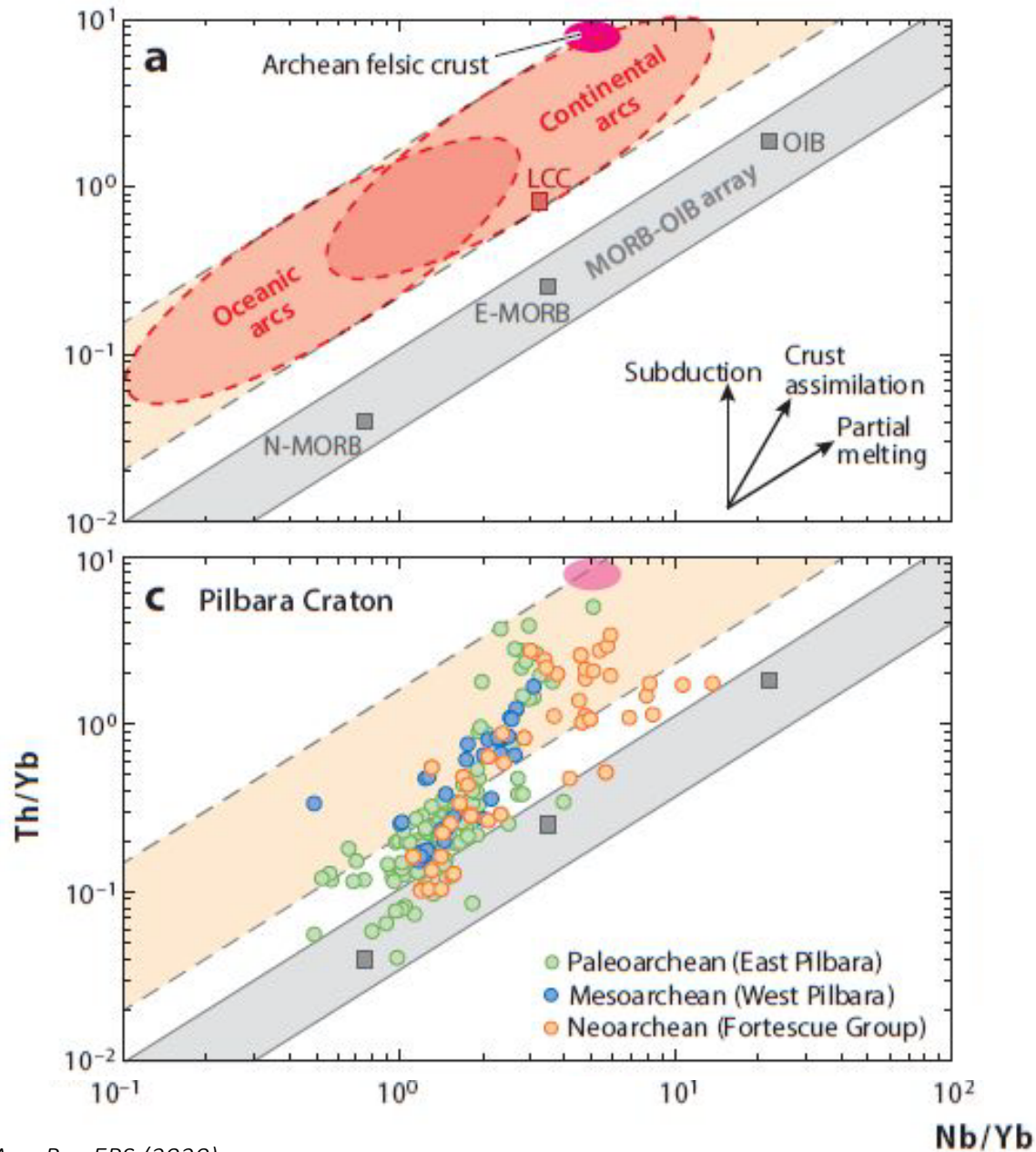
THE ARCHEAN ROCK RECORD

Key Features of Archean Geology

Petrogenesis of Archean Crust compared to present-day Crust

- Around 20% of TTGs record a high-pressure signature, considered to record extraction from an eclogite residue at pressure >2.0 GPa, corresponding to the extreme depths (>60 km) experienced by younger crustal rocks only during deep subduction.
- such high-pressure TTGs have recently been interpreted to represent fractionated sanukitoid (high-magnesian diorite) melts derived by partial melting of chemically enriched hydrated lithospheric mantle.

How to interpret isotope signatures



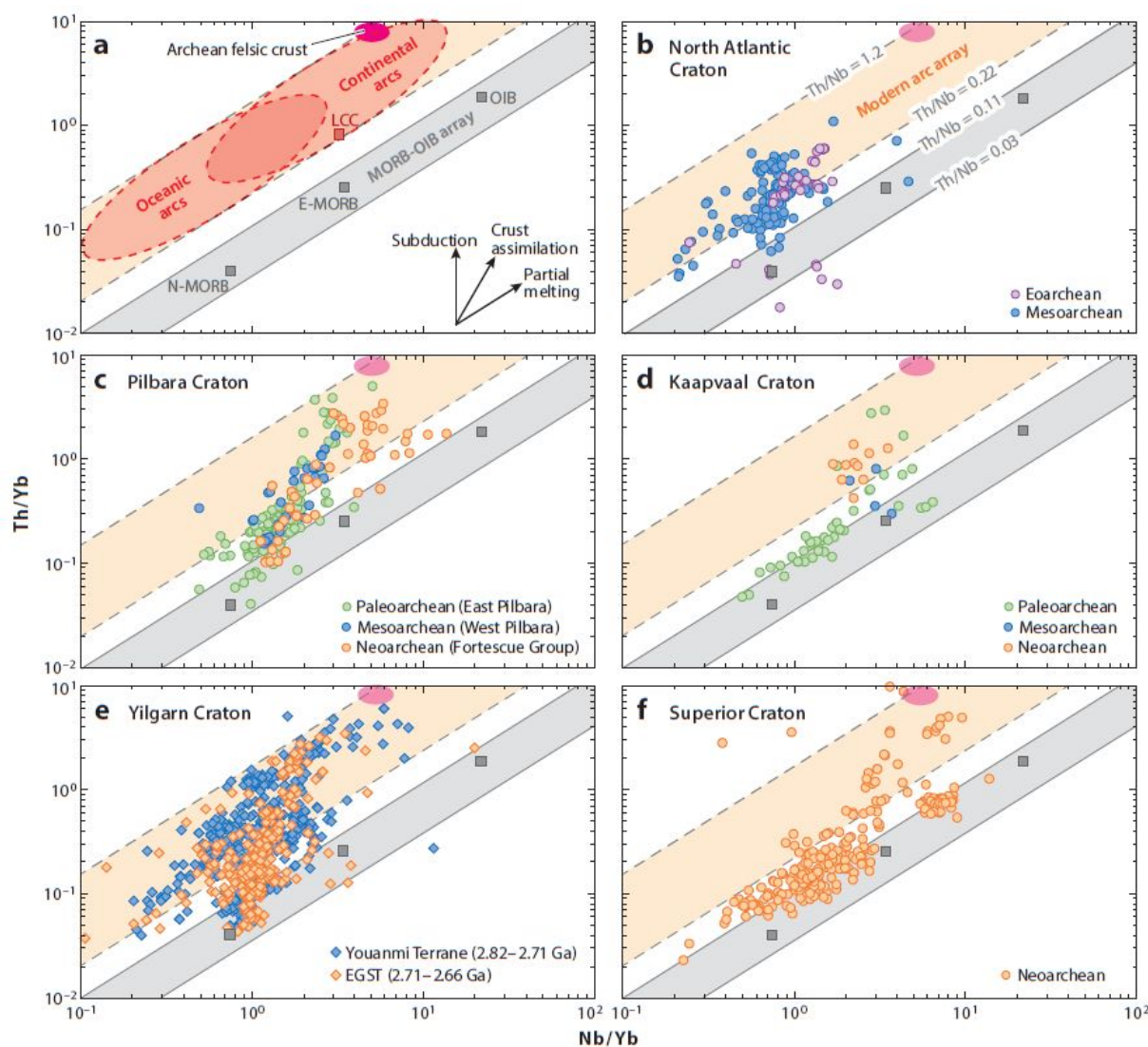


Figure 4

(a) The Th/Yb–Nb/Yb plot of Pearce (2008) showing main fields as well as composition vectors expected during subduction enrichment of a mantle source, crustal assimilation, and partial melting. Panel *a* adapted from Smithies et al. (2018). Copyright 2018, with permission from Elsevier; data for ocean floor basalt compositions (N-MORB, E-MORB, and OIB) from Sun & McDonough (1989); for the average composition of Archean felsic crust from Moyen (2011); and for modern LCC from Rudnick & Gao (2014). (b)–(f) Plots of Th/Yb versus Nb/Yb for basalts from the North Atlantic Craton (southwest Greenland), the Pilbara Craton, the Kaapvaal Craton (Barberton Granite–Greenstone Belt), and the Superior Craton (Abitibi Greenstone Belt) colored by age, and for the Yilgarn Craton colored by terrane. Data for panels *b*–*f* from GeoRoc (<http://georoc.mpch-mainz.gwdg.de/georoc/>) and GSWA (2019), filtered by MgO (<18 wt%) and SiO₂ (>45 and <57 wt%) content. Abbreviations: EGST, Eastern Goldfields Superterrane; E-MORB, enhanced mid-ocean ridge basalt; LCC, lower continental crust; MORB, mid-ocean ridge basalt; N-MORB, normal mid-ocean ridge basalt; OIB, ocean island basalt.

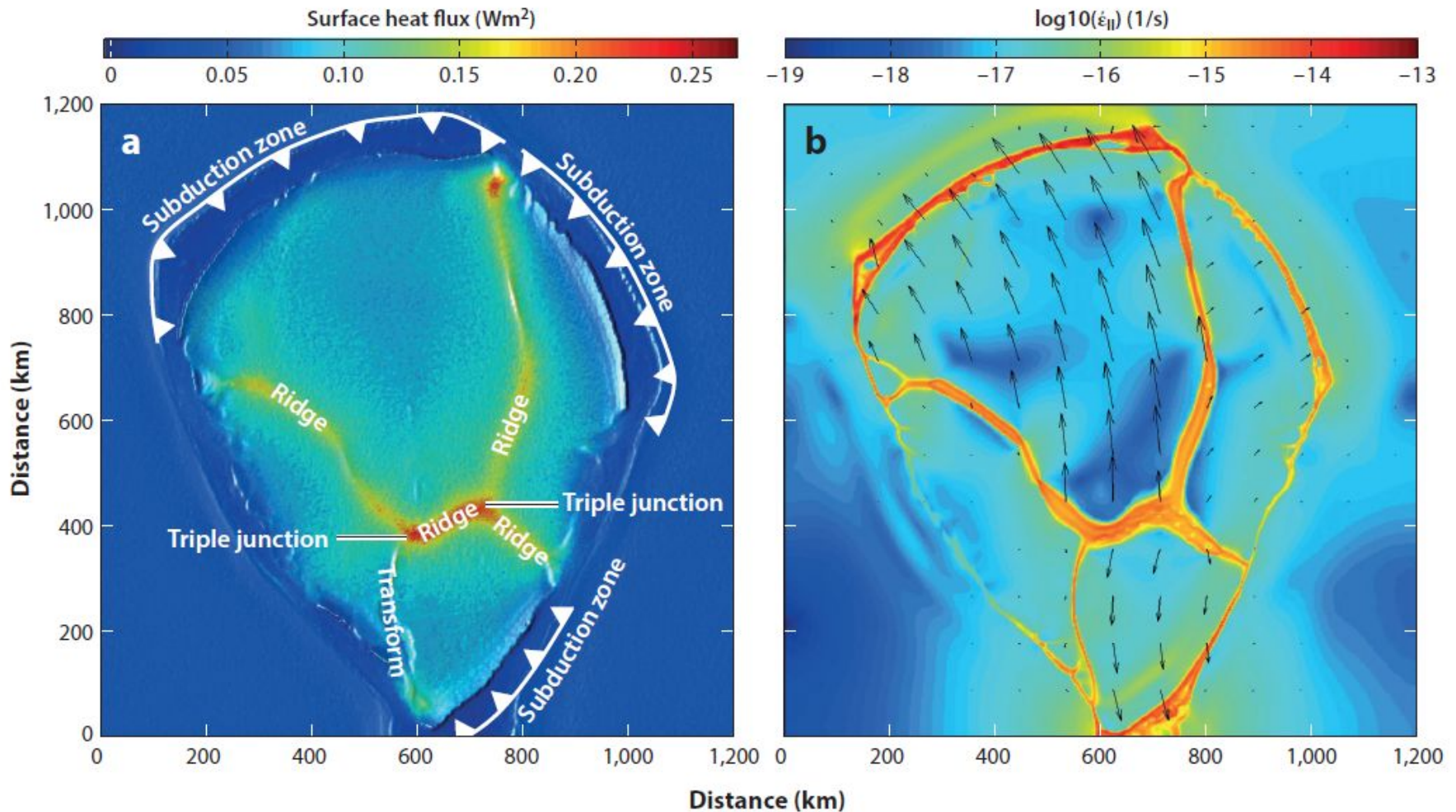


Figure 5

Development of an embryonic mosaic of plates separated by spreading centers (ridges), triple junctions, and transform faults at the latest stage of plume-induced subduction. (a) Surface heat fluxes projected onto the modeled surface topography, showing a pattern of spreading centers (*white lines with triangles* show dip directions of retreating subducting slabs). (b) Spatial distribution of the second strain rate invariant at a depth of 20 km (*arrows* show horizontal velocities of individual, young, nonsubducting plates moving toward retreating subducting slabs). Figure adapted from Gerya et al. (2015). Copyright 2015, with permission from Springer Nature.

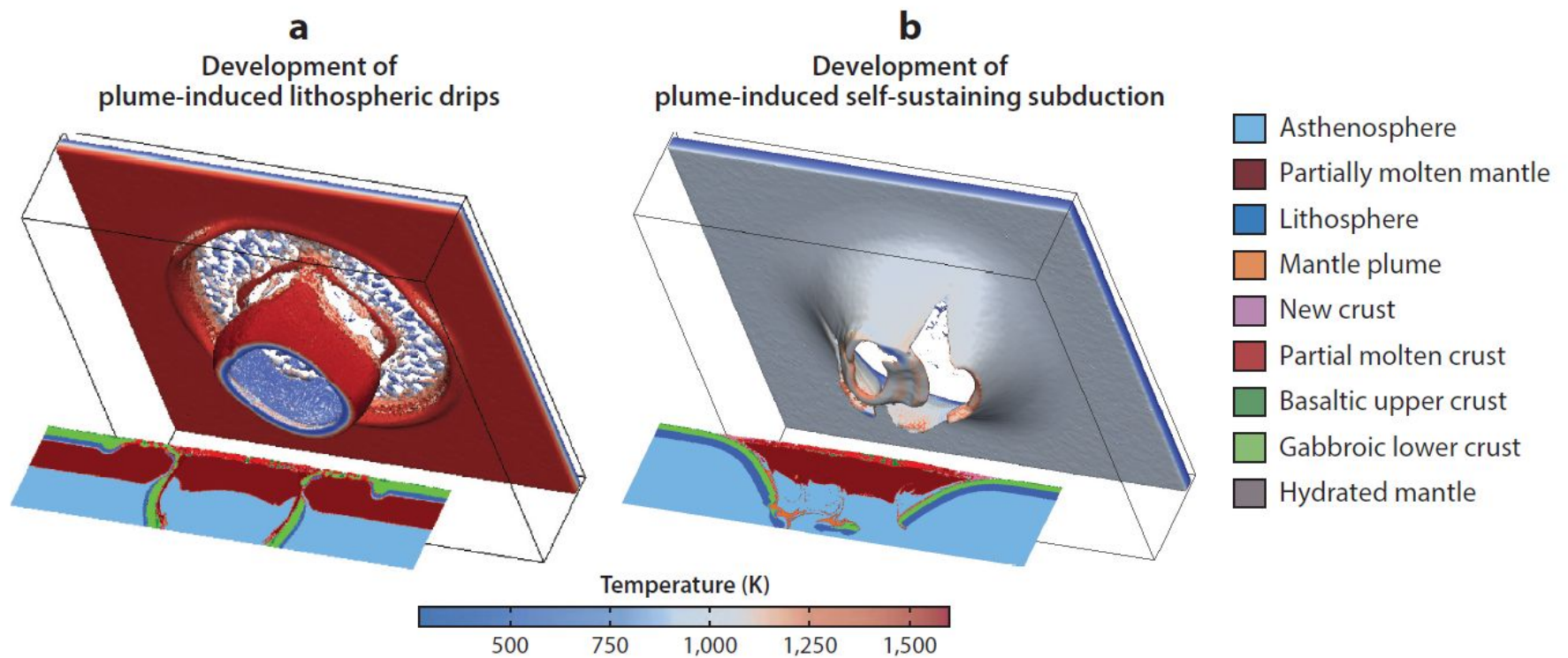


Figure 6

Plume–lithosphere interaction for hotter mantle temperature (ΔT_p of $+200^\circ\text{C}$) and thicker oceanic crust. (a) Development of plume-induced lithospheric drips for 20-Myr oceanic plate with 30-km-thick crust. (b) Development of plume-induced self-sustaining subduction for 80-Myr oceanic plate with 20-km-thick crust. Figure adapted from Gerya et al. (2015). Copyright 2015, with permission from Springer Nature.

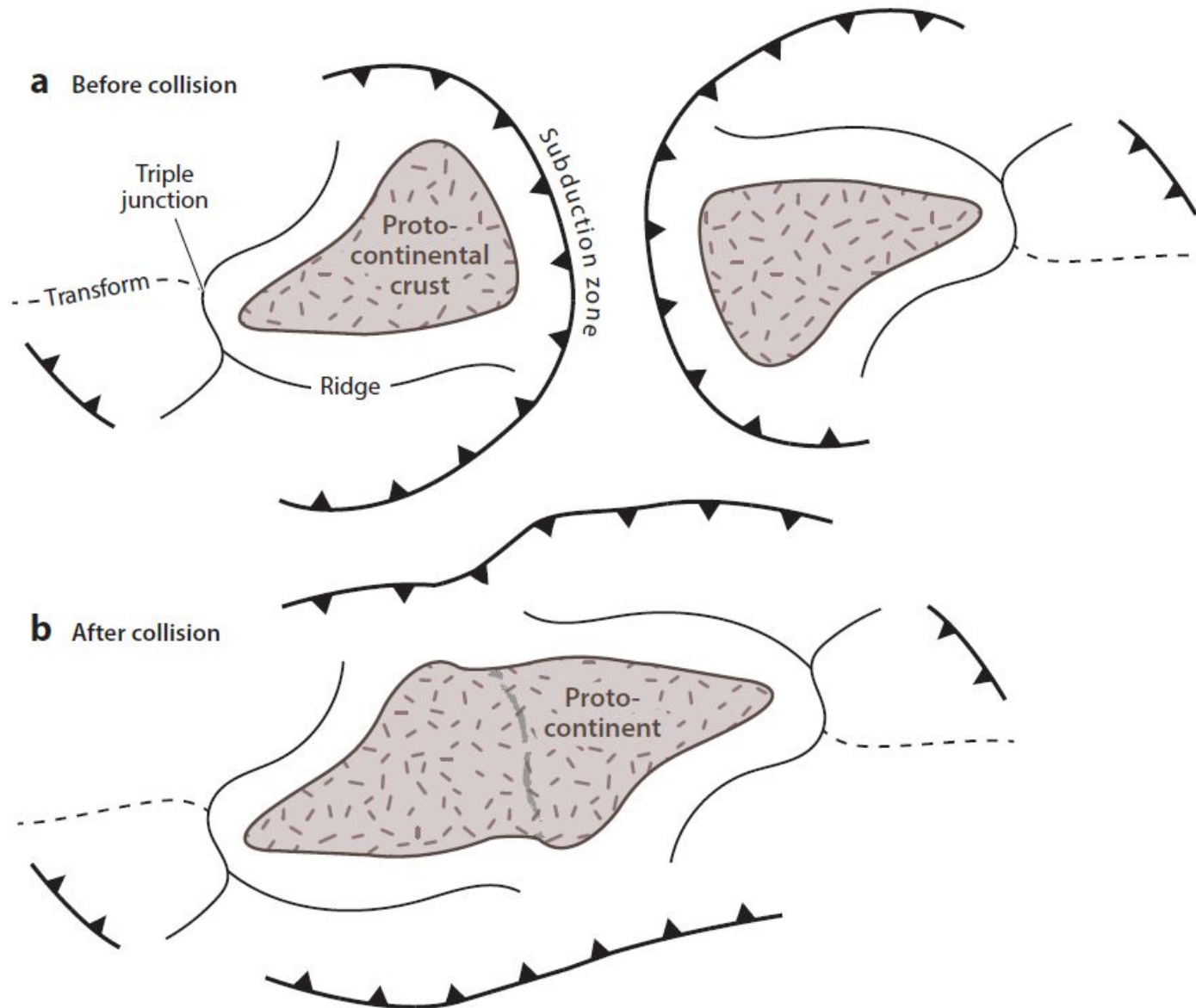


Figure 7

Sketches showing approaching plume-induced subduction cells (*a*) before elimination of the intervening oceanic lithosphere and collision and (*b*) after collision and formation of a proto-continent.

Plate Tectonics and the Archean Earth

Summary Points

1. Before the Mesoarchean–Neoproterozoic, a stagnant lid or sluggish lid or lid and plate tectonics mode, with a deformable (squishy) lithosphere and either intermittent (unstable) subduction or subduction on a locally confined scale, may have been dominant. A hotter mantle prohibited widespread stable subduction and plate tectonics, and magmatism was largely due to upwelling mantle and plume–lithosphere interactions.
2. During a Mesoarchean–Neoproterozoic transition, as secular cooling overwhelmed heat production, plate tectonics emerged, possibly in part via plume-initiated retreating subduction cells that generated proto-continents.
3. The rise of proto-continents and enhanced erosion to provide sediments at their edges may have enabled initiation of subduction under the proto-continents by spreading of continental margins over oceanic lithosphere. This process could have stabilized subduction and promoted the spread of plate tectonics globally, as recorded by the widespread appearance of high and intermediate T/P metamorphism in the Neoproterozoic. The formation and breakup of the supercratons, and the formation of the first supercontinent Columbia, demonstrate that plate tectonics was fully developed by the early Paleoproterozoic.

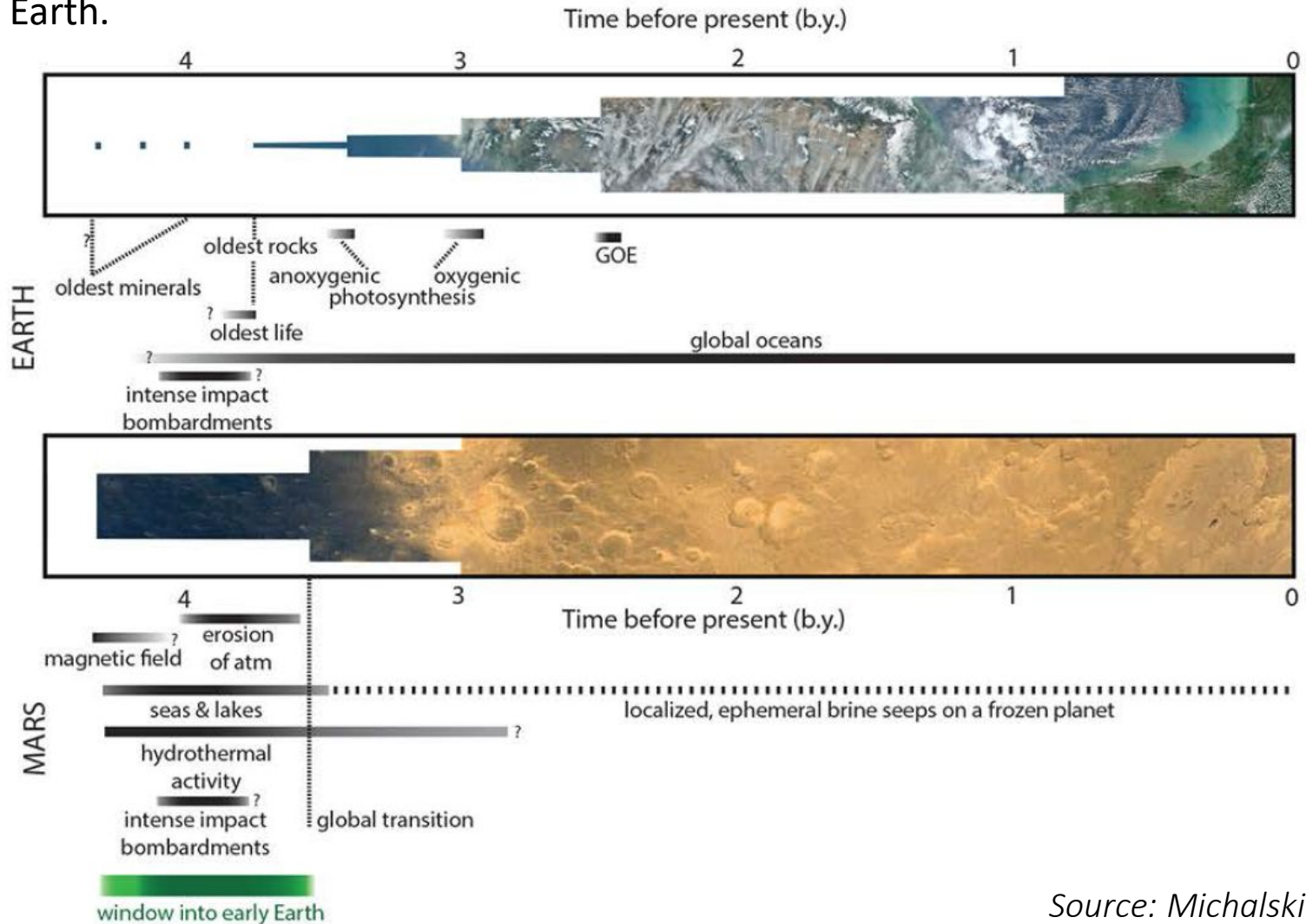
Plate Tectonics and the Archean Earth

Future Issues

1. Geochemical criteria need to be identified to distinguish impact-induced from plume-induced melt products, so that we may determine the contribution of each process to the formation of the Hadean and Eoarchean tonalite-trondhjemite-granodiorite crust.
2. To evaluate hypotheses regarding the tectonics of early Earth, it is necessary to increase the number of metamorphic pressure, temperature, and age data from exposures of ancient (older than 2.8 Ga) continental crust worldwide. Retrieval of such data should be a priority of metamorphic studies.
3. To understand secular change in tectonics on Earth requires a better knowledge of the thermal evolution of Earth and mantle potential temperature and further research to resolve the contentious issue of the amount and temporal evolution of water in the mantle.
4. To understand the evolution of life on Earth, it is necessary to assess linkages between secular change in tectonic mode and the evolution of Earth's atmosphere, oceans, and landscape, since these control nutrient supply and environment.

A comparison of key events in the histories of the Earth and Mars.

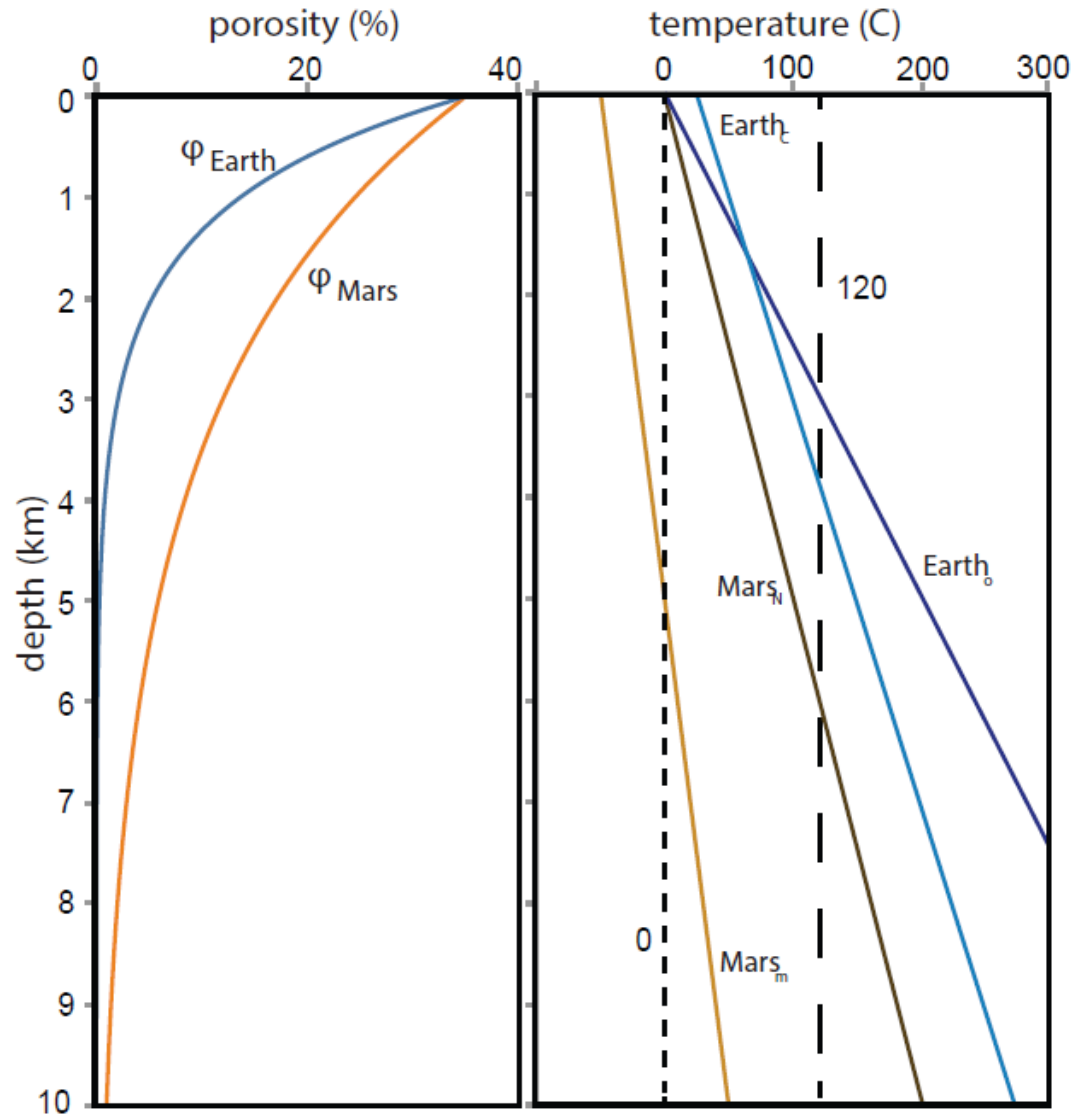
The area of each time line is an approximation of the amount of crust preserved from over different epochs. The generally unmetamorphosed and well-preserved geologic record of early Mars is an invaluable window into the geology and prebiotic chemistry of the early Earth.



Source: Michalski et al.

A comparison of the average porosity of thermal gradients of the crusts of Earth and Mars.

For similar rock types and surface porosities, the martian crust contains significantly more porosity to greater depth than that of the Earth (left). Estimated thermal gradients for Noachian (ϕ_N) and modern (ϕ_m) Mars are lower than that of the modern continental (ϕ_c) or oceanic (ϕ_o) crust of Earth (right). A hypothetical 120°C limit is encountered at 3-4 km depth on Earth, where the porosity is 1-2%. The same temperature limit would not be encountered until ~6 km depth on Noachian Mars or much deeper on modern Mars.



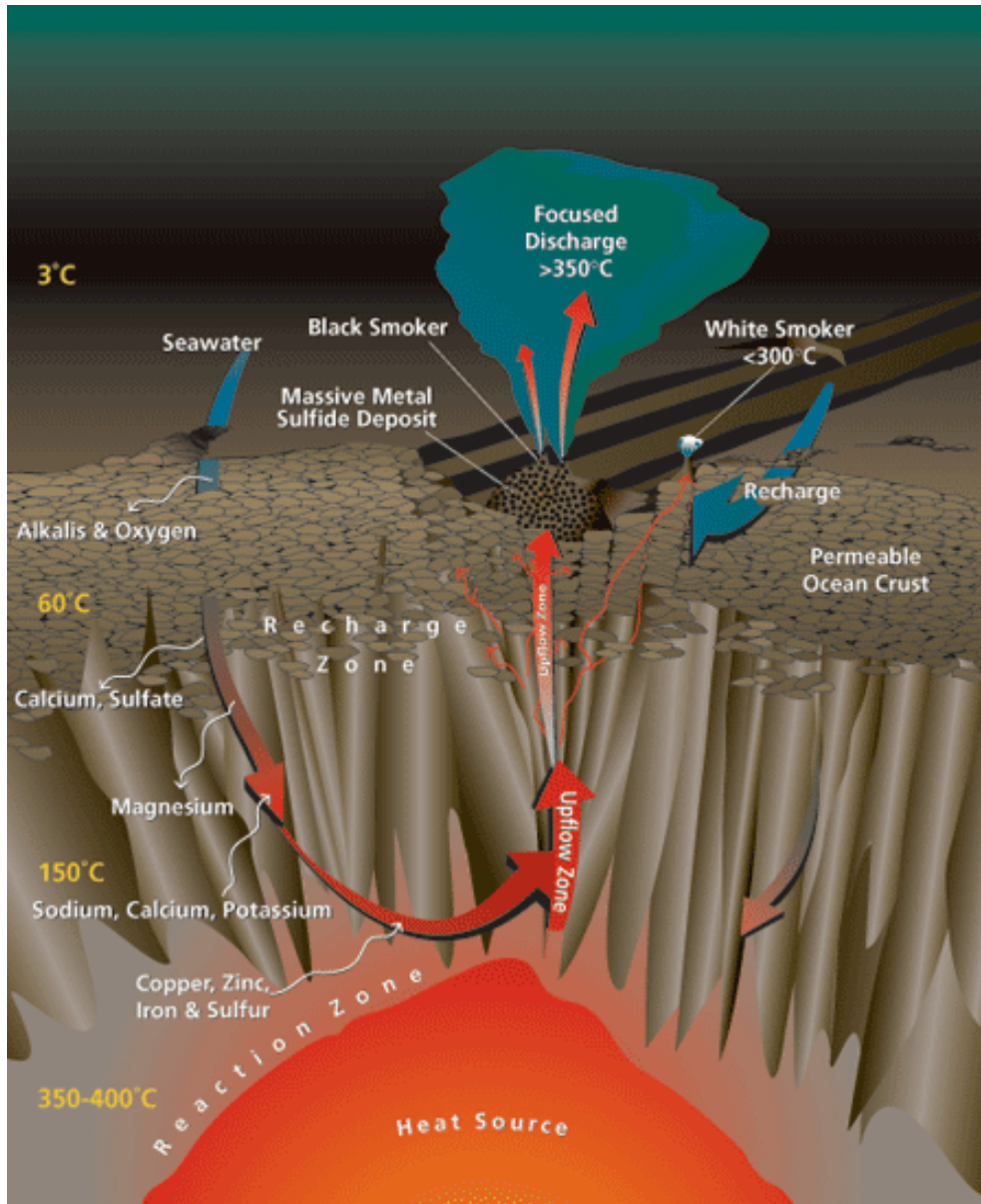
A Hydrothermal-Sedimentary Context for the Origin of Life

F. Westall,¹ K. Hickman-Lewis,^{1,2} N. Hinman,³ P. Gautret,⁴ K.A. Campbell,⁵ J.G. Bréhéret,⁶
F. Foucher,¹ A. Hubert,¹ S. Sorieul,⁷ A.V. Dass,¹ T.P. Kee,⁸ T. Georgelin,^{1,9} and A. Brack¹

Abstract

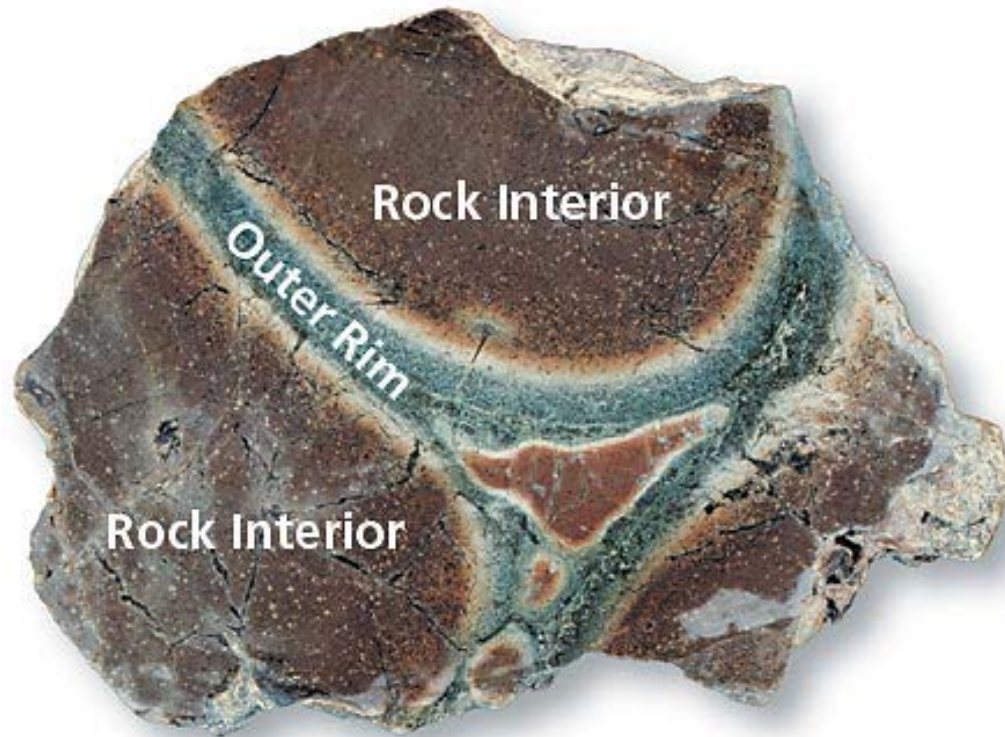
Critical to the origin of life are the ingredients of life, of course, but also the physical and chemical conditions in which prebiotic chemical reactions can take place. These factors place constraints on the types of Hadean environment in which life could have emerged. Many locations, ranging from hydrothermal vents and pumice rafts, through volcanic-hosted splash pools to continental springs and rivers, have been proposed for the emergence of life on Earth, each with respective advantages and certain disadvantages. However, there is

Submarine hydrothermal systems & Black Smokers



In a hydrothermal circulation system, cold seawater seeps through the permeable seafloor and deeper subsurface dikes. It undergoes a series of chemical reactions with subsurface rocks at various temperatures to create hot hydrothermal fluid that eventually vents at the seafloor.

Examples of fluid-rock interactions



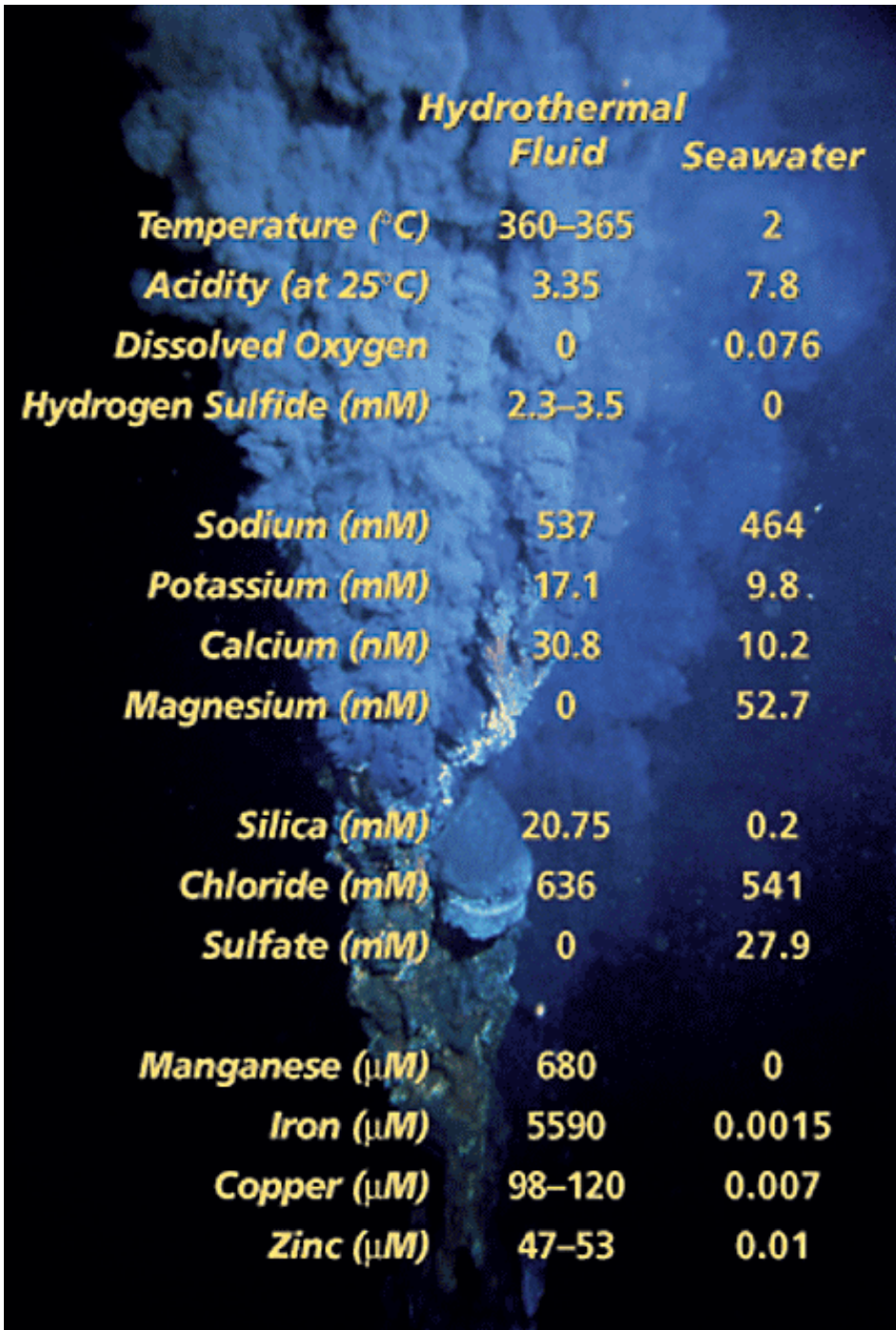
A rock sample dredged from the Mid-Atlantic Ridge shows how seawater flowing between subsurface rocks alters them and cements them together. The rocks' outer rims (gray) have been chemically changed by interaction with hot seawater and can be easily distinguished from the relatively unaltered interior (brown). By comparing the geochemistry of the rim and the interior, researchers can determine the ways in which elements are exchanged between seawater and rock

Examples of fluid-rock interactions



A rock sample, recovered by drilling 116 meters below the active seafloor hydrothermal vent site at 26°N on the Mid-Atlantic Ridge, shows how the rock has been altered by reactions with seawater at temperatures of about 300°C. Pieces of highly altered rock (gray) are cemented together with minerals such as iron sulfides (gold-colored) and quartz (white).

Fluid-Rock Interaction: Black Smoker

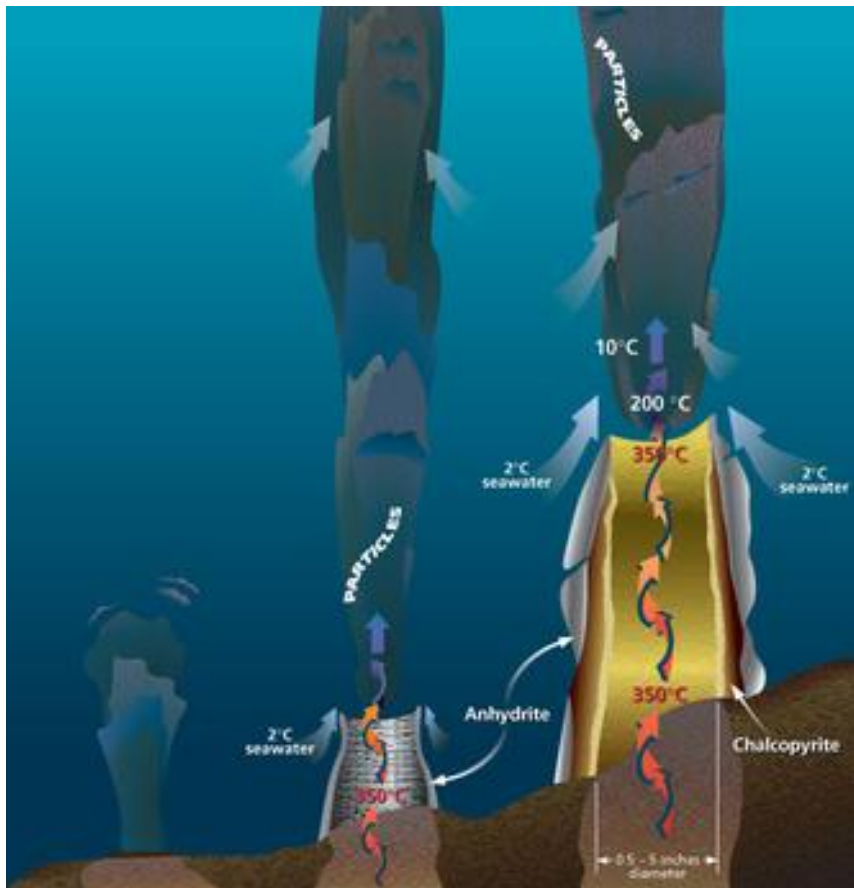


	<i>Hydrothermal Fluid</i>	<i>Seawater</i>
<i>Temperature (°C)</i>	360–365	2
<i>Acidity (at 25°C)</i>	3.35	7.8
<i>Dissolved Oxygen</i>	0	0.076
<i>Hydrogen Sulfide (mM)</i>	2.3–3.5	0
<i>Sodium (mM)</i>	537	464
<i>Potassium (mM)</i>	17.1	9.8
<i>Calcium (nM)</i>	30.8	10.2
<i>Magnesium (mM)</i>	0	52.7
<i>Silica (mM)</i>	20.75	0.2
<i>Chloride (mM)</i>	636	541
<i>Sulfate (mM)</i>	0	27.9
<i>Manganese (μM)</i>	680	0
<i>Iron (μM)</i>	5590	0.0015
<i>Copper (μM)</i>	98–120	0.007
<i>Zinc (μM)</i>	47–53	0.01

A comparison of characteristics and chemical composition shows the distinct differences between seawater and hydrothermal vent fluid, in this case fluid from the TAG hydrothermal site on the Mid-Atlantic Ridge at 26°N.

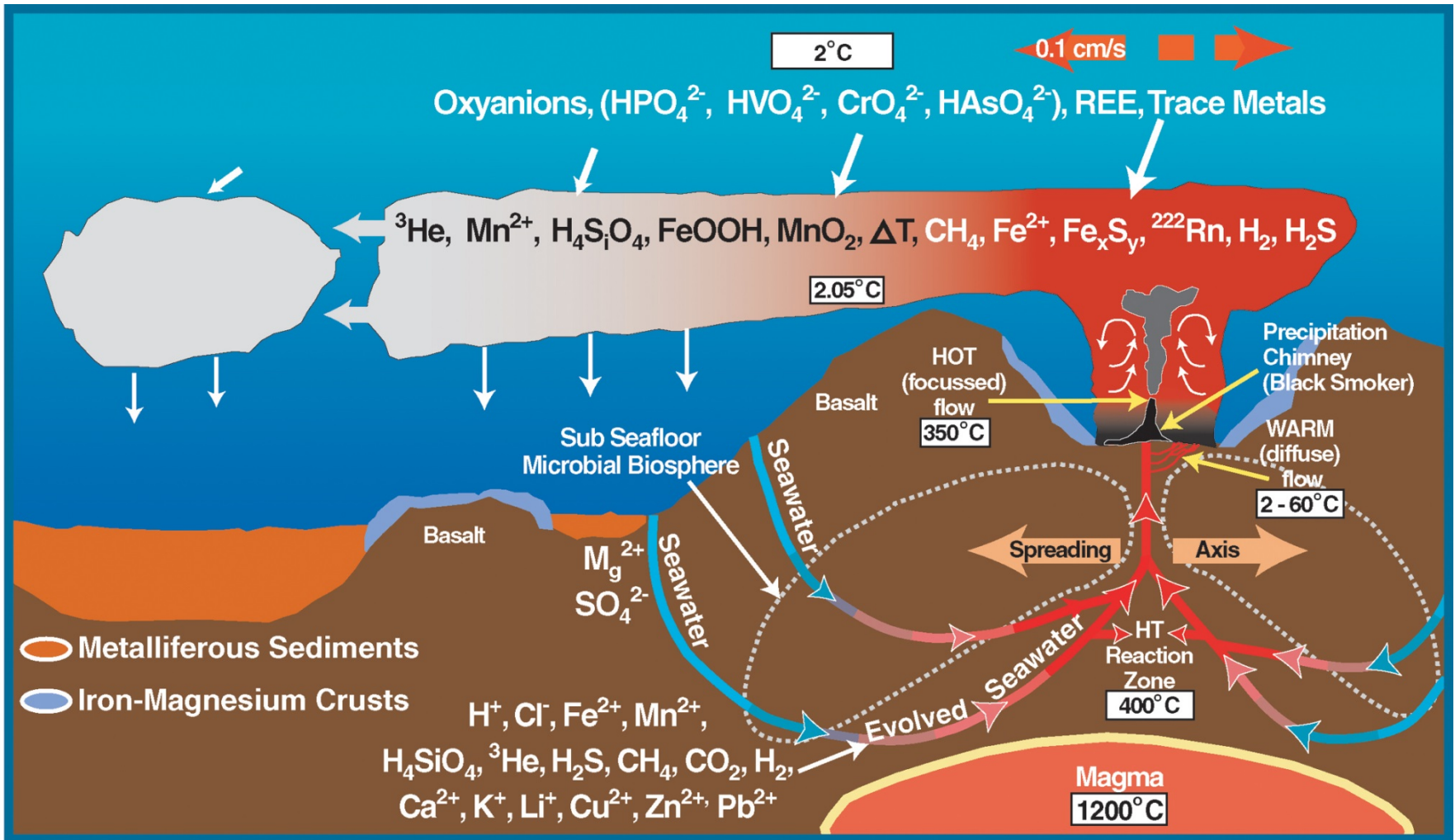
Fluid-Rock Interaction: Black Smoker

A Black Smoker is also known as a sea vent, which is a type of hydrothermal vent or underwater hot spring found on the ocean floor. They are formed in fields of hundreds of meters wide. When it comes in contact with cold ocean water, many minerals precipitate, forming black chimney-like structure around each vent



Fluid-Rock Interaction: Importance for Ore deposits

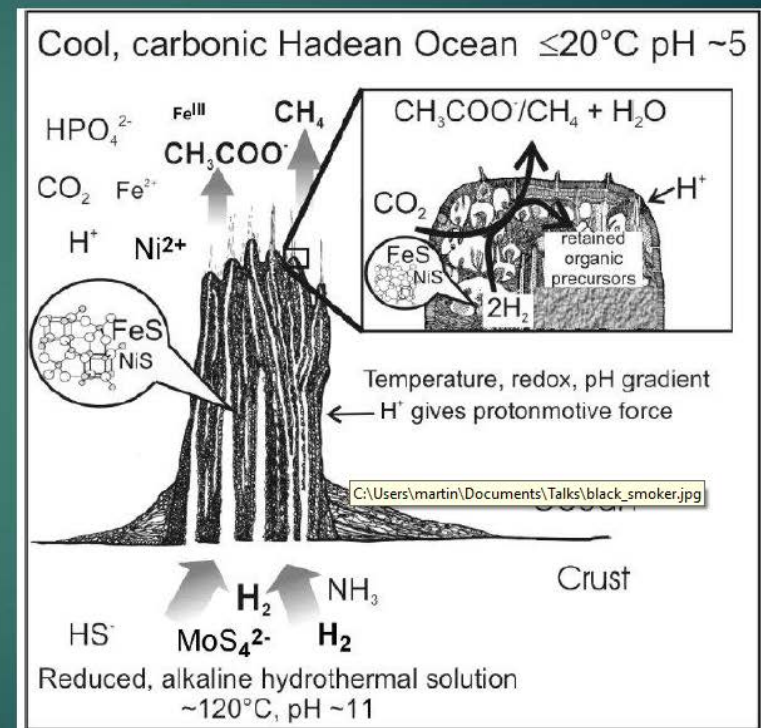
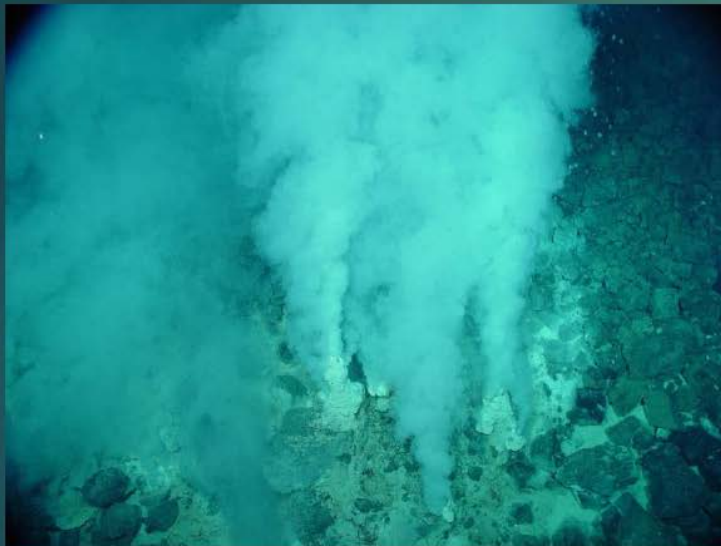
Black smoker metal precipitation



<http://oceanexplorer.noaa.gov/explorations/02fire/background/hirez/chemistry-hires.jpg>

Submarine hydrothermal vents

White Smokers - Alkaline chimneys in warm vents (off-axis)



Submarine hydrothermal vents

TABLE 3A. ENVIRONMENTS AVAILABLE FOR THE EMERGENCE OF LIFE

<i>System</i>	<i>Prebiotic chemistry</i>		<i>Emergence of life</i>	
	<i>Advantages</i>	<i>Disadvantages</i>	<i>Advantages</i>	<i>Disadvantages</i>
Submarine hydrothermal vents Temperatures >100–150°C Fluid dynamics pH—alkaline-acid Ionic strength Energy sources Mineralogy, <i>e.g.</i> , sulfides and various mafic/ultramafic minerals and their alteration products Element availability Porous structures (minerals, edifices, <i>e.g.</i> , beehive structures) Protection from external environment Distribution of products	Facilitates molecular interactions Low in porous edifice Favors prebiotic processes Variable Heat; exothermal breakdown of organic molecules Reactive surfaces favor molecule- organic interactions (Table 1) CHNOPS Concentration of prebiotic components, compartmentalization UV protection, disruption caused by impacts In hydrothermal fluid effluent	Agitation can break up molecules High in vent throat	Diffusion of nutrients Any pH for protocells Salts necessary for protocells Breakdown of organic molecules; redox reactions of reactive minerals; gradients (pH, temperature...) Energy from redox reactions at mineral surfaces CHNOPS, Cu, Fe, Ni, Zn... Protected environment for protocells Protected environment—from UV, etc. In hydrothermal fluid effluent	Temperatures too high unless the vents are inactive and flushed with lower- temperature seawater Disruption if too high

Source: Westall et al., *Astrobiology*, 2018

Pumices



TABLE 3B. ENVIRONMENTS AVAILABLE FOR THE EMERGENCE OF LIFE

System	Prebiotic chemistry		Emergence of life	
	Advantages	Disadvantages	Advantages	Disadvantages
Pumice				
Temperatures <70°C	Temperatures conducive to prebiotic chemistry; occasional freezing possible		Temperatures above freezing conducive to protocell activity	
Fluid dynamics pH—variable, depending on the composition of the pumice and the properties of the seawater	Low in porous edifice	Does not favor ribose formation	Diffusion of nutrients Any pH for protocells	
Ionic strength	Variable, depending upon ambient seawater		Salts necessary for protocells	
Energy sources	Heat if in vicinity of volcanic or hydrothermal edifices		Energy from redox reactions at surfaces of volcanic glass; gradients (<i>e.g.</i> , pH, <i>T</i>)	
Mineralogy	Volcanic glass of felsic to more rarely basaltic origin		Energy from redox reactions at surfaces of volcanic glass	
Element availability		No CHNOPS but could adsorb organics from seawater	Na, K, some transition metals, Fe	No CHNOPS but could adsorb organics from seawater
Porous structures	Micro-pores could act as mini reactors; concentration of prebiotic components, compartmentalization		Protected environment for protocells	
Protection from external environment	Protection from UV and disruption caused by impacts		Protected environment—from UV, etc.	
Distribution of products	Floating on ocean surface		Floating on ocean surface	

Source: Westall et al., *Astrobiology*, 2018

Subarial Geysers

TABLE 3C. ENVIRONMENTS AVAILABLE FOR THE EMERGENCE OF LIFE

<i>System</i>	<i>Prebiotic chemistry</i>		<i>Emergence of life</i>	
	<i>Advantages</i>	<i>Disadvantages</i>	<i>Advantages</i>	<i>Disadvantages</i>
<i>Properties</i>				
Subaerial geysers				
Temperatures < ~130°C; possibly freezing	Facilitates molecular interactions; freezing temperatures stabilize ribose and promote catalytic activity of RNA		Cellular activity up to 120°C	
O ₂ production from production of H ₂ O ₂		Will destroy organic molecules		Will destroy organic molecules
Fluid dynamics	Low in porous edifice surrounding geyser	High in vent throat	Diffusion of nutrients	Disruption of structures in vent throat
pH—alkaline-acid	Favors prebiotic processes	Acidic pH unfavorable for ribose	Any pH for protocells	
Ionic strength	Variable		Salts necessary for protocells	
Energy sources	Heat; exothermal breakdown of organic molecules		Breakdown of organic molecules; redox reactions of reactive minerals; gradients (pH, temperature...)	
Silica (carbonates today depending upon underlying lithology)	Silica surfaces favor molecule-organic interactions (Table 1)		Energy from redox reactions at country rock mineral surfaces	
Element availability	CHNOPS from hydrothermal fluids		CHNOPS, Cu, Fe, Ni, Zn...	
Porous structures (minerals, edifices, e.g., beehive structures)	Concentration of prebiotic components, compartmentalization		Protected environment for protocells	
Protection from external environment	Some UV protection in porous sinter deposits	Desiccation and exposure to UV	Some protection from UV, etc.	Desiccation and exposure to UV
Distribution of products		Difficult		Difficult

Source: Westall et al., *Astrobiology*, 2018

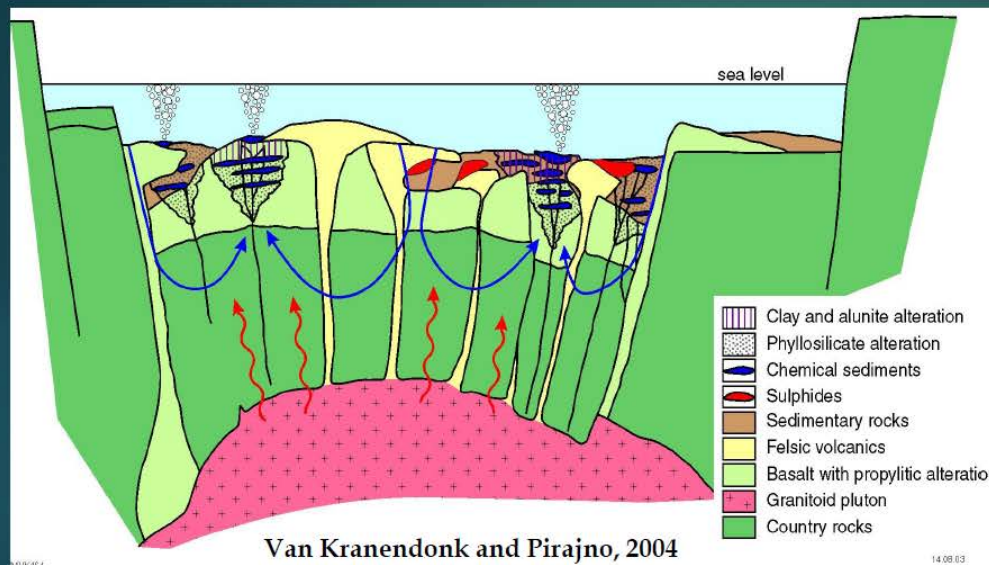
Volcanic coastal environments

TABLE 3D. ENVIRONMENTS AVAILABLE FOR THE EMERGENCE OF LIFE

System	Prebiotic chemistry		Emergence of life	
	Properties	Advantages	Disadvantages	Disadvantages
Volcanic coastal environments (seawater heated by hot lava and rock pools)				
Temperatures, high on lavas (200°C), low in rock pools (<100°C), to possibly freezing depending on early Earth scenario	Relevant for prebiotic chemistry		Temperatures <120°C permissive of cellular activity	
Fluid dynamics—variable	Variable due to tidal energy, splashing but negligible salt crusts on hot lava	Too much agitation in tidal pools could break up the molecules	Permissive of cellular activity	
pH acid	Necessary for oligopyrrol synthesis	Does not favor ribose formation and stability	Any pH for protocells	
Ionic strength	High		Salts necessary for protocells	
Energy sources (heat, UV, redox)	Heat necessary for salt precipitation and pyrrol volatilization; UV fluxes to lava surface and rock pools would have been high	Heat and UV not good for stability of ribose	Redox reactions on reactive minerals; gradients (pH, temperature...)	UV deleterious to cellular life
Mineralogy, <i>e.g.</i> , mostly basalt lava (pyroxene, olivine, feldspars, accessory oxides) and their alteration products	Redox reactions important for oligopyrrol formation		Energy from redox reactions at mineral surfaces	
Element availability	CHNOPS from organics in water and mantle carbon in basalts; Fe ²⁺ and Mg ²⁺ from altered basalts		S and transition elements Cu, Fe, Ni, Zn...	
Porous structures (minerals, edifices, <i>e.g.</i> , beehive structures)	Altered basalts in rock pools, mineral porosity, sediments		Protected environment in rock pools for protocells	
Protection from external environment		No protection from UV, disruption caused by impacts or volcanic eruptions		No protection from UV, disruption caused by impacts or volcanic eruptions
Distribution of products	Possible if pool is tidal		Possible if pool is tidal	

Source: Westall et al., *Astrobiology*, 2018

Low-eruptive, hydrothermally-dominated, volcanic caldera setting

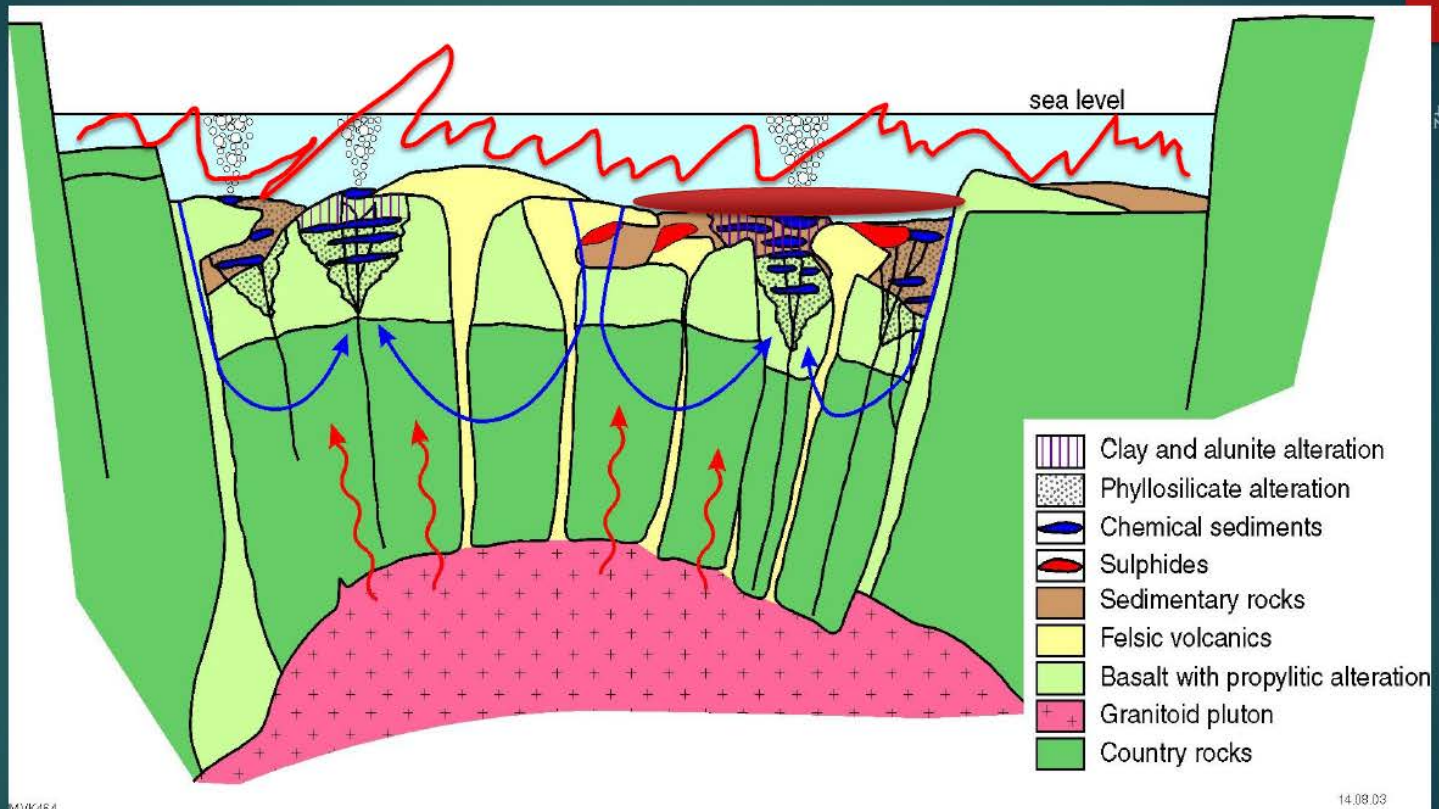


36

White Island,
New Zealand

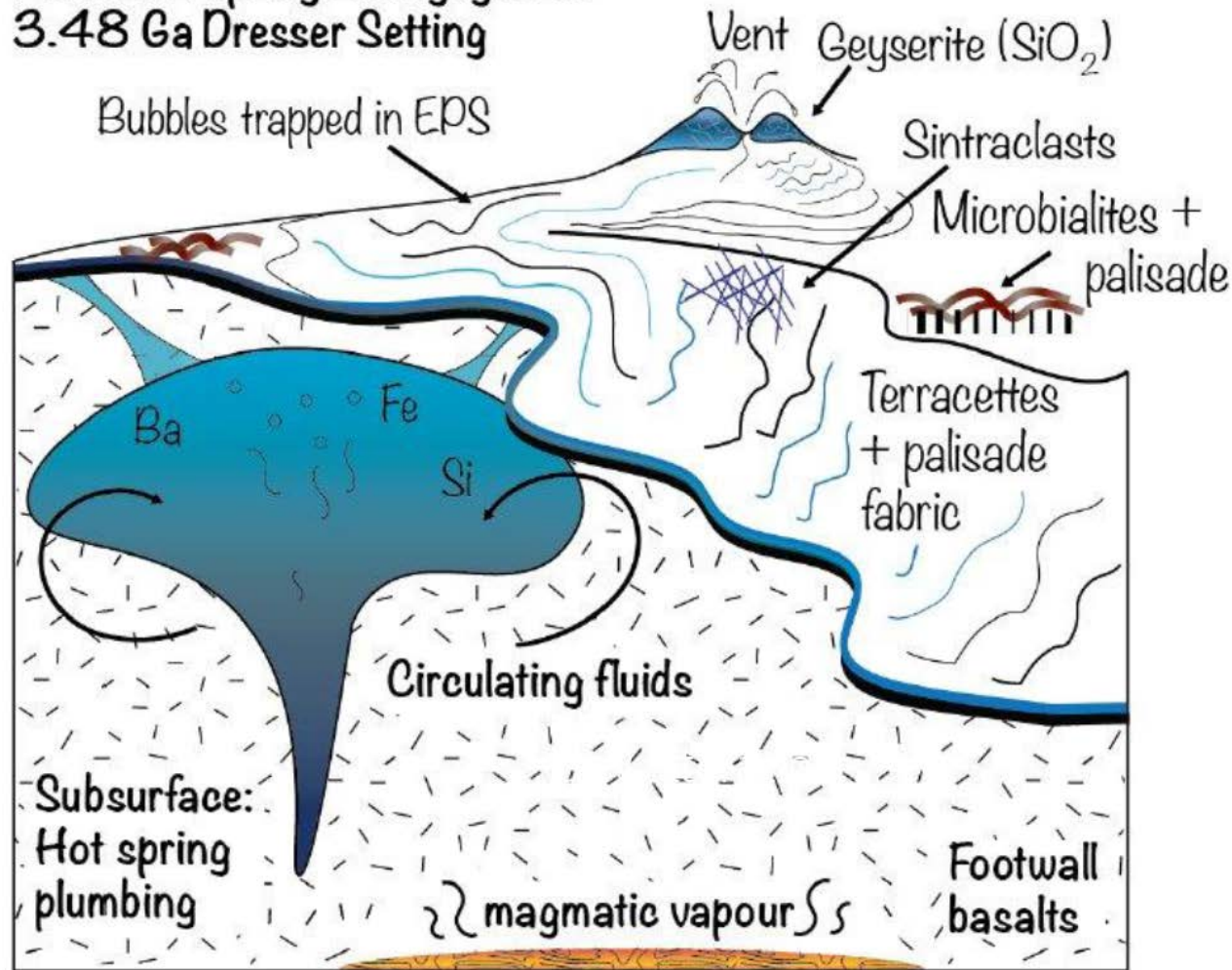


Volcanic caldera, *Plus* an emergent land surface



Van Kranendonk and Pirajó

Active hot springs and geysers :
3.48 Ga Dresser Setting



Dresser Fm geyserite

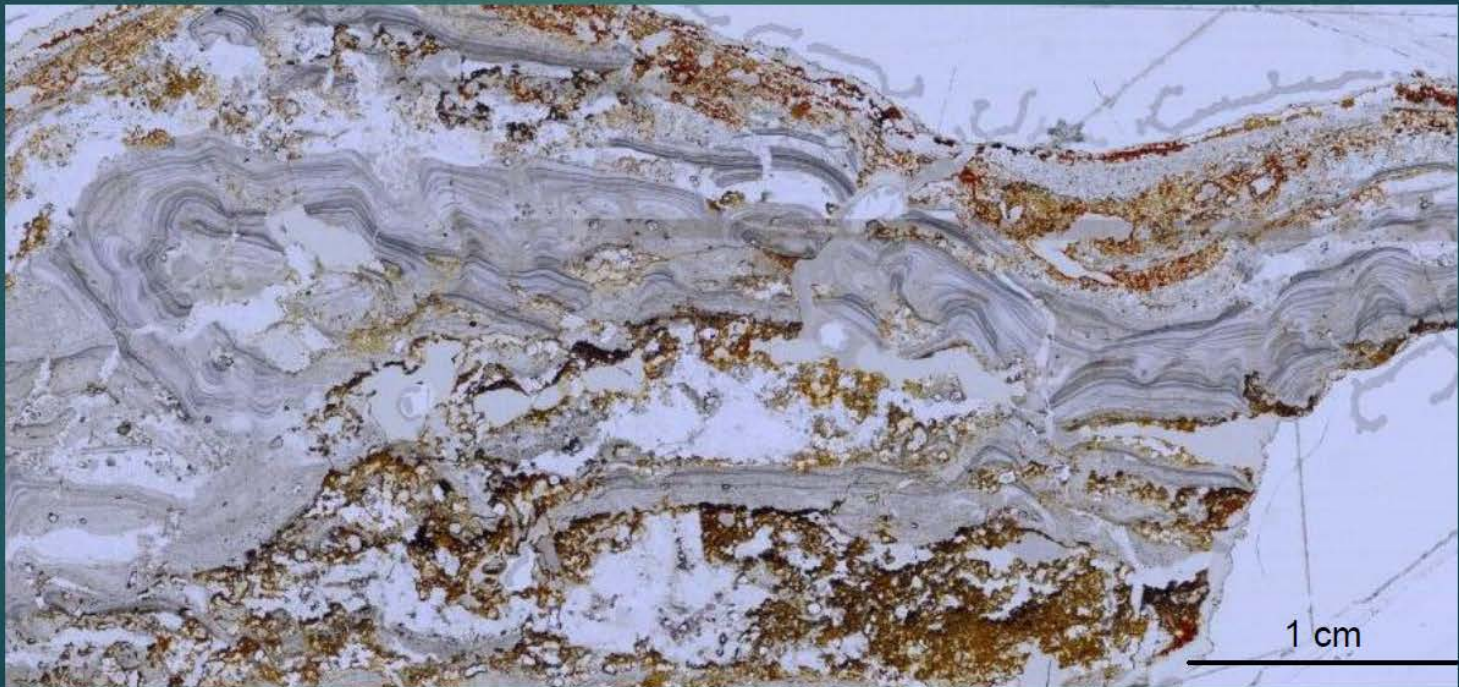
ARTICLE

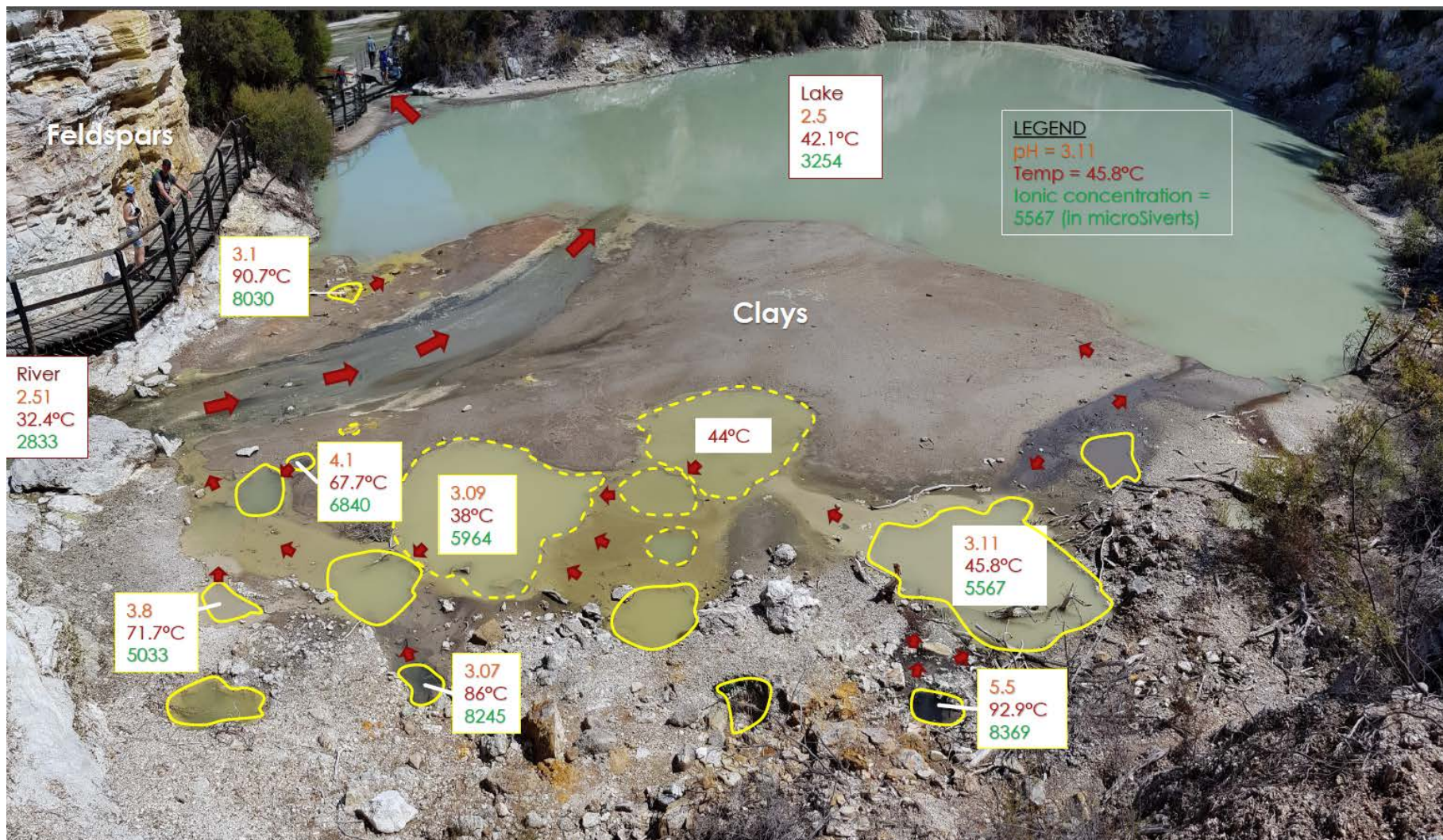
Received 18 Jul 2016 | Accepted 15 Mar 2017 | Published 9 May 2017

DOI: 10.1038/ncomms15263 OPEN

Earliest signs of life on land preserved in ca. 3.5 Ga hot spring deposits

Tara Djokic^{1,2}, Martin J. Van Kranendonk^{1,2,3}, Kathleen A. Campbell⁴, Malcolm R. Walter¹ & Colin R. Ward⁵





Source: invited Talk by Prof Martin van Kranendonk (University of New south Wales), Brixen February 2020

3. Ability to concentrate prebiotically important elements

Boron



Puga geothermal field, India

Iron



Chocolate Pots, Yellow

Organic matter



Wai-O-Tapu, New Zealand

Arsenic-gold



Champagne Pool, New Zealand

Sulfur



Wai-O-Tapu, New Zealand

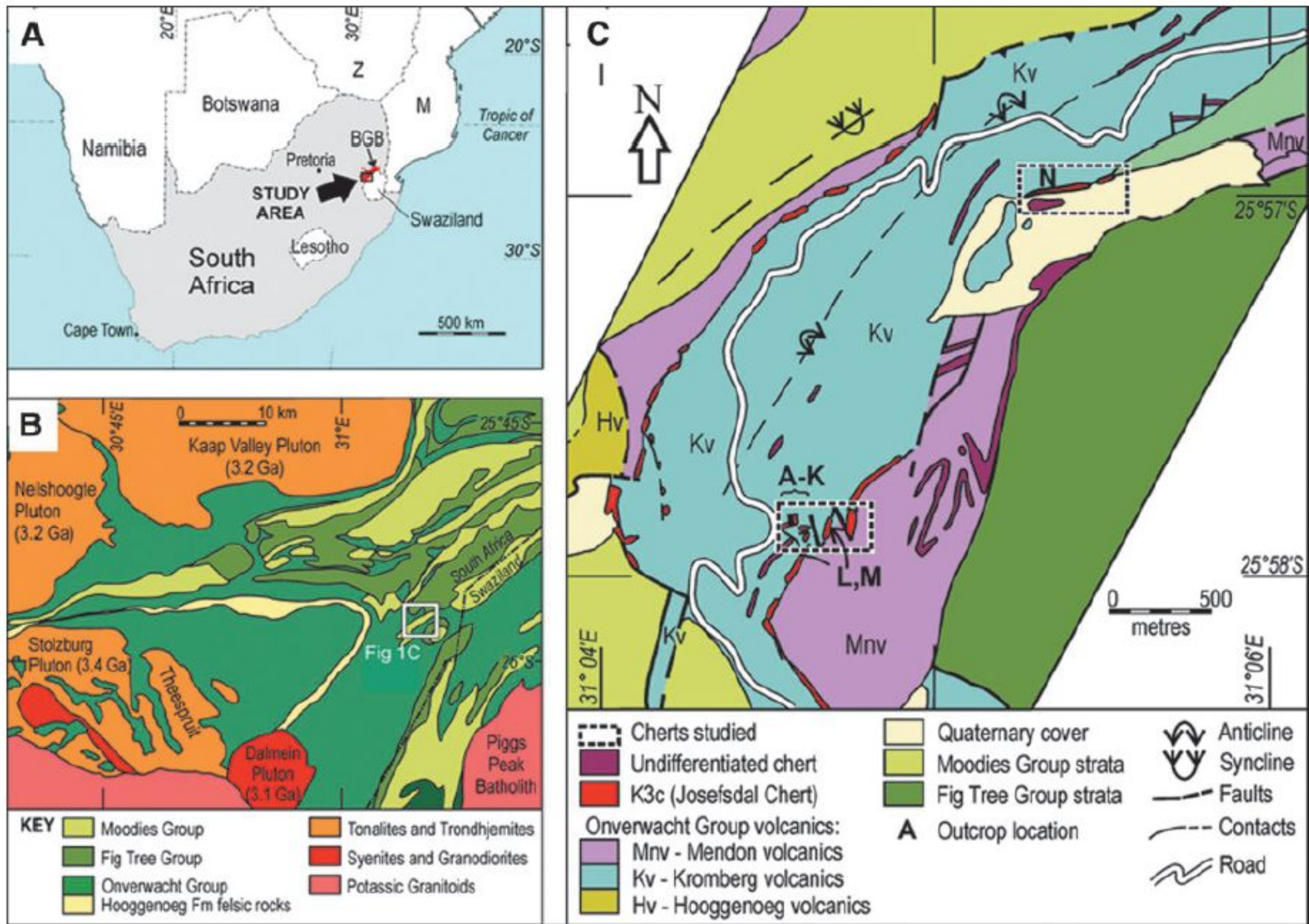


FIG. 1. (A) Location of the study area within South Africa. (B) General geological map of the Barberton Greenstone Belt showing location of the JC (white box). (C) Detailed geological map of the thin JC sediment exposures (red) within large thicknesses of mafic and ultramafic volcanics. Adapted from Westall *et al.* (2015a).

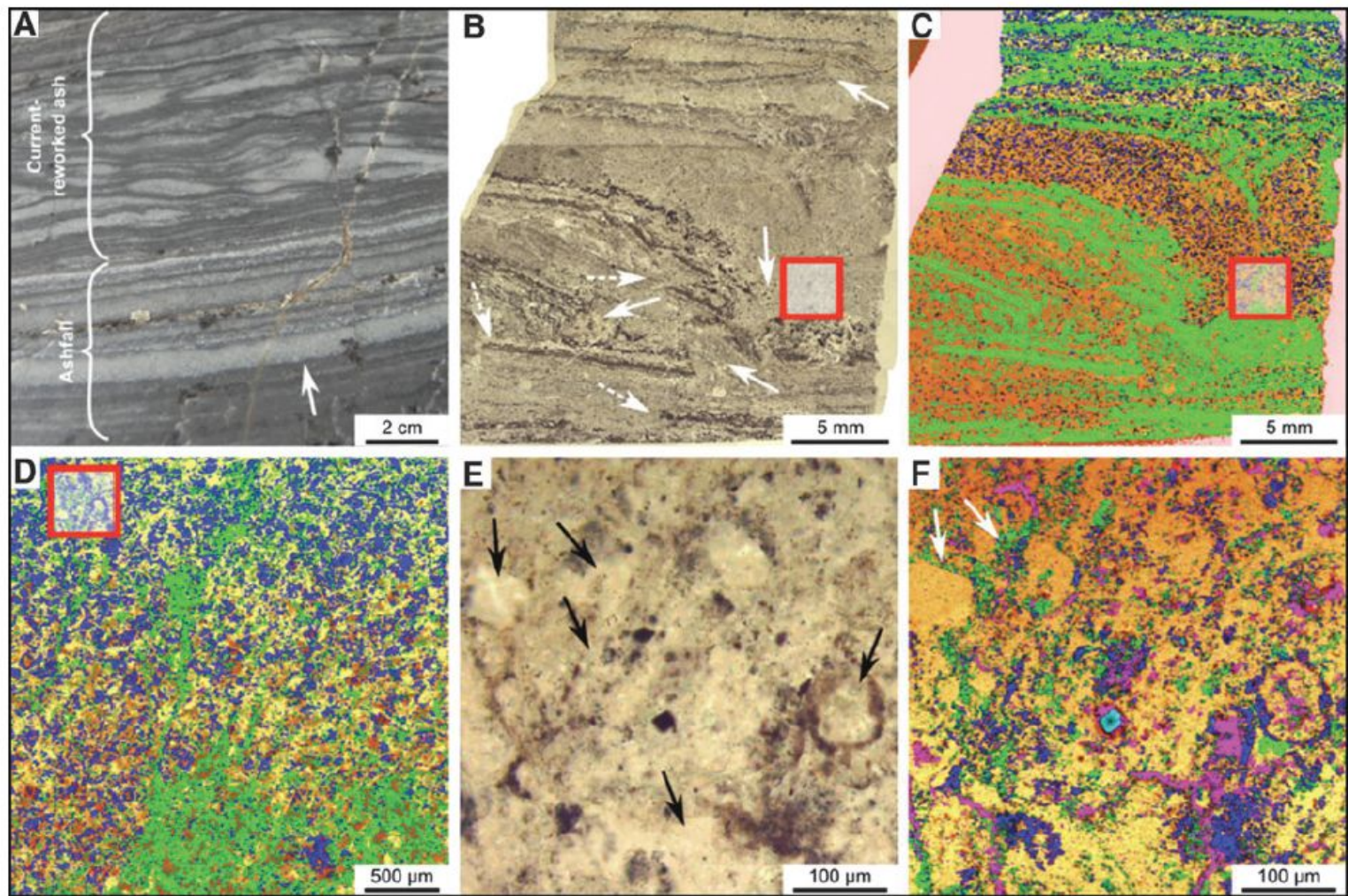


FIG. 2. Early Archean, laminated shallow marine volcanogenic sediments interacting with pervasive hydrothermal effluent from the 3.33 Ga JC. (A) Field photograph of alternating ash (light) and carbonaceous (dark) layers. (B) Photomicrograph of a thin section from the same facies documenting layers disrupted, through soft sediment deformation, by infiltrating hydrothermal fluids (arrowed). Red box outlines detail in (D). (C) Raman map of (B), showing carbon (green) within the silicified matrix (orange, quartz); anatase (blue) represents altered volcanic clasts. Red box outlines details in (D). (D) Raman map (red boxes in B, C) showing carbon (green) intermixed with volcanic particles (represented by alteration phases: anatase, blue; muscovite, pink); the quartz matrix (yellow/orange) represents the silica precipitated by hydrothermal fluids. Optical image (E) and Raman map (F) are details of the red box in (D) showing carbon (green) coating volcanic particles (arrowed), which have been replaced by muscovite (pink), anatase (blue), and quartz (yellow/orange). Additional minerals: magnetite, light blue; rutile, red.

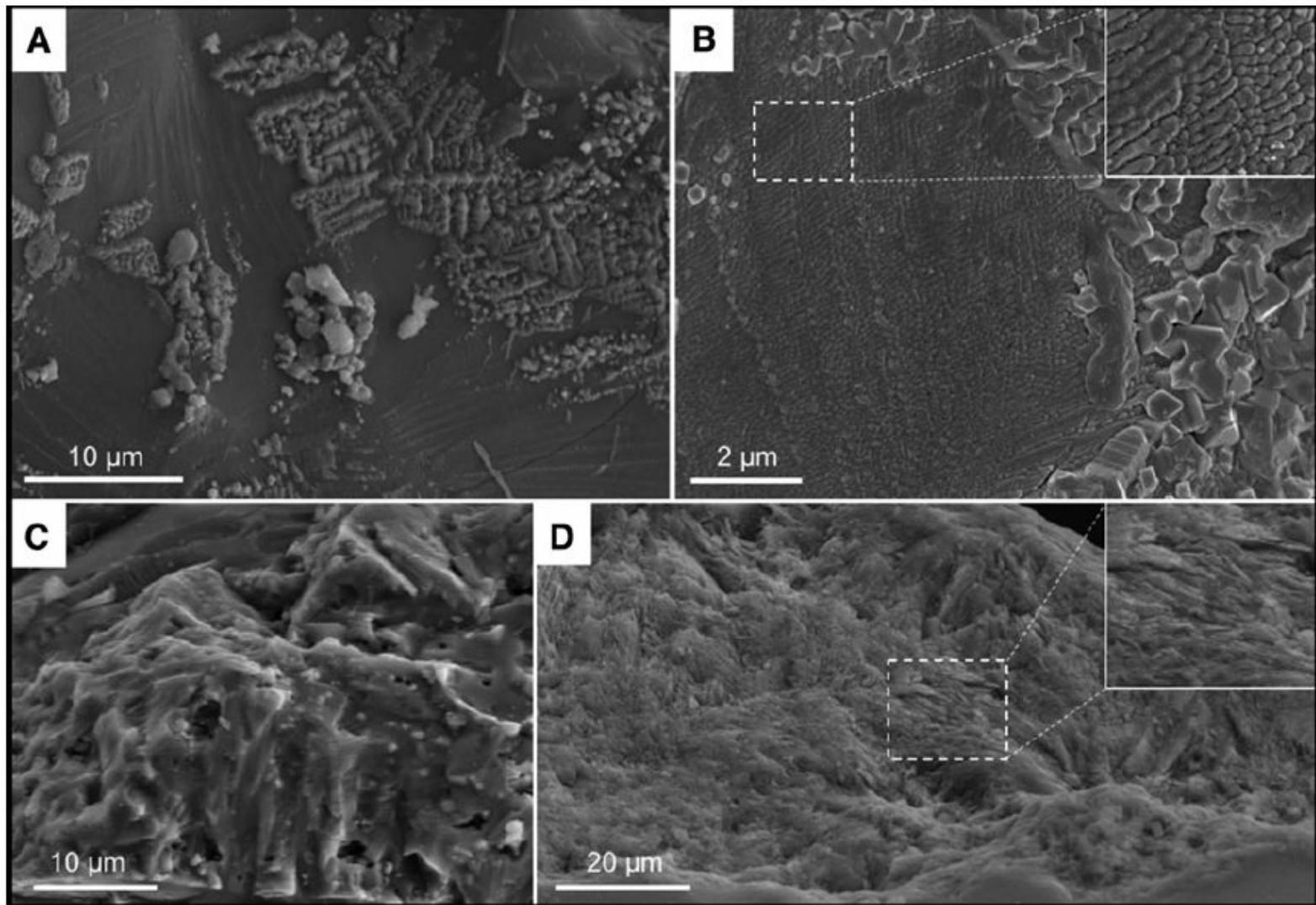


FIG. 3. Crushed volcanic rocks (mixture of East Pacific Rise basalt and komatiite) before and after corrosion in artificial seawater (starting pH = 6.24). (A) Scanning electron microscope view of the surface of basalt glass with skeletal pyroxene crystals showing mineralogical and morphological variability on the micron scale. (B) Detail of the volcanic glass surface (with inset) documenting submicron-scale morphological heterogeneity. (C) Sample from the same crushed volcanic rocks after 15 days of corrosion (ending pH = 7.1). The pyroxene crystals show pits and pores ranging in size from submicron to a few microns. (D) Phyllosilicate-coated surface of a volcanic glass shard corroded for 15 days (ending pH = 7.1).

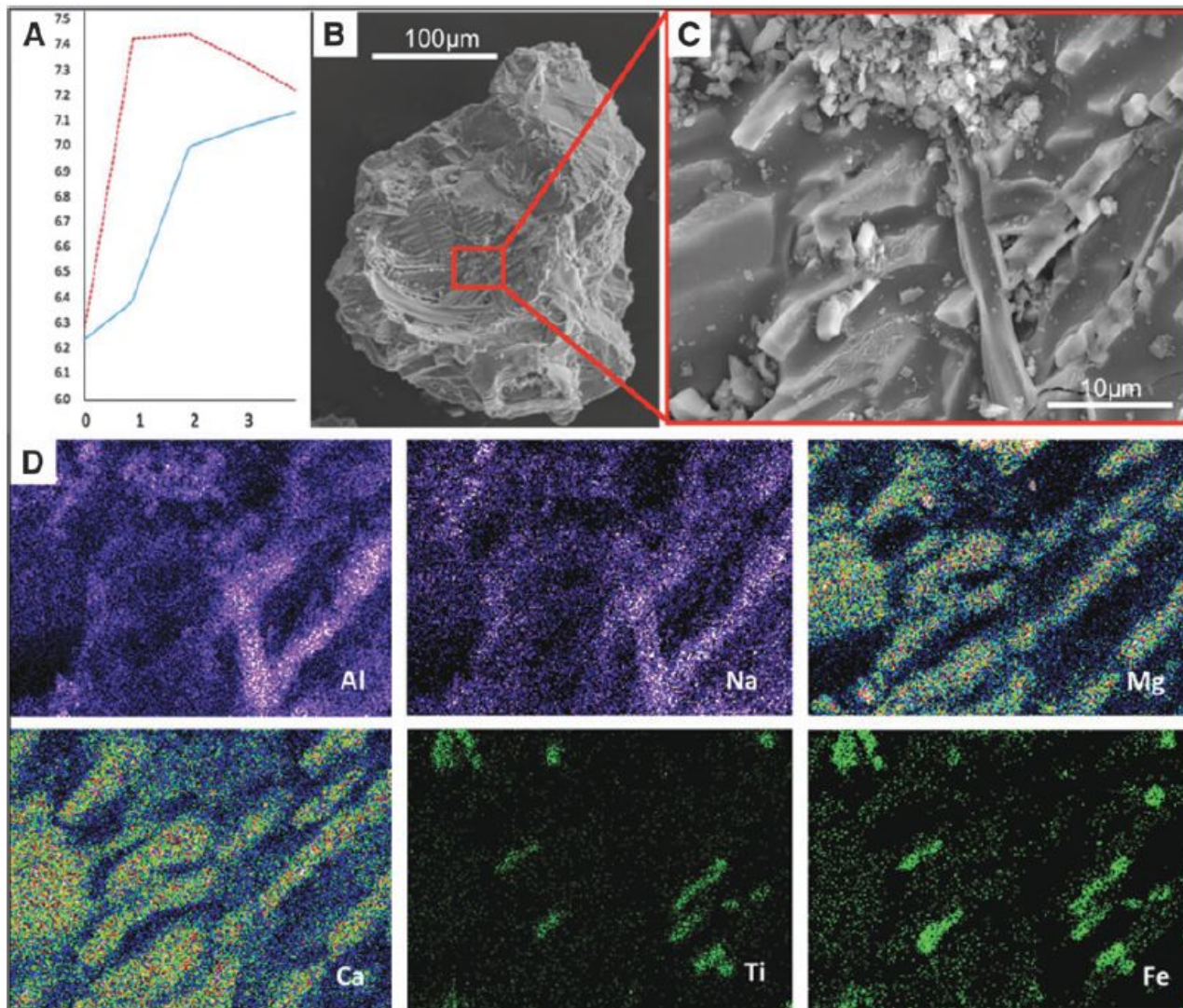


FIG. 4. Corroded volcanic grains from a mixture of East Pacific Rise basalt and komatiite (as in Fig. 3). (A) Changing pH during the first 3 days of corrosion of a mixture of East Pacific Rise basalt and komatiite in artificial seawater with a starting pH of 6.24. The red curve denotes pH changes in the sediment, blue curve changes in the overlying seawater. The rapid change in pH to more alkaline conditions from an initial weak acid is ascribed to the reaction of this seawater with particularly reactive minerals in the volcanic grains; the pH gradient in the pore spaces of volcanic sediment can thus be initiated in days. (B, C) Scanning electron micrographs of an ex-gas bubble in a pyroxene grain, documenting variable surface textures including porosity and protrusions associated with compositional variability (D). (D) EDX elemental maps showing two main phases: needle-shaped crystals of pyroxene (Na, Mg, Al, Ca, trace Fe; Si not shown) co-precipitated with ilmenite (FeTiO_3).

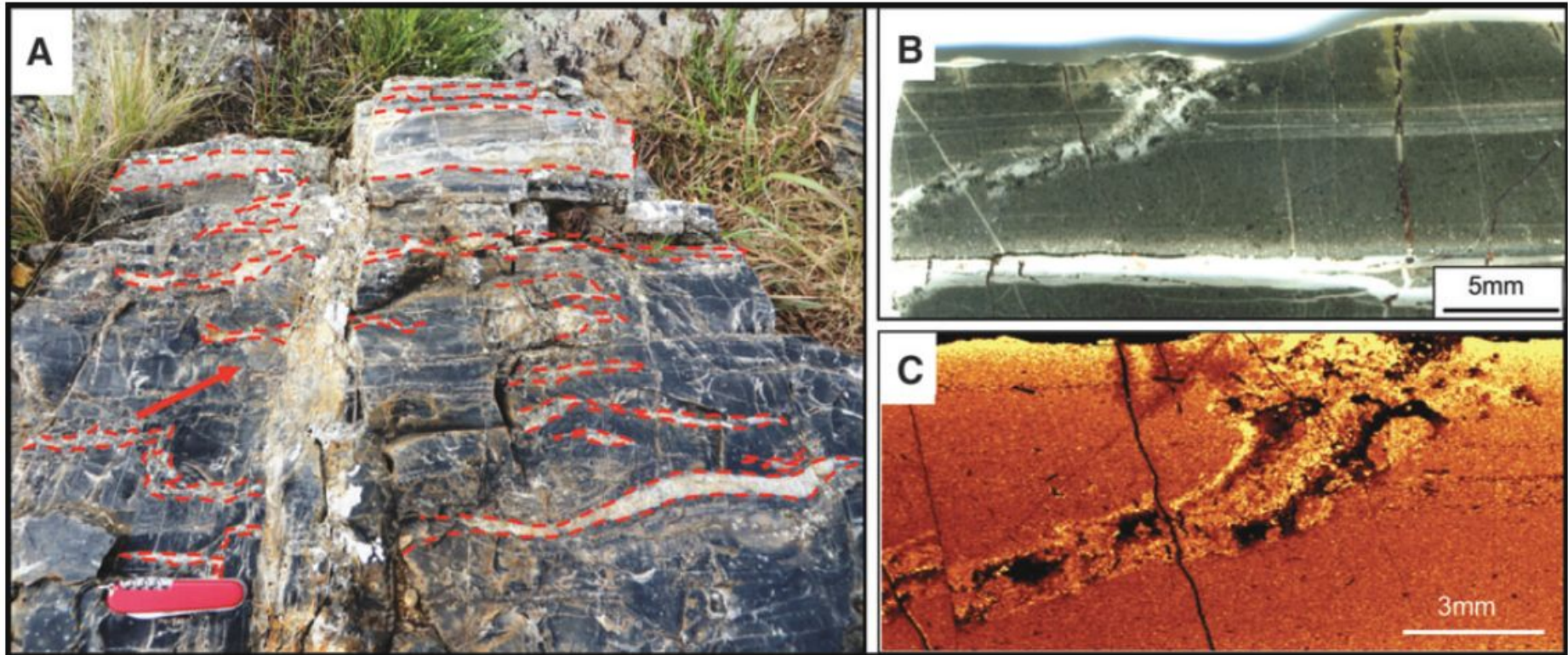


FIG. 5. Macroscopic to microscopic hydrothermal veins. (A) Late diagenetic, vertical hydrothermal vent (full arrow) cross-cutting hummocky-swaley storm deposits in the JC (Facies A of Westall *et al.*, 2015a). Note also infiltrations of hydrothermal chert, emanating from the central vent, parallel to the sediment layering (outlined by dotted red lines). (B) At the thin-section scale, this optical micrograph shows a hydrothermal veinlet cross-cutting finely laminated, fine-grained sediments. (C) Raman map of carbon distribution in the sediment and in the vein shown in B); brighter color indicates higher concentration, *i.e.*, carbon is at its highest concentration when entrained within the vein.

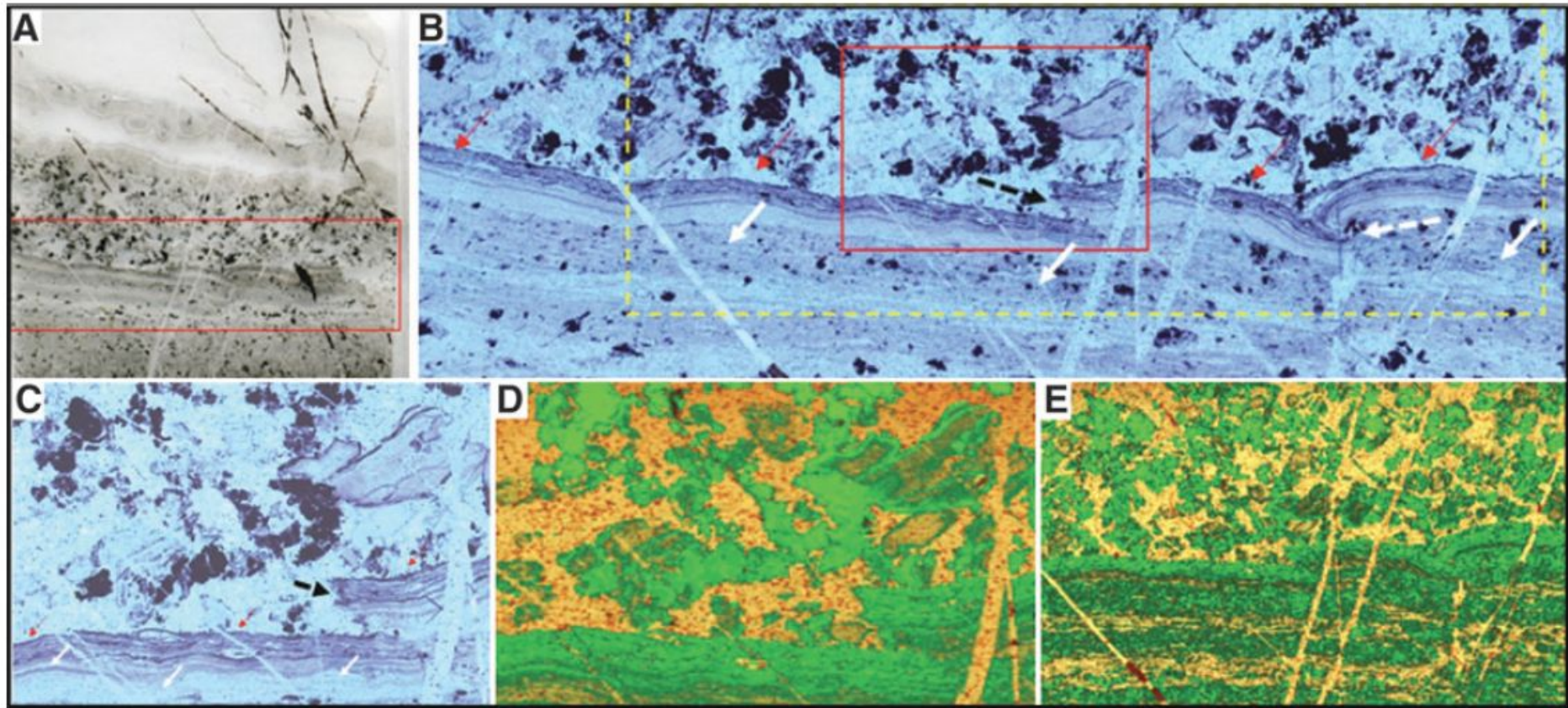


FIG. 6. Silica gel-like sediment from the 3.33 Ga JC. (A) Scanned thin section slide of a deposit of hydrothermal silica containing carbonaceous clots and layering. (B) Detail of red box in (A) showing fine-scale carbonaceous layering in the lower part of the image and a mottled carbonaceous texture in the upper part. The top of the layered section shows plastic deformation (dashed white arrow) and tearing, indicative of disruption by the dynamic flow of hydrothermal fluids. Red arrows indicate the cohesive layer above the plastically deformed layer, and solid white arrows indicate detrital sedimentation below. The red box denotes the detail in (C) and the Raman scan in (D), while the yellow box denotes the area of the Raman map in (E). (C) Detail showing tearing of the cohesive surface of the finely laminated layer (black arrow). (D, E) Raman maps demonstrate that the sample consists of only quartz (yellow-orange) and carbon (green).

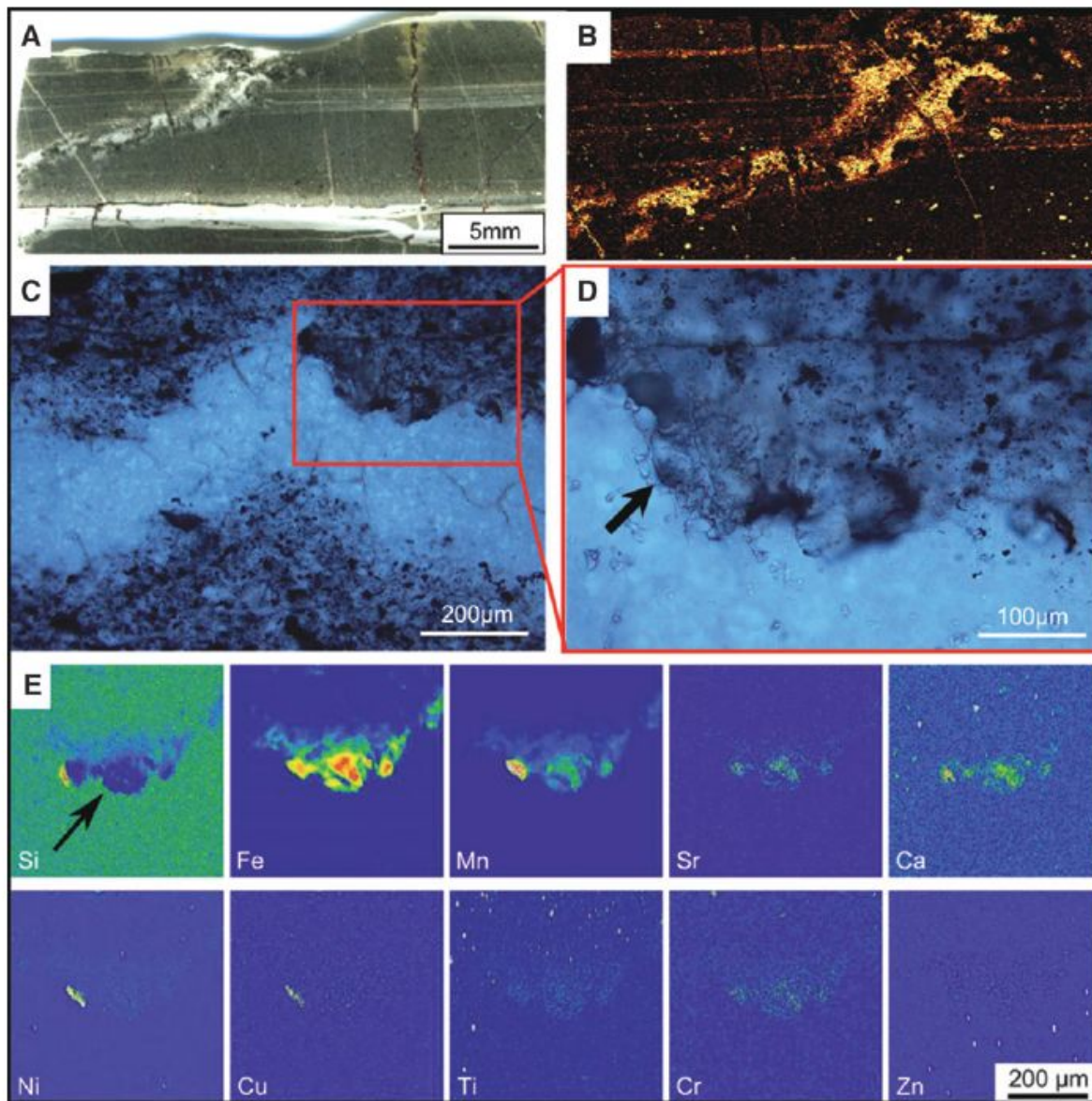


FIG. 7. Hydrothermal veinlet in fine-grained carbonaceous sediments from Josefsdal. (A) Optical micrograph showing a hydrothermal veinlet cross-cutting finely laminated, fine-grained sediments. (B) Raman map of the siderite distribution in the sediment and in the veinlet; brighter color indicates higher concentration. (C, D) Optical micrograph views of a siderite (FeCO_3) and rhodochrosite (MnCO_3) co-precipitate at the edge of the veinlet shown in (A). Red box in (C) shows location of detail in (D). Arrow in (D) points to the same location as the arrow in (E). (E) PIXE elemental maps (beam size: $2\ \mu\text{m}$; map size: $500 \times 500\ \mu\text{m}$; resolution: 256×256 pixels; 11 h acquisition time) of area denoted by red box in (C) document concentrations of other elements associated with the siderite/rhodochrosite precipitation, including Mn, Sr, Ca, Ni, Cu, Ti, Cr, and Zn scavenged from the hydrothermal fluids.

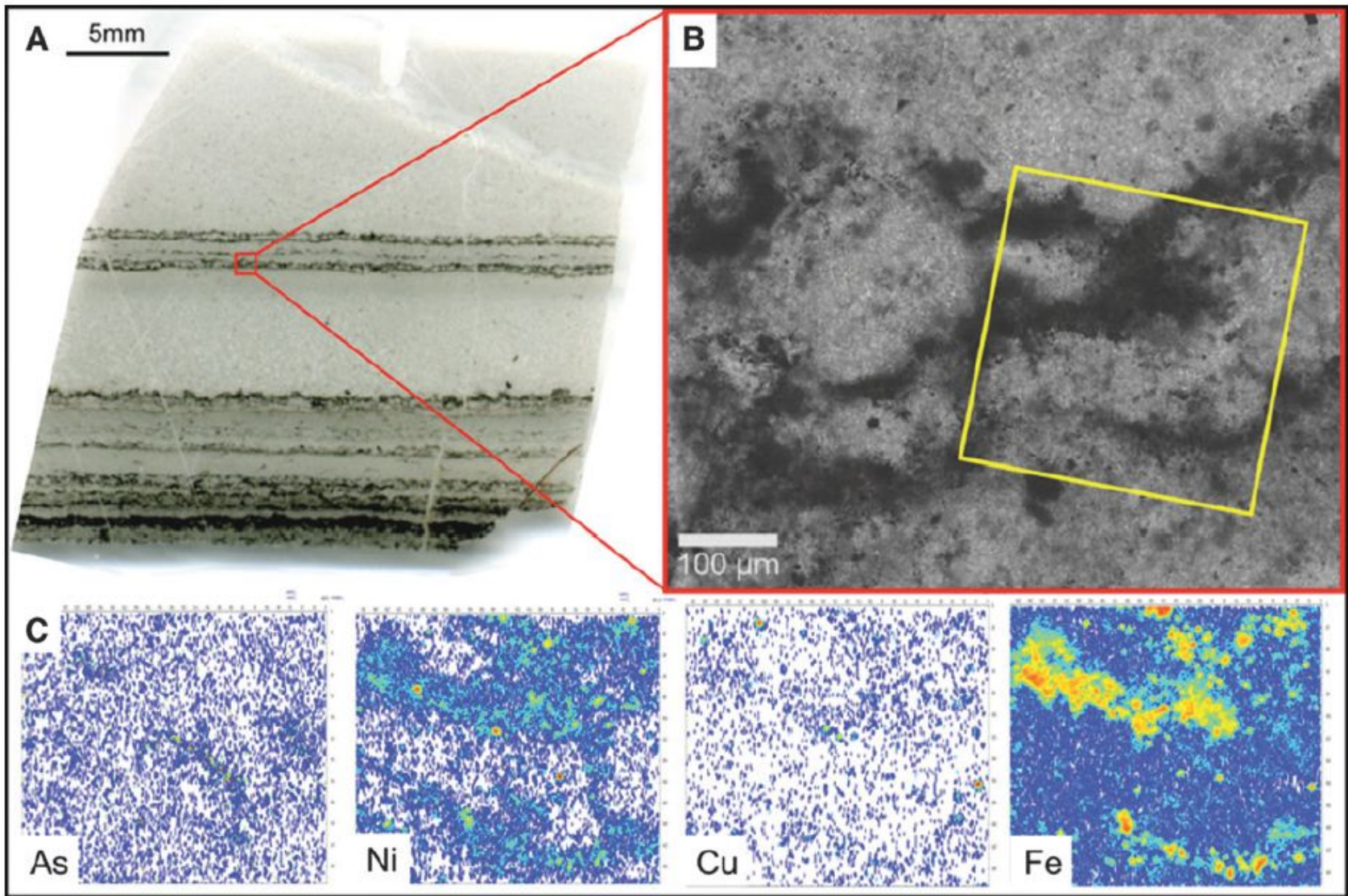


FIG. 9. Hydrothermal element scavenging by altered volcanic particles. (A) Thin section of sedimented volcanogenic particles showing dark layers comprising concentrations of volcanic particles (including spherules), as well as traces of carbon and microcrystalline pyrite (Facies D, after Westall *et al.*, 2015a). (B) Optical micrograph of the volcanic particles in a black layer in the JC sediments. Yellow box denotes the area of the regions in (C). (C) PIXE elemental maps (beam size: 2 μm; map size: 300×300 μm; resolution: 256×256 pixels; 3.5 h acquisition) showing the concentration of Fe, As, Ni, and Cu, trace elements of hydrothermal genesis scavenged by the altered volcanic particles.

Submarine hydrothermally influenced sediments

TABLE 5. ENVIRONMENTS AVAILABLE FOR THE EMERGENCE OF LIFE

<i>System</i>	<i>Prebiotic chemistry</i>		<i>Emergence of life</i>		
	<i>Properties</i>	<i>Advantages</i>	<i>Disadvantages</i>	<i>Advantages</i>	<i>Disadvantages</i>
Submarine hydrothermally influenced sediments					
Temperatures ~ 50 to >100°C	Facilitates molecular interactions			Temperatures acceptable for protocellular activity	
Fluid dynamics	Low to high		High dynamics will disrupt molecular bonds	Diffusion of nutrients	
pH—alkaline-acid	Favors prebiotic processes			Any pH for protocells	
Ionic strength	Variable			Salts necessary for protocells	
Energy sources	Heat, redox reactions			Small organics (from Fischer-Tropsch and ultramafic fluid inclusions); redox reactions of reactive minerals; gradients (pH, temperature...)	
Mineralogy, <i>e.g.</i> , sulfides and various mafic/ultramafic minerals and their alteration products	Reactive surfaces favor molecule-organic interactions (Table 1)			Energy from redox reactions at mineral surfaces	
Element availability	CHNOPS			CHNOPS, Cu, Fe, Ni, Zn...	
Organics (from hydrothermal fluids, volatile and degraded ET organics)	Volatiles, small organic molecules, components of macromolecular building blocks of life			Presence of nutrients (small organics, CH ₄)	
Porous sediments	Concentration of prebiotic components, compartmentalization			Protected environment for protocells	
Silica hydrogels	Very common, compartmentalization, confinement			Hydrogels as protocells, compartmentalization and autoreplicative system	
Protection from external environment	UV protection, disruption caused by impacts			Protected environment—from UV, etc.	
Distribution of products	Mixing of pore water and sediments with seawater, current transport			Mixing of pore water and sediments with seawater, current transport	

Source: Westall et al., *Astrobiology*, 2018

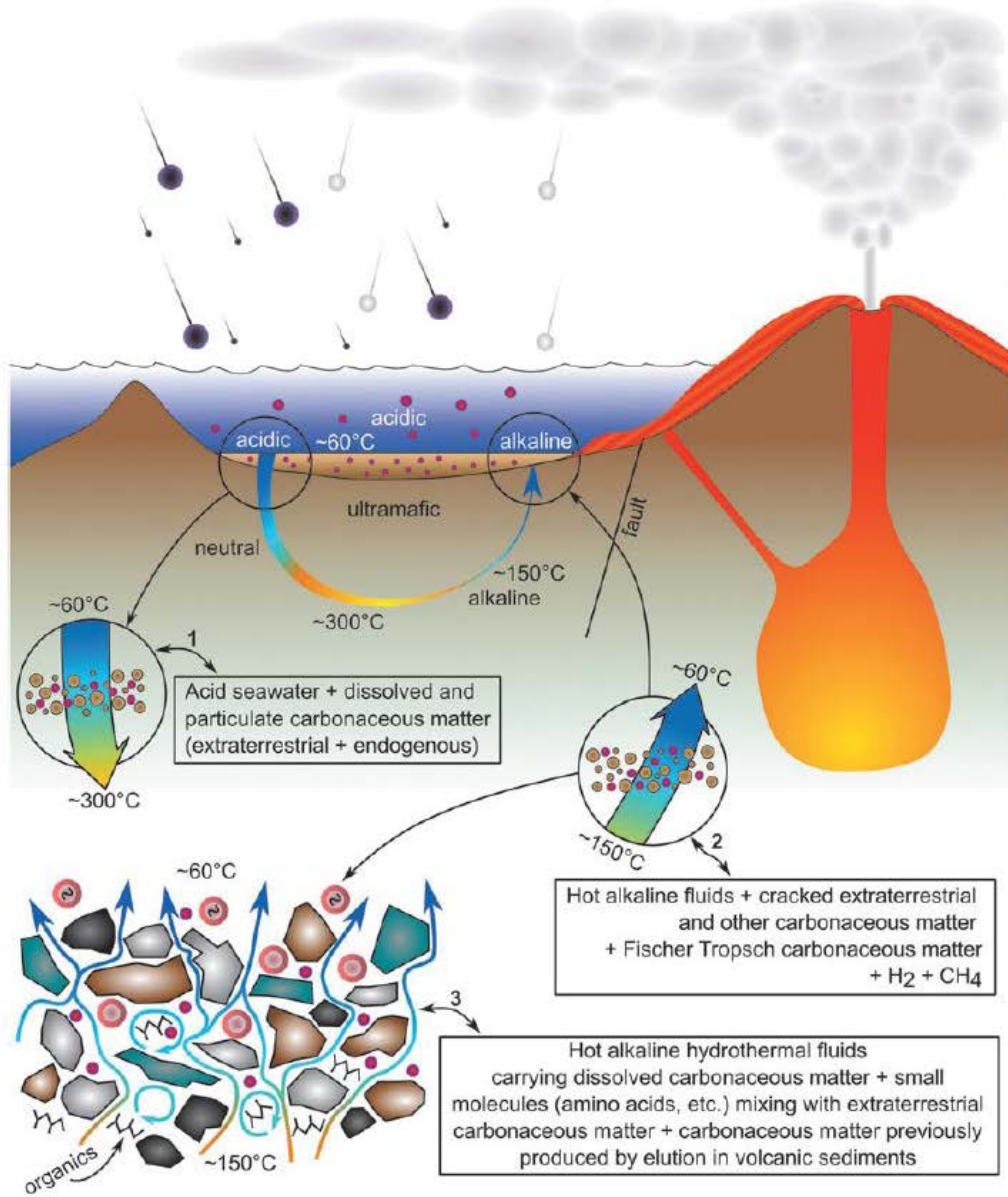


FIG. 11. Schematic synthesis of the proposed Hadean, hydrothermal-sedimentary micro-reactor environment for complexification of prebiotic chemistry. Slightly acidic seawater entraining dissolved and particulate carbonaceous matter of diverse origins permeates through ultramafic/mafic sediments into the crust (insert 1), altering the ultramafic rocks and becoming more alkaline during these reactions. Light-weight carbon molecules and gases (*e.g.*, H₂, CH₄) formed by Fischer-Tropsch-type processes (Shock *et al.*, 2002), as well as molecules from ultramafic fluid inclusions (Van Kranendonk *et al.*, 2015), were convected into reactive porous sediments at the bottom of the sea (the sediment-water interface, insert 2), where a temperature and pH disequilibrium (insert 3) with the overlying acidic seawater existed. Convection of warm, carbon-bearing hydrothermal fluids allowed prebiotic molecules to concentrate and self-assemble in pore spaces and on the surfaces of chemically reactive minerals, resulting in the formation of increasingly complex molecules.

Competing models for the Origin of Life

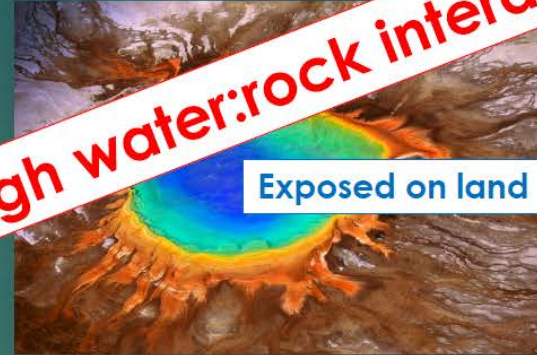
Deep sea hydrothermal vents



Permanently wet

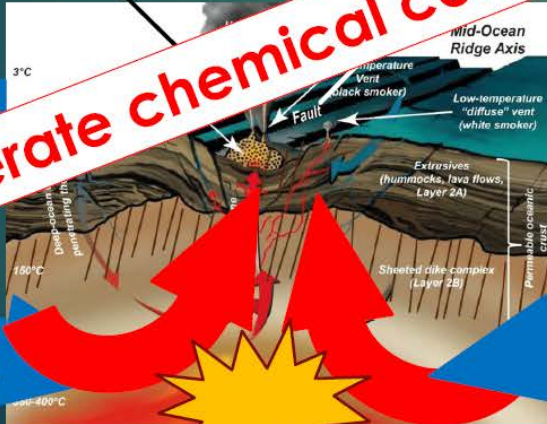


Terrestrial hot spring fields

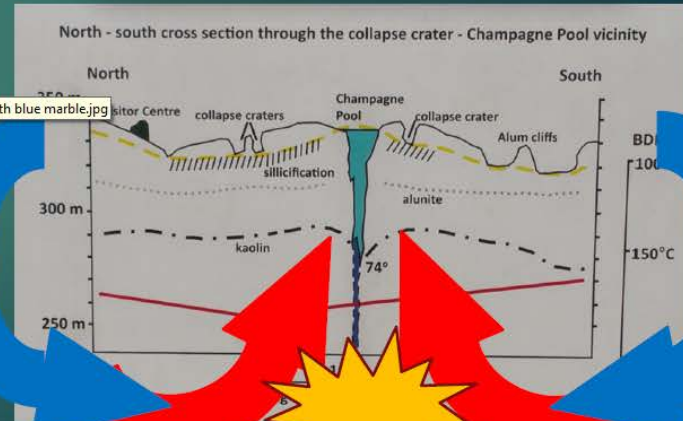


Exposed on land

Generate chemical complexity through water:rock interaction



G:\astronomy pics\Earth blue marble.jpg



2. Compositionally varied pools

pH=6.7, T = 85°C
Gold, Arsenic

pH=8.5, T = 68°C

pH=1, T = 88°C
High ionic concentrations

pH=3, T = 92°C
Sulfur-rich

pH=2, T = 14°C
Sulfur-rich

The water problem:

Biopolymer formation requires dehydration via condensation reactions

PROTEINS H_2O H_2O H_2O H_2O H_2O H_2O

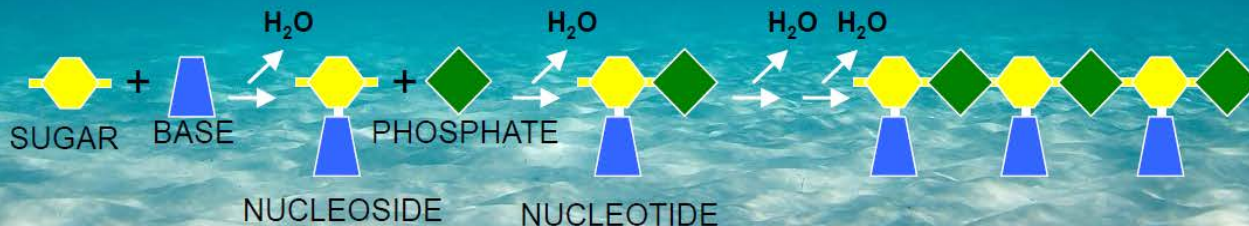
Water may be essential for life, but Cairns-Smith (1982) noted that "all the major biopolymers are metastable in aqueous solution in relation to their (deactivated) monomers."

CARBOHYDRATES

H_2O H_2O H_2O H_2O H_2O

"You can heat a solution of amino acids in water forever, but no polymers will be produced. On the other hand, polymer synthesis can occur if the amino acids are in a dry state... The source of energy is that water molecules have the potential to leave the system. Deamer, 2011: First Life. U. California Press

NUCLEIC ACIDS: DNA and RNA



Benefits of Terrestrial hot spring fields



- ▶ 1) They have the capacity for wet-dry cycles that promote condensation reactions to make polymers
- ▶ 2) Have multiple, chemically and thermally distinct pools – they are geologically the most complex areas on Earth
- ▶ 3) Can concentrate organic molecules, other elements, and biopolymer products that would be diluted in oceans
- ▶ 4) Include acidic conditions in which lipid vesicles can form
- ▶ 5) Have additional water : air and air : rock interfaces
- ▶ 6) Composed of fresh, not salty water
- ▶ 7) Exposed to atmosphere-filtered UV, which aids polymerisation

Drying: evaporation

1. Wet-dry cycles

Timescales of
minutes → hours → days → seasons → years



Wetting:
Geyser splashing

Water may be essential for life, but Cairns-Smith (1982) noted that "all the major biopolymers are metastable in aqueous solution in relation to their (deactivated) monomers."

"You can heat a solution of amino acids in water forever, but no polymers will be produced. On the other hand, polymer synthesis can occur if the amino acids are in a dry state... The source of energy is that water molecules have the potential to leave the system.

Deamer, 2011: First Life. U. California Press



SUGAR

BASE

PHOSPHATE

NUCLEOSIDE

NUCLEOTIDE

Drying: water drawdown



Chemical Evolution

International Edition: DOI: 10.1002/anie.201503792
German Edition: DOI: 10.1002/ange.201503792

Ester-Mediated Amide Bond Formation Driven by Wet-Dry Cycles:
A Possible Path to Polypeptides on the Prebiotic Earth**

Jay G. Forsythe, Sheng-Sheng Yi, Irena Mamajanov, Martha A. Grover,
Ramanarayanan Krishnamurthy,* Facundo M. Fernández,* and Nicholas V. Hud*

Angewandte
Chemie

Three recent papers suggest that early crust was at least partly differentiated to felsic crust in the Hadean-early Archean

Potassic, high-silica Hadean crust

Patrick Boehnke^{a,b,1}, Elizabeth A. Bell^f, Thomas Stephan^{a,b}, Reto Trappitsch^{a,b,2}, C. Brenhin Keller^d, Olivia S. Pardo^{a,b}, Andrew M. Davis^{a,b,c}, T. Mark Harrison^{c,1}, and Michael J. Pellin^{a,b,e,f}

Titanium isotopic evidence for felsic crust and plate tectonics 3.5 billion years ago

Science 2017

Nicolas D. Greber,^{1,2,3} Nicolas Dauphas,¹ Andrey Bekker,^{2,3} Matouš P. Ptáček,¹ Ilya N. Bindeman,⁴ Axel Hofmann³

nature
geoscience

Article | Published: 13 August 2018

An impact melt origin for Earth's oldest known evolved rocks

Tim E. Johnson[✉], Nicholas J. Gardiner, Katarina Miljković, Christopher J. Spencer, Christopher L. Kirkland, Phil A. Bland & Hugh Smithies

Nature Geoscience 11, 795–799(2018) | Cite this article

Kemp et al. 2010

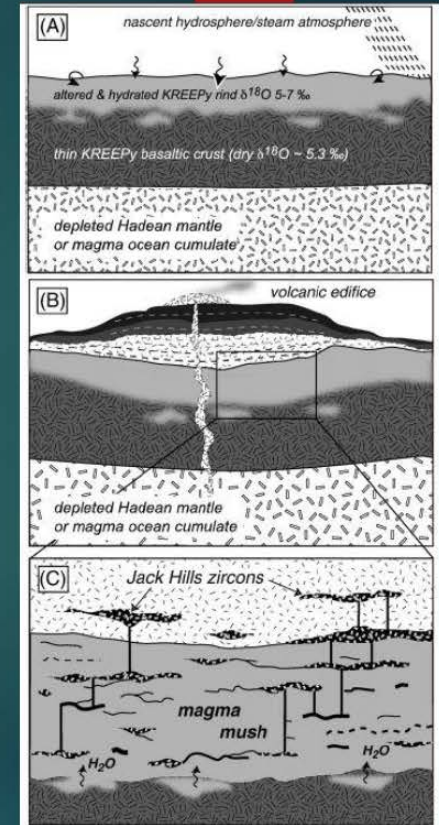


TABLE 2. THE PHYSICOCHEMICAL ENVIRONMENT OF THE ORIGIN OF LIFE

<i>Parameter</i>	<i>Prebiotic chemistry</i>		<i>Emergence of life</i>	
	<i>What</i>	<i>How or where</i>	<i>What</i>	<i>How or where</i>
Element availability	CHNOPS essential for life	From endogenous and exogenous CHNOPS molecules	Chemical bonding of these elements—CHNO—range in covalency, allowing sufficiently strong yet penetrable bonding among these elements. S and P are also penetrable but not involved in long chain formation. Assembly of atoms into discrete molecules is also a form of molecular complexification. Mutual cooperative interactions between molecules so that self-organization can emerge and function can be expressed.	By enabling stable linear carbon chains while introducing elements with different oxidation-reduction and pH reactivities that allow reactions without destruction (enzymes) or formation of metastable intermediates leading, ultimately, to sustainable, stable products. Within environments which presented free energy, molecular building blocks and conducive gradients of physicochemical properties so as to encourage mutually cooperative molecular interactions in localized spaces.
Temperature	Increases the frequency with which energetic molecular collisions can occur; helps pass activation energy barrier	Probability of intermolecular collision is increased, activation energy supplied by thermal means to cross the energy barrier (heat in hydrothermal systems), helps in dehydration for condensations by removal of water	High temperatures will break up molecular bonds (DNA/RNA nucleotides are stable up to 120°C)	Mixture of high <i>T</i> hydrothermal fluids with lower <i>T</i> seawater varies temperature between the two end members according to flux—see gradients, but also advective flux
pH	Different chemical processes occur at different pH values	Alkaline-acid hydrothermal fluids; acidic seawater; mixtures of hydrothermal and seawater; <i>e.g.</i> , amino acid coupling to produce peptides at high pH and general acid-catalyzed hydrolysis processes at low pH.	Variable pH changes structure and surface properties of colloids, sols, and polymers. Also allows nucleophilic reactions (substitutions), condensation reactions.	Variable pH for protocells, by allowing reversible and irreversible reactions involving CHNO (S, P) components

(continued)

TABLE 2. (CONTINUED)

<i>Parameter</i>	<i>Prebiotic chemistry</i>		<i>Emergence of life</i>	
	<i>What</i>	<i>How or where</i>	<i>What</i>	<i>How or where</i>
Ionic strength	Helps stabilization and structural organization of organic molecules, spontaneous self-assembly phenomena; gradients are important for physicochemical properties	Complexification processes, <i>e.g.</i> , self-assembly, form a concentration of monomers through the formation of surfactant micelles, interfacial adsorption of ionic surfactants and formation of aqueous colloidal crystals	Salts necessary for protocells, but minimum water activity is 0.5	By changing the surface charge of particles and by changing the properties and stability of micelles. Seawater, hydrothermal, pore water fluids.
Energy	Energy is necessary for fueling reactions and primitive metabolisms	<i>e.g.</i> , ionizing radiation for prebiotic reactions; energy from exothermic reactions; heat from hydrothermal systems	For primitive metabolism	Assuming that there were, originally, only reduced compounds with various oxidation states (inorganic components) and that organic components delivered to Earth were in variable oxidation states. Oxidation of reduced inorganic compounds, <i>e.g.</i> , NH ₄ , NO ₂ , S ₂ , S ₀ , H ₂ and Fe ²⁺ ; oxidation of organic compounds produces phosphorylated molecules.
Radiation	Useful for some prebiotic reactions but mainly destructive for organic molecules	UV, radiogenic species (U, Th, etc.)	Destructive for biomolecules	By introducing random flaws in the structure of organic molecules. By introducing temporary elevated energy states in inorganic components and transition elements that enable potential bonding with organic components. UV, radiogenic species (U, Th, etc.). <i>e.g.</i> , temperature, pH, ionic gradients
Gradients	A means of maintaining systems out of equilibrium	Dissipation of energy. Sinks for this dissipated energy are potential reaction sites ...	Necessary for maintaining far-from-equilibrium systems; to gain and dissipate energy, reactants, and products	<i>e.g.</i> , temperature, pH, ionic gradients
Molecular diffusion	Diffusion of molecules into and out of the above-mentioned compartments to permit molecular reactions	In solvents, <i>e.g.</i> , hydrothermal fluids, seawater, pore waters, mixtures	Diffusion of molecules into and out of the above-mentioned compartments to permit molecular reactions	In solvents, <i>e.g.</i> , hydrothermal fluids, seawater, pore waters, mixtures

Source: Westall et al., *Astrobiology*, 2018